Francesco Pio Lionetti

Preliminary evaluation of joining Al-PEEK via Through Hole Extrusion Welding

School of Engineering

Dissertation for the Degree of Master of Science in Mechanical

Engineering Espoo

July 2020

Supervisor: Professor Pedro Vilaça

Advisor: Prabilson Khadka

Abstract

Author Francesco Pio Lionetti

Title of thesis Preliminary evaluation of joining Al-PEEK via Through Hole Extrusion Welding

Degree programme Master of Science Mechanical Engineering

Major/minor Mechanical Engineering | **Code** ENG 25

Thesis supervisor Professor Pedro Vilaça

Thesis advisor Prabilson Khadka

Date 31/07/2020 | **Number of pages** 104 | **Language** English

Abstract

The guideline for future automotive and structural application is to reduce the weight with high performance in terms of mechanical resistance. In automotive field this has an additional benefit that is related to the environmental issues that are becoming increasingly stricter. The competitiveness in this industrial field will be guaranteed through hybrid solutions which involve lightweight metals and engineering polymers. Different joining techniques between dissimilar materials were already proposed and established, but sometimes these methods are not very effective. The purpose of this work is to introduce a preliminary evaluation of a new approach to join dissimilar materials.

THEW (Through Hole Extrusion Welding) is the new tested joining technique for dissimilar materials. The process consists to extrude the viscoplasticised aluminum alloy through an extrusion die to soften, penetrate, and pressurise the polymer component. The aluminum alloy is brought to the condition of viscoplastic through the stirring effect due to the probe used for this technology. At the same time the shoulder guarantees a total closure of the welding surface and a forging action on the welding region. The penetration of the aluminum will cause a pressurisation and a consequent upward flow of the polymer ensuring the formation of the so called "Crab Claw" joint. The most important involved joining mechanisms are mechanical interlocking and adhesive bonding. The material involved for the final version of the THEW joint are AA5754-H111, PEEK and Ti Gr 1 with a respective thickness of 5 mm, 5 mm, and 0.6 mm.

To implement this new kind of dissimilar materials joining technique an experimental plan is made involving the design of new tools, process parameters and clamping system. Different set of tools and process parameters are tested on different base materials. After the experimental phase, a best set of preliminary process parameters, tools and base materials are selected. The process is also implemented for non-linear paths and in a double side version.

Mechanical, microstructural, and macrostructural tests are used to analyse the joint from different point of views (mechanical, geometric, and microstructural point of view). The results are analysed and commented to do appropriate analyses on the possible impact of this new joining technique.

Keywords Through Hole Extrusion Welding (THEW), Al-alloy, PEEK, Crab Claw Joint, Friction Stir Welding, Dissimilar engineering materials

Acknowledgments

The results of this challenging work were not possible without the help of all the people who surrounded me during this period.

First, I would like to thank my supervisor Prof. Pedro Vilaça who gave me the opportunity to explore the wonderful world of the scientific research and encouraged me even in the worst periods when everything seemed to go in a bad way.

A big thank you to my advisor Prabilson Khadka who helped me in every single moment of this wonderful experience and reassured me in the most stressful periods.

Thanks to the colleagues who assisted me, Gonçalo, Antti, Hamidreza and Sofia.

Thanks to the technicians Seppo, Kim, Laura and Samuli who supported me during the testing and machining phase.

Finally, thank you to my family. Your support from distant Italy was fundamental to complete this work and to achieve the maturity deriving from it.

Francesco Pio Lionetti

Espoo, 31.07.2020

Contents

Symbols and acronyms

THEW	Through Hole Extrusion Welding
AA	Aluminum Association
PEEK	Polyether Ether Ketone
SS	Stainless Steel
CFRT	Carbon-Fiber-Reinforced Thermoplastics
GFRT	Glass-Fiber-Reinforced Thermoplastics
T_g	Glass Temperature
T_m	Melting Temperature
ICJ	Injection Clinching Joinining
E-ICJ	Electrical-Heating ICJ
F-ICJ	Friction-Based ICJ
PTFE	Polytetrafluoroethylene
Ag/PPy	Silver/Polypyrrole
GTAW	Gas Tungsten Arc Welding
SMAW	Shielded Metal Arc Welding
GMAW	Gas Metal Arc Welding
VOC	Volatile Organic Compound
LAMP	Laser-Assisted Metal and Plastic
YAG	Yttrium-Aluminum-Garnet
PA	Polyamide
PC	Polycarbonate
PET	Polyethylene Terephthalate
FSpJ	Friction Spot Joining
FLW	Friction Lap Welding
FSW	Friction Stir Welding
PMH	Polymer-Metal Hybrid
NDT	Non-Destructive Testing
PLC	Programmable Logic Controller
Q&T	Quenched And Tempered
AISI	American Iron And Steel Institute
CNC	Computer Numerical Control
EDS	Energy Dispersive X-ray Spectrometry

List of figures

List of tables

Introduction

1.1 Scope of the thesis

The present thesis is an extension of the previous works made in Aalto University by Prabilson Khadka [1] and Gnana Sambandhan Meikandaan [2] about the technology of THEW (Through Hole Extrusion Welding) under the supervision of Professor Pedro Vilaça. THEW technology is a disruptive manufacturing technique to produce hybrid multilayer structures based on joining metal to polymer-based components.

In this work, the joining process is carried out for aluminium alloy plates (AA1050, AA5754-H111) and polymer plates (PEEK). Alternatively, to a stainless-steel extrusion die, Ti Gr 1 was proposed, for its low thermal conductivity.

In THEW process, the aluminium alloy is stirred and viscoplasticised by a non-consumable rotating tool. Afterward, the stirred viscoplasticised aluminium is pushed by the tool through the slot made on the thin extrusion plate, to flow in polymeric material. Here, there will be the formation of the typical hook joint where two bonding mechanisms are involved to achieve the final joint: mechanical interlocking and adhesion.

Since this work represents an extension of the previous works, an alternative joint shape is proposed instead of the hook joint of the earlier attempts. This is the so called "Crab Claw" joint.

For this reason, the scope of the thesis can be resumed to bring into feasibility the new version of THEW, with several improvements in the quality of the joint and of the surrounding conditions. This is done to demonstrate that this technology can be used as a serious alternative to the different existing methods to join dissimilar materials, ensuring a completely sealed joint. Since, this is a public version of the work, all the sensitive data were removed or blacked and the process parameters were replaced with letters. All the sensitive information that can be extracted from pictures were hidden.

In the section 1.2 the objectives of this work are listed.

1.2 Objectives of the thesis

As already stated in the previous section, the present work is intended as an extension of the previous works made in Aalto University about THEW process. For this reason, new objectives and improvements from the earlier works are proposed to obtain a better concept of joint between aluminium alloys and polymer-based materials.

The objectives are:

1. Evaluation of a new concept of the rigid extrusion die with an alternative material (Ti Gr 1) and reduction of its thickness from 1 mm to 0.6 mm.

2. Development and improvement of the conditions to implement the process in a new way ("Crab Claw" joint) such as design of a new concept of clamping system, new tools, material geometry and process parameters.

3. Development of single side THEW joint in different shapes:
   - Long linear (≈ 200 mm);
   - Non-linear: circular Ø200 mm and rectangular 200 mm × 200 mm.
   - Mechanical testing: tensile shear and cross tension.

4. Development of double side THEW joint:
   - Long linear (≈ 200 mm);
   - Non-linear: circular Ø200 mm and rectangular 200 mm × 200 mm.

5. Establishment of a best set of preliminary process parameters.

6. Microstructural and mechanical characterisation of the joints.

2 Literature review

In this chapter different available joining techniques for dissimilar materials are presented since they are considered the direct competitors of THEW technology.

2.1 Introduction

Nowadays, the most important and urgent challenge of the main dominating companies in the industrial scene is to reduce the environmental impact due to the use of some materials in structural and automotive application.

For this reason, there is a continuous demand for lightweight design in every industrial sector, but especially in automotive and aerospace fields. Many times, this can be achieved with the exploitation of new lightweight alloys like Al, Mg and Ti, as well as of advanced polymer-based composite materials, such as carbon-fiber-reinforced thermoplastics (CFRT) and glass-fiber-reinforced thermoplastics (GFRT) [3].

Sometimes, the mechanical features of lightweight alloys and polymer materials allow the use on their own. However, they are not always able to fulfill the requirements for a certain product design. For this purpose, the idea to join them, in order to leverage their best properties together, is taking hold in the industrial field. In fact, industrial communities have started to develop combinations of different classes of lightweight materials, like fiber-reinforced thermoplastics and aluminum alloys, giving birth to the so called multi-materials structures [4].

The main aim of this recently developed class of materials is to reduce the weight and costs of the final product, and to enhance their coupled properties [5].

There are big dares when materials which have different mechanical, chemical, thermal and electrical properties must be joined. In fact, the incompatibility of them can lead to problems related to the joining process, but also to the structural performance of the joint [6].

Different joining techniques are already state of the art to join the various dissimilar materials and new promising joining methods are popping up especially in the automotive field [7].

For this reason, in the next section several methods to join dissimilar materials are introduced. Moreover, the advantages and disadvantages of the different techniques are clarified to understand which method is more suitable depending on the different set of materials and applications.

2.2 Dissimilar materials joining processes

Joining includes several processes whose objective is to assemble individual parts into a larger and more complex one. In addition, joints make possible to transfer or distribute the loads due to the service of the assembly from one component of it to the other one. Joints can be temporary or permanent [8].

The most important joining methods for dissimilar materials are mechanical joining processes, chemical joining processes (adhesive bonding), thermal fusion joining processes, solid state welding processes and hybrid joining processes [6].

In the next subsections, all these macro-categories will be discussed and some variants of them will be introduced and described.

2.2.1 Mechanical joining processes

In this case the joint formation is obtained through a mechanical way using strictly mechanical forces to create a physical interference or interlocking through fasteners [9]. There are two major subgroups in mechanical joining processes: mechanical fastening and integral mechanical attachment [10]. They work in the same way, because both avail of physical interference and interlocking to have a unique part. The only difference is related to the means to reach it.

Mechanical fastening

In mechanical fastening further members, called fasteners, like screws and rivets are used to obtain the joint. In this case, some good rules should be followed to obtain a tight joint. For example, in some kinds of fastening, rivets are subjected to a proper heating cycle before the fastening, in order to have a compact clamp after the cooling [11].

The fasteners are used to have a macroscopic interlocking between the elements to be joined. In fact, the fasteners are in contact with each element of the joint in order to transfer the load from one to the other both in shear, tension and compression [12].

They can be classified depending on the service load which are subjected. Tension fasteners are designed to carry tensile load (pan head, truss head, hex head, socket screws, blind rivets, grooved pins, etc.), compression fasteners are designed to carry compression load (set screws and washers), shear fasteners are designed to carry loads perpendicular to their axis (dowel pins and roll pins) [13]. They can be permanent or nonpermanent [14].

Another way to differentiate fasteners is in threaded and unthreaded fasteners. The first category is preferred when disassembly is required because the unscrewing does not cause the break of the components. Moreover, threaded fasteners are designed primarily to develop clamping forces or preload using threads, while unthreaded fasteners are designed primarily to resist shear through bearing with a pinning action [12].

Hex Bolts
Bolts with a hexagonal head with threads for use with a nut or tapped hole. Abbreviated HHMB or HXBT.

Carriage Bolt
Bolts with a smooth rounded head that has a small square section underneath.

Eye Bolts
A bolt with a circular ring on the head end. Used for attaching a rope or chain.

J-Bolt
J shaped bolts are used for tie-downs or as an open eye bolt.

U-Bolt
Bolts in U shape for attaching to pipe or other round surfaces. Also available with a square bend.

Elevator Bolt
Elevator bolts are often used in conveyor systems. They have a large, flat head.

Wood Screws
Screws with a smooth shank and tapered point for use in wood. Abbreviated WS

Machine Screws
Screws with threads for use with a nut or tapped hole. Abbreviated MS

Thread Cutting Machine Screws
Machine screws with a thread cutting (self tapping) point.

Sheet Metal Screws
Fully threaded screws with a point for use in sheet metal. Abbreviated SMS

Self Drilling SMS
A sheet metal screw with a self drilling point.

Socket Screws
Socket screws, also known as Allen Head, are fastened with a hex Allen wrench.

Eye Lag
Similar to an eye bolt but with wood threads instead of machine thread.

Lag Screw
Screw with a wood thread and pointed tip. Abbreviated Lag.

Figure 1: Different types of threaded fasteners

Figure 2: An example of unthreaded fastener (rivet)

Integral mechanical attachment

Integral mechanical attachment is obtained through geometric features present on the parts to be joined. In this case the mechanical fasteners are replaced by the geometric features which allow the joining of the components. One of the most widespread method of integral mechanical attachment between dissimilar materials is staking. This is a mechanical attachment where the plastic deformation of one of the joining parts is exploited to form the joint.
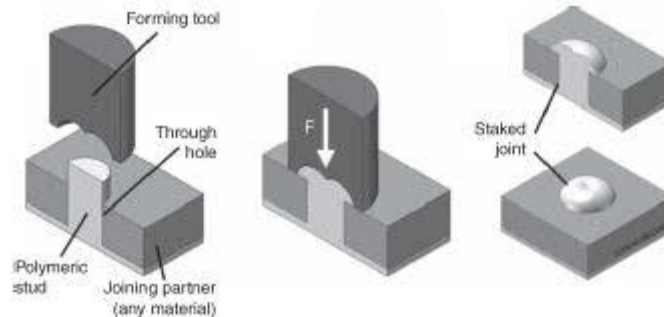
Figure 3: Example of staking [3]

In figure 3 there is an example of the traditional staking process. A thermoplastic workpiece with a protruding stud fits in a through-hole made on the second workpiece. A forming tool shapes the stud into a stake, which entraps the parts together [3].

It is possible to distinguish two kinds of staking processes based on the energy used to deform the stud into a stake: cold staking and hot staking. In cold staking processes there is no melting of the polymer and the service temperature is below the glass temperature (T_g) for the amorphous polymers and crystalline melting temperature (T_m) for semi crystalline polymers. In this case only the mechanical energy is used to form the joint. On the other hand, in hot staking there is the softening or the melting of the polymer above its T_g or T_m in order to soften or melt the polymer, facilitating the deformation [3]. For this reason, hot staking is usually preferred. In fact, some limitations in cold staking are the recovery effect in the polymer, which leads to a partial/total loss of the designed shape reducing the clamping effect of the joint. Other advantages of the hot staking over the cold staking are lower forces exerted both on the forming tool and polymer and more precise tolerances due to the softening of the material. In contrast, an extra heating should be avoided because it could lead to the degradation of the polymer and higher cooling times. Examples of hot staking processes are thermal staking, infrared and laser staking, hot air cold staking and ultrasonic staking.

Traditional staking methods are applied for dissimilar materials, but they are limited to low-strength thermoplastics and blends. The challenges of advanced polymer-metal joining create further interest for new advanced staking processes [15].

Injection Clinching Joinining (ICJ) is a staking-based method developed for polymer-metal structures. The technique was developed and patented by the Research Center Helmholtz Zentrum Geesthacht (HZG), in Germany in 2010 [16]. In this technology the softened/melted polymer is injected in the cavities made internally in the through-hole metal workpiece. There are two variants of ICJ: Electrical-Heating ICJ (E-ICJ) which uses

electricity to produce heat to soften/melt the polymer and Friction-Based ICJ (F-ICJ) that exploits the frictional heating obtained through the contact between the tool and the polymeric stud. A cross section of a joint obtained through ICJ is represented in Figure 4. While in Figure 5 there is a representation of the F-ICJ process using different tools.

Figure 4:Cross section of a joint using cavities in the metallic partner [3]
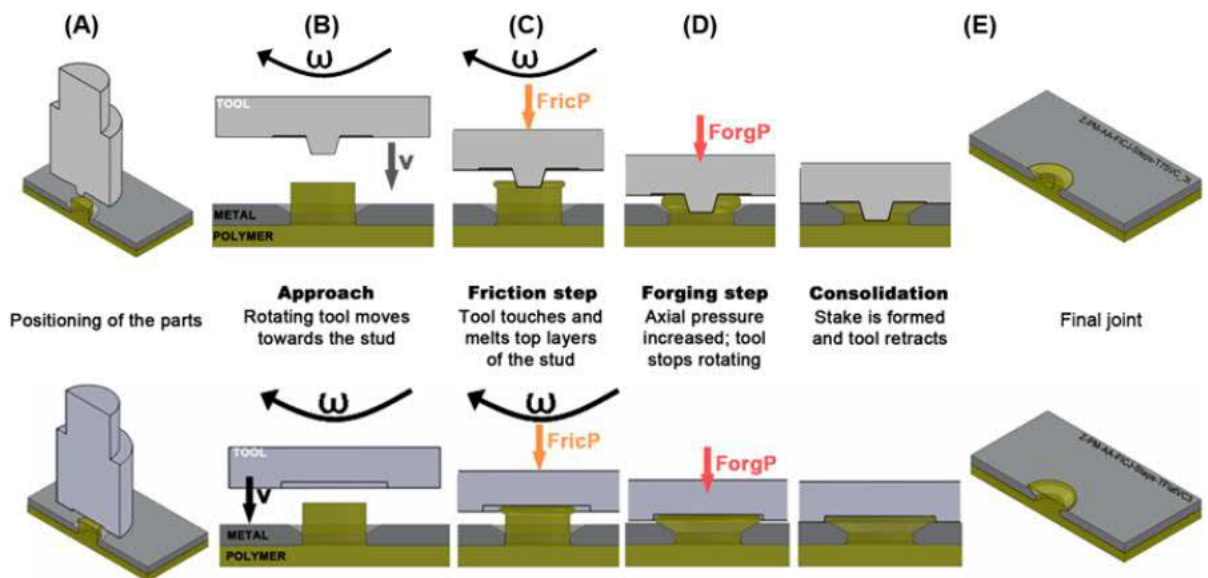
Figure 5: F-ICJ steps using flat tool and conical-pin tool [17]

Ultrasonic upsetting is an innovative ultrasonic-based staking process. It was developed by Brückner *et al.* [18]. In this process the polymer stud has a tubular shape until the middle of its height. The sonotrode hits and deforms the material at this height with an ultrasonic frequency leading to a selective deformation. At the same time, the shoulder presses on the top part of the stud supporting the deformation for a restricted volume. The deformation zone allows the joining of the two components.

The process is represented in Figure 6.
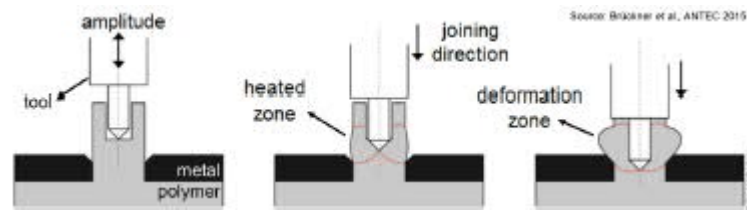
Figure 6: Ultrasonic upsetting phases [19]

Gude *et al.* [20] developed a new approach to join continuous fiber-reinforced thermoplastics and metallic components. In fact, thermoplastic composites have very small deformation range. For this reason, all the known joining techniques which exploit the forming of the fiber-reinforced thermoplastics can be partially used. The new process is called "thermoclinching".

The different steps of the process are represented in Figure 7.
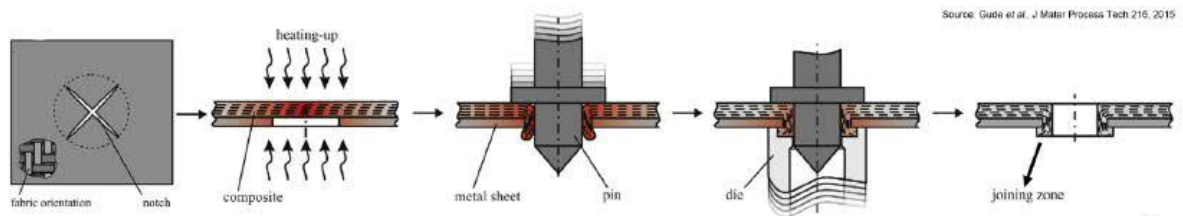
Figure 7: Schematic illustration of the thermoclinching joining process [20]

First, a pre-cut notch is made on the polymer surface to improve the local deformation of the polymer. The two parts are aligned in the mold to start the heating process that helps the plastic deformation capability of the thermoplastic polymer. After that, the tapered pin is shifted through the pre-machined metal sheet and the fiber-reinforced polymer is pressed outside the hole made in the metal sheet. Subsequently, when the polymer is still hot, it is pressed through the ring-shaped die to obtain the typical form-locked joint. After the cooling, the die is removed [20].

Other detailed information and methods to join dissimilar materials through mechanical processes can be found in [3].

Advantages and limitations of mechanical joining processes

In the previous subsections the state of the art about the different ways to join dissimilar materials through mechanical interactions have been discussed very extensively.

In this subsection, the advantages and limitations related to these processes are presented.

First, mechanical joining does not depend on the materials to be joined. In fact, no bonds are needed to accomplish the joining. For this reason, dissimilar materials can be joined too and in some cases the disassembly is obtained without damages in the workpieces. This leads to the possibility of a replacement of the single pieces in case of damages. Moreover, there are not any modifications to the chemical composition or microstructures of the two parts. Another advantage is that any special-purpose preparation of the pieces is not required, because impurities or external agents are not involved in the process of joining. Sometimes, a certain degree of movement is allowed depending on the different ways exploited to obtain the mechanical joining of the structures.

The big deal with mechanical joining is the stress concentration at the point of fastening or attachment. For instance, in the process of riveting the preparation of holes is required. Mohammadi *et al.* makes some studies about the effect of the hole in a non-homogeneous plate showing that the presence of the hole changes the elastic field in the vicinity of the hole both in case of biaxial tension or pure shear loading [21]. The presence of the stress raisers plays a central role in the fatigue cracks initiation, because they usually initiate at stress concentration features [22]. To reduce the presence of the stress concentration near the hole a compressive residual stress can be created in this region to offset the tension stress (procedure of shot peening). Another disadvantage is that these systems allow the presence of moisture, water, and air on the interface between the fastener and the pieces if no sealants are used. This permits the fluid leakage and acceleration of corrosion in presence of oxygen or other active gas. Finally, sometimes accidental loosening can occur as a result of the service loads and vibrations.

2.2.2 Adhesive bonding

Adhesive bonding is a solid-state joining technique that relies on the formation of intermolecular forces between the workpieces and the polymeric adhesive itself for joint formation [11]. An adhesively bonded joint is formed by adherends, adhesive, primers and interphase regions as it is represented in Figure 8 [3].
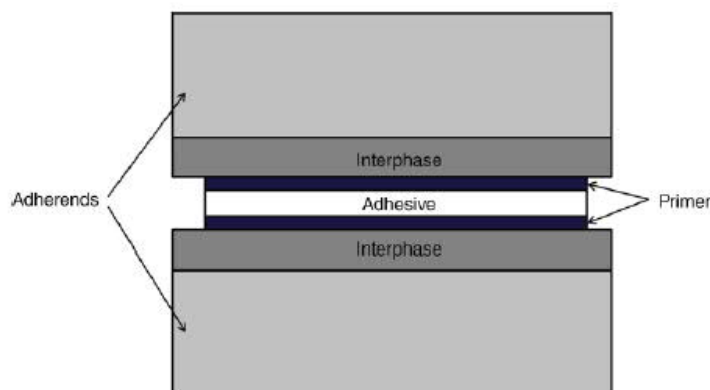
Figure 8: Components of an adhesively bonded joint [3]

The adherends represent the two bulk materials to be joined. The interphase is the region in contact with the adhesive. Usually, it is chemically or physically treated to obtain different features with respect to the adhesive and the bulk materials. In fact, depending on these features the adhesive joint could be more or less effective. The use of the primers can lead to the enhancement of the joint structural properties.

It is worth to distinguish the different types of adhesives. Structural adhesives are defined as adhesives that can resist substantial loads and that are responsible for the strength and stiffness of the structure [23]. In fact, they are used to transmit the loads between the two adherends in a uniform manner and through interfacial shear [24] [25]. From an engineering point of view structural adhesives are relevant because they are used for load-bearing components, in fact they are also called engineering adhesives. On the other hand, non-structural adhesives can be used for non-load bearing components. They are not able to transmit the load from one component to the other one and, consequently, they are not able to withstand loads.

The most important application for structural adhesives is aerospace field. In fact, it is used, as a direct competitor of riveting, to bond stringers to skins for both fuselage and wing to stiffen them against buckling [26]. Common structural adhesives are epoxies, cyanoacrylates, and some urethanes and acrylic adhesives.

In contrast, the main field of application for non-structural adhesives is in automotive industry to have sealing to prevent fluid leakage, thermal insulation and vibration damping [2].

Various theories about adhesion mechanisms can be found in literature, but in this section only the most important and widespread will be discussed.

First, to have adhesion, good wetting of the adhesive on the adherend is required. Liquids will wet only solid surfaces of higher surface energy than their own. For instance, there are not any common liquids able to wet PTFE and in fact there are not very good adhesives for it. In this case, some treatments (flaming, acid etching, ultraviolet radiation, etc.) can be used to increase the surface energy of low surface energy materials [27].

Mechanical interlocking

In mechanical interlocking the bonds depend on the roughness of the surface of the bulk material. The adhesive fills the asperities or pores on the surface that can be natural or created through different mechanisms (sandblasting, plasma treatment, wet etching, etc.) to gain the adhesion between the adhesive and adherend.

For instance, also impenetrable and uniform material as PTFE can be penetrated by silver/polypyrrole nanocomposite [28] [29].
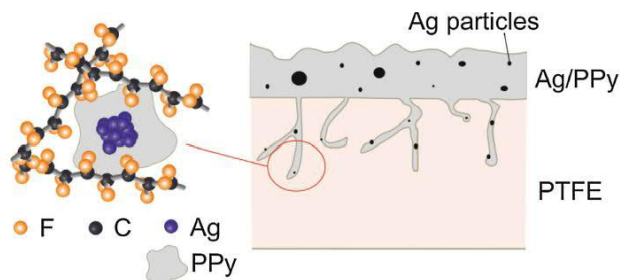
Figure 9: Schematic illustration about mechanical interlocking between Ag/PPy and PTFE [29]

Diffusion

The diffusion theory suggests that the atoms on the surface can mix leading to a kind of interlocking. In fact, when two materials show a certain degree of solubility, they form a solution at their interface. The atoms movement and mixing to form the solution is called diffusion. When it happens between a solid adhesive and an adherend it is slower, and it is called solid-state diffusion. On the other hand, when the adherend is in a liquid state, the diffusion mechanism is faster. Naturally, when the mechanism takes place between chemically similar adhesives and adherends, like when both are polymers, it is easier to happen and there is a stronger adhesion [30].

Contact   Healing/Diffusion   Bonded Material
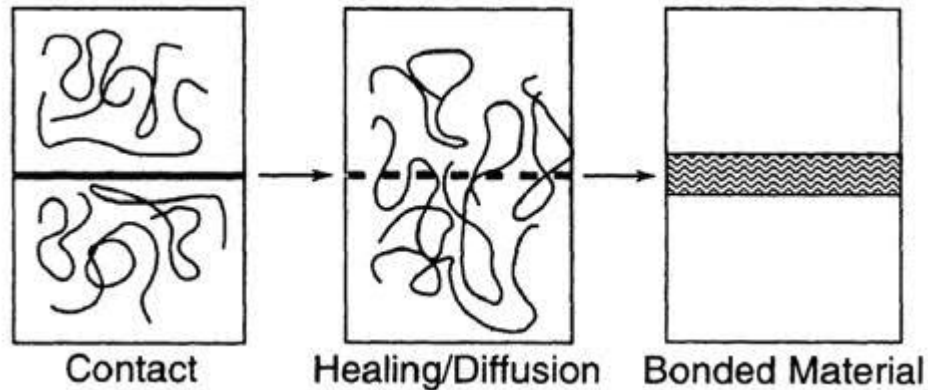
Figure 10: Different steps of diffusion process [29]

Adsorption

The adsorption theory suggests that, after that an intimate contact between the adhesive and the adherend has been reached through the wetting mechanism explained before, the permanent adhesive bond derives from the forces of chemical bonding. These chemical bonds can be either primary (ionic, covalent and metallic), but usually they are secondary (van der Waal's bonds or hydrogen bonds). The predominant type of bonding depends on the reciprocal chemical nature of the adherend and the adhesive [30].

Electrostatic theory

The electrostatic theory of adhesion ascribes the process of adhesion to the presence of forces of attraction on the interface between the adherend and the adhesive. These forces arise from a flow of charges due to the electronegativity difference between the two materials, which is a measure of the degree of attraction between a specific atom and an electron. The flow of charges leads to the reverse polarization of the two materials that attract to each other. In fact, most of the force of adhesion derives from dipole interactions [30].
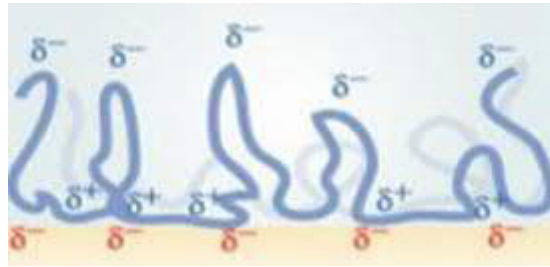
Figure 11: Schematic illustration of dipole interactions [31]

Advantages and limitations of adhesive bonding

As in the case of the discussed joining methods, in this chapter the advantages and disadvantages of adhesive bonding are discussed.
First, the adhesives have the role to transmit the stresses between the two adherends through a larger contact area than the other joining processes. This leads to a uniform distribution of the stress on the joint in case of the application of a load and to a consequent possibility to carry higher loads than the traditional joining processes [32]. Moreover, there is an improved joint stiffness due to the continuous bond area rather than point contact as in mechanical fastening, which avoids the presence of stress concentration points. This feature is very important also in terms of fatigue behavior. In fact, adhesive bonds have better fatigue resistance and damage tolerance [3]. Another advantage of adhesive bonding is that, together with mechanical joining, it is the only technique which avoids microstructural and large chemical alteration of the adherends. For this reason, all the dissimilar materials can be joined from a theoretical point view. A theory that strengthens this point is that the adhesive avoids the contact between the two adherends. In this way, galvanic corrosion between dissimilar materials is prevented better than mechanical fastening [3]. Additionally, adhesives are widely used in aerospace/aircraft industries, because they offer an excellent strength/ratio that allows to exploit them for lightweight designs [33].

In contrast, a big disadvantage of adhesive joints between polymers and metals is the relatively low resistance compared to metals. In fact, there is a limitation on the operating temperature, that is generally in the range 175-200 °C [32]. In addition, they are intrinsically very sensitive to the peel loads. For this reason, there is the need to consider this problem during the design phase [33]. Another disadvantage is that moisture and other contaminants negatively affect the adhesive joint performance, mainly when they are stressed. An adequate surface cleaning is required to avoid this negative feature.
Finally, even if the use of the adhesives is becoming increasingly wide in each structural sector, it is not yet possible to develop a reliable mathematical model about the

performance in terms of durability for adhesive joints. Nevertheless, some adhesive bonded can be reliably made based on empirical values obtained through experimental tests [3].

2.2.3 Thermal fusion joining processes

In this section the most important fusion welding processes are included. Welding is the process of joining two components through the creation of metallurgical bonds at their interface by combining atoms and molecules of the materials into intimate contact by heat, pressure, or both. When the heat causes the melting of the considered materials, the welding process is called fusion welding process [32].

The most widespread fusion welding technique is electric arc welding. Different specific electric arc techniques as gas tungsten arc welding (GTAW), shielded metal arc welding (SMAW) and gas metal arc welding (GMAW) have been used to weld only slightly dissimilar metals, such as carbon steel and stainless steel. In fact, the high energy inputs of the fusion welding processes can result in material metallurgical mismatch. This issue hinders their use to create dissimilar metal-to-metal joints as well as polymer-to-polymer and metal-to-polymer joints [11].

Welding of polymers to metals is a very hard process due to the quite different nature of the materials. Polymeric materials can be divided in thermoplastics, thermosets and elastomers as represented in figure 12.
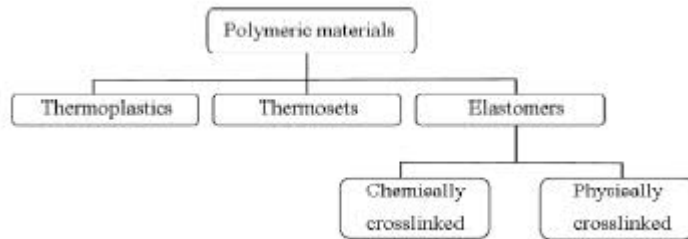
Figure 12: Polymeric materials classification [34]

They are characterised by structural macromolecules (monomers) that are held together by the Van der Waals force, while metals are organised in a densely packed crystal structure with high cohesive energy (usually two orders of magnitude higher than the one of the polymers). This means that the solubility of metal in polymers is very low, in fact metals tend to form round clusters (the most stable shape under "nonwetting" conditions [35]) instead of mixing when they are processed during the welding [36]. The temperature required to plasticise the metal to allow the mixing flow during the welding process are too high for the polymer which deteriorate before metal becomes softer or molten. Furthermore, among polymeric materials, only thermoplastics can be welded, while thermosets can be joined only by mechanical fastening and adhesive bonding [3]. Indeed, the heating process of thermosets leads to an irreversible crosslinking reaction resulting in degradation, which makes impossible to reshape them by means of heating [11] [37].

Despite these difficulties, an example of an emerging fusion welding technique to join dissimilar materials is explained in the next paragraph.

Laser welding

The joining of metals to thermoplastic has usually obtained through adhesive bonding and mechanical fasteners. Both these two last joining methods present problems. The main limitation for adhesives is related to the restriction of volatile organic compound (VOC) emission. While, mechanical joining is characterized by non-flexible design or low productivity. For this reason, Kawahito *et al.* have developed a new Laser-Assisted Metal and Plastic (LAMP) joining method [38]. Different laser sources can be used. The most widespread are yttrium aluminum garnet (YAG), fiber, disc laser and diode laser. The laser beam is focused though a proper optic system and depending on focal position, different power densities can be obtained. Moreover, a shielding gas is used as in metal laser welding.

The procedure consists of a laser beam that is irradiated in continuous or pulsed wave mode through the transparent thermoplastic sheet or directly on the metal plate to obtain the melting of the thermoplastic. Polymers with high values of laser transparency (more than 70%) can be directly subjected to the laser beam from the plastic side. While, the laser hit on the metal surface can be used either for transparent or non-transparent thermoplastics. The two plates are arranged in a lapped configuration. The high temperature leads to the formation of small bubbles in the molten thermoplastic near the interface due to the expansion of air and a partial decomposition of the polymer. The high pressure generated by the bubbles, forces the molten plastic compound to flow onto the metal surface. Here, the molten polymer starts to fill the pits or concave parts on the metal surface and interacts with the oxide film creating bonding.

The process leads to the production of strong joints due to the combination of different mechanisms: mechanical interlocking, Van der Waals forces (physical bonding) and chemical bonding [3][38].
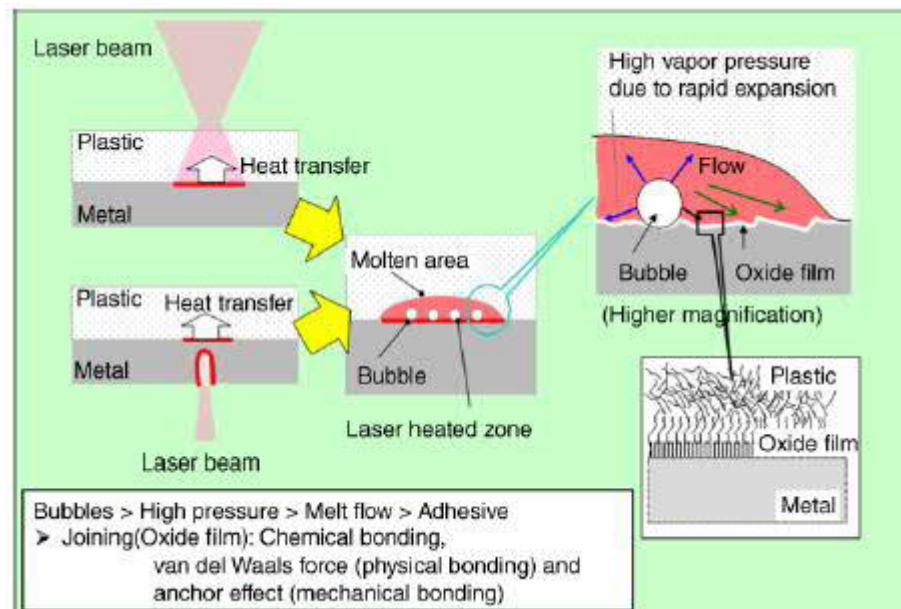
Figure 13: Mechanisms of LAMP joining process [3]

Kawahito *et al.* have demonstrated that LAMP can be applied successfully to obtain strong joints between type 304 stainless steel and different thermoplastics such as PA (polyamide), PC (polycarbonate) and PET (polyethylene terephthalate), reaching a maximum tensile shear strength of 3390 N for PA [38].

Advantages and limitations of laser welding

Laser welding was introduced to eliminate limitations present in other joining processes for dissimilar materials. Different advantages can be found in this advanced technology.

First, laser welding has very low environmental impact. Low or no VOC emissions are detectable for this technique, differently from adhesive bonding which is limited from this point of view. Another big advantage compared to adhesive bonding is that no surface cleaning or preparation is required in laser welding. This feature enables to have shorter processing time and higher productivity thanks also to the possibility to have automated process. In addition, since the joint is less sensitive to external factors like moisture, long term stability of the joint can be noticed. No further components are added to obtain the joints, differently from mechanical fastening. For this reason, no extra weight is added to the bulk components, keeping unaffected the initial purpose of joining dissimilar materials, namely, to obtain lightweight structures [2] [39]. Finally, different experiments, as mentioned in the previous paragraph, have demonstrated that high tensile shear strength of the joint can be obtained with a specific set of polymer-metal [38].

However, there are also drawbacks related to the nature of this process. It is suitable only for thermoplastic polymers and not for thermosets. This is closely related to the physical nature of thermosets that cannot be reshaped by heating once the irreversible crosslinking reaction takes place. The last important disadvantage of laser welding is that tight contact interface is required to avoid any presence of air gap during the joining, otherwise during the joining there will be release of oxygen and nitrogen from the air on the joint interface, which makes the joint less strong [3].

2.2.4 Solid state welding processes

Solid state welding processes include the welding processes which allow the joining at the faying surfaces of the parts, principally but not exclusively, through plastic deformation of the parent materials due to the application of pressure, at temperature lower than their melting point and without addition of a filler material. The energy sources for solid state welding processes are usually mechanical. They can be either directly the pressure applied or obtained through frictional forces, as occurs in most cases. The heat that is generated intrinsically in the process is fundamental to obtain plastic deformation at low stresses and without melting [32].

Different solid-state welding processes have been tested to obtain sound joints for dissimilar materials. For our purpose, two of these processes will be analysed in the following subsections. In particular, the attention is focused on friction-based processes. As in any chapter, a subsection will present the advantages and disadvantages of this kind of welding process.

Friction spot joining

Friction spot joining (FSpJ) is a solid-state joining technique for lightweight metals/polymer structures that was developed at Helmholtz Zentrum Geesthact by Sergio T. Amancio-Filho. The bonding mechanism for this technique applied to dissimilar materials is based on a competition between adhesive bonding and mechanical interlocking.

FSpJ uses a three-piece non-consumable tool system with a clamping ring, a sleeve and a pin as it is represented in Figure 14.

Figure 14: FSpJ tools with principal dimensions in millimetres and final assembly [40]

The components are assembled coaxially in such a way that they can rotate and move in and out independently of each other. The technique can be conducted through two variants: sleeve plunge and pin plunge. In the sleeve plunge variant, the two pieces are overlapped and clamped between a backing plate and the clamping ring with the metal on the top part over the polymer partner. Then, the sleeve and the pin start to rotate in the same direction and the sleeve moves towards the metal surface touching it and producing heat by friction. Meanwhile, the sleeve penetrates the metal, while the pin retracts, forming an annular space, known as reservoir. Due to the rotation and the plunging of the sleeve, the metal that is thermally plasticised is squeezed into the reservoir. After that, the sleeve retracts to the metal surface and the pin plunges to push back the entrapped plasticized metallic material, refilling the created keyhole. The plunge depth is set to have it only in the metallic part to avoid damage or degradation in the polymer. Moreover, the plasticised metal is also deformed by the pin plunging movement. This leads to the creation of a "nub" on the polymer surface which allows a kind of mechanical interlocking. Frictional heat created by the contact between the tool and the metallic part is transferred via conduction to the polymer, to create a melted thin layer of polymer which improves the joint strength with further adhesive bonding. Figure 15 gives a schematic representation of the process steps.
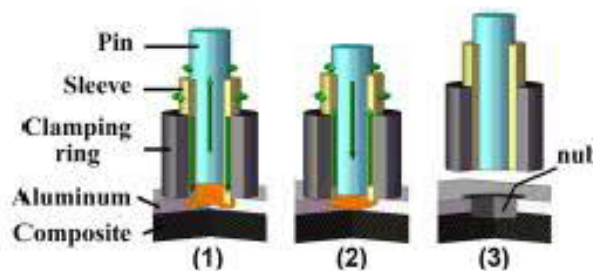
Figure 15: FSpJ steps; (1) the sleeve plunging plasticises the metal, (2) spot refilling, (3) nub formation and joint consolidation [40]

Pin plunge variant is equal for all the process steps except for the fact that the pin penetrates the metal piece while the sleeve is retracted. Different experiments were conducted using this technique. Gouseghir *et al.* analysed the feasibility of FSpJ between aluminium AA2024-T3 (bare and alclad) and carbon fiber reinforced poly(phenylene sulphide). From lap shear tensile testing and considering the nominal area of the sleeve (corresponding to an outer diameter of 9 mm) as the joint area, a maximum lap shear tensile strength of 27 MPa was achieved for bare aluminium samples and 43 MPa for alclad aluminium samples. These values are very promising from a mechanical point of view and further investigations are justified for them [41]. Another feasibility study was made by Amancio *et al.* creating FSpJ joints with good mechanical performance between the magnesium alloy AZ31 and two thermoplastic composites, glass fiber- and carbon fiber-reinforced poly(phenylene sulphide). Lap shear tensile testing revealed an average ultimate shear strength ranging from 20 to 28 MPa [42].

Friction lap welding

Friction lap welding (FLW) was developed by joining and welding research institute (JWRI), Osaka University. It is a new method to obtain hybrid joints between metal and plastic. A non-consumable rotation tool is pressed on the metal surface and moves along the overlap region. The purpose of the tool is to heat the material to be joined, but it also applies a pressure on the joint interface. The surface appearance of FLW joint is very similar to the one of friction stir welding (FSW) process. However, there is a fundamental difference in the tool. In FSW, a stirring probe is used to promote the flow of the viscoplasticised material around it, while in FLW there is no stirring probe. Therefore, in FLW the function of the tool is only to press and heat up the metal. Indeed, the friction due to the rotating tool shoulder and the metal leads to heat production. Then, the heat is transferred from the metal workpiece to the thermoplastic material via conduction and a narrow-melted region of the plastic material is achieved on the joint interface. The joining of the metal and the plastic is obtained when the plastic solidifies under the pressure imposed by the tool shoulder on the metal surface [43]. Several mechanisms have been proposed as the driving force for the joining. They include anchor effect, Van der Waals force, hydrogen bonding force and chemical bonding [44].
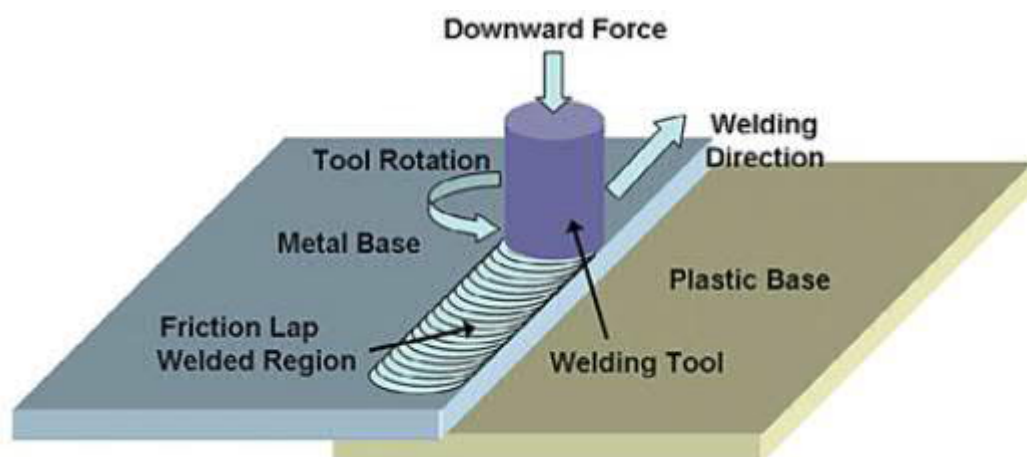
Figure 16: Illustration of the FLW process [45]

Nagatsuka *et al.* investigated the effect of surface treatments and joining speed on the joint properties for aluminum alloy A5052 and polyamide 6 with 20 wt% carbon fiber addition. The obtained results showed that the tensile shear strength increased as the joining speed increased from 100 to 1600 mm/min and decreased thereafter. Surface grinding of A5052 leads to an increase of the tensile shear strength of the joint too [43].

Advantages and disadvantages of friction-based solid-state welding processes

Solid state welding processes have several advantages compared to the common fusion welding and other joining techniques for dissimilar materials. First, the temperature reached during the process is much lower than the case of fusion welding. This leads to less perturbation to the microstructures of the materials involved in the joining and less effect on the mechanical properties. Problems related to the porosity are also avoided. In addition, since there is no fusion or there is just local fusion, the intermixing of the materials involved is minimal and this advantage allows the use of dissimilar materials. These processes do not involve the use of shielding gas and they are environmentally friendly, because no emissions are generated due to lower processing temperatures. Furthermore, since they are friction-based processes and the parent technology is FSW, the same technological equipment can be used leading to a gain in terms of flexibility and costs [32] [42] [45].

Disadvantages are related to the impossibility to do complex weld shape, or welded joints in difficult access places. The applied forces are higher than previous described processes, due to the contact between the rotating tools and the workpiece. This means that workpieces need to be properly clamped to prevent the relative movement of the workpieces. Moreover, only overlap joints can be produced for the two analysed processes and in many of the friction-based processes. Finally, there is also a limitation about the thickness of the samples, because a minimum thickness is required [3] [32].

2.2.5 Hybrid joining processes

Hybrid joining processes are also known as polymer-metal hybrid (PMH) technologies in which metals and polymers are integrated in singular component or subassembly. These processes are widespread in the automotive industry, because through the combination of different requirements of several adjacent parts into a singular component/subassembly is possible to obtain a customer-specific solution. Moreover, the integration of metals and polymers into a single component/subassembly leads to greater benefits than the simple joining of proximal parts. The advantages of PMH technologies will be discussed in the last subsection of this section. Different PMH technologies can be defined: injection over-molding technologies, metal over-molding technologies combined with secondary joining operations, PMH technologies involving adhesive bonding and direct-adhesion PMH technologies [3]. In the next paragraph the first category will be analysed in depth.

Injection over-molding

Injection over-molding is part of polymer metal hybrid (PMH) technologies in which metals and polymers are integrated in a singular component/sub-assembly. The process was introduced and patented by Bayer [46]. The process consists of different stages: 1) sheet-metal raw parts are stamped to obtain the desired shape (usually U-shape); 2) flared

through-holes are obtained by punching the metal inserts; 3) inserts are placed in the injection-molding die and 4) injection molding is used to over-mold the metal inserts with a cross-ribbed integrated structure made of 30% short glass-fiber-filled polyamide. In this technology, the tight interlocking between the metal and the short-fiber-filled polyamide cross-ribbed structure, and the achievement of a better stiffness and buckling resistance of the PMH component is obtained through: 1) formation of rivets from the molten polyamide which penetrates the holes of the metal insert; 2) over-molding of the U-shaped insert flanges [47]. A schematic model of a simplified injection overmolded load-bearing automotive component is given in figure 17.
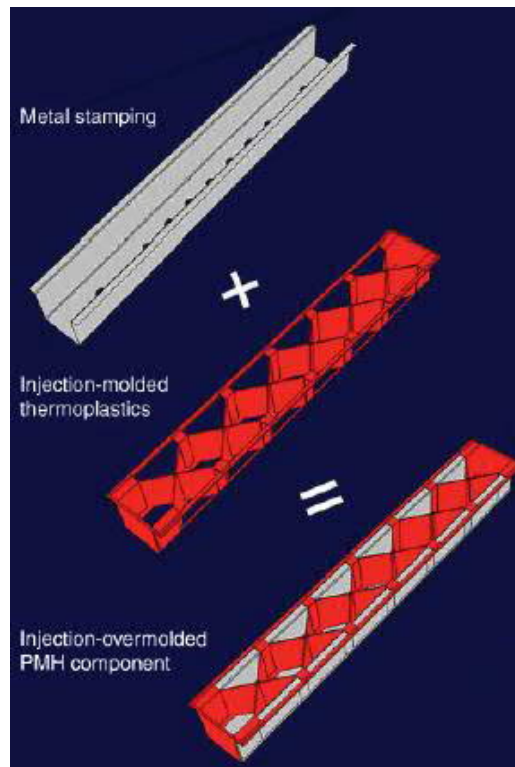
Figure 17: Exploded view of an injection overmolded component [47]

For what concerns the load-bearing capacity of these components, it is well known that the mechanical performance of a PMH component depends on the degree of load transfer through the polymer-metal interface, which it is directly controlled by the mechanism and strength of polymer to metal joining. For this reason, it is fundamental to understand the nature of the joining process.

In injection over-molding the load transfer between polymer and metal is based on the shrink-fit mechanism [47]. Shrink-fit is an interference fit obtained through a size change in the components that are assembled after the assembly. One common technique is to heat or cool one component before assembly and to bring it to the ambient temperature after the assembly. The joint is obtained through the thermal expansion. An example of shrink fit is the assembly of a railway axle with the wheels. The assembly is performed by heating the wheel in such a way that the diameter of the hole increases. After cooling, the wheel remains connected with the shaft because of the pressure created due to the diameter difference between the gear and the shaft. Indeed, the elastic deformation of shaft and hub determines a system of pressures that, through friction, enables the torque and force

transmission. Further strength is given to the joint through the formation of mechanical interlocks that are promoted by the presence of geometric features in the metal subcomponent.

Advantages and limitations of hybrid joining processes

Many technical and economic advantages can be found in PMH technologies, but some of them are the most important. First, since the components are prepared directly to be assembled, there is a reduction of the number of used components to make the final product [47].

Obviously, as in every polymer-metal hybrid structure, there is a weight reduction compared to the traditional all-metal solutions. This advantage is more related to most important purpose of hybrid structures, that is environmental impact reduction and cost saving in terms of fuel consumption for automotive industry [47].

The last important advantage is the increase in bending strength of the metal section. This is attributed to the polymer subcomponent because it forces the metal section to maintain its shape and cross-sectional properties during the application of an external load. Indeed, this feature delays also the buckling failure, typical of thin-wall structures like the stamped metal section. An example of it is given in figure 18 where it is demonstrated how a thin-wall sheet-metal component can immediately buckle under compressive load. However, the addition of the injection-molded thin-wall cross-ribbed plastic subcomponent increases the buckling resistance and the total stiffness of the assembled component [47].
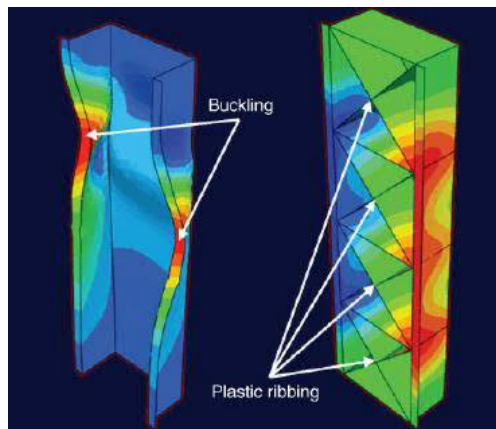
Figure 18: Improvement of the buckling resistance through the cross-ribbed plastic substructure [47]

3 Through Hole Extrusion Welding (THEW) process

3.1 Introduction

Through Hole Extrusion Welding Process is an experimental welding process developed at Aalto University by Pedro Vilaça *et al.* [1]. Two versions of it were developed. The first one is the spot variant, where the process is performed in a precise point on the aluminium ceiling. The experiments and mechanical testing made on the first trial suggest going for an improvement of the process. The improvement is represented by the second variant of the process, the slot variant, where the tool stirs the material and in the meanwhile it travels for a certain length. The experimental results from the mechanical testing reveal the achievement of an improved performance of the joint.

For this reason, in this work only the slot variant will be considered. In section 3.2 there is a description of the overall process developed before this work.

In section 3.3 the main benefits of this technology are shown together with the comparison to the other existing processes to join dissimilar lightweight materials.

Finally, in section 3.4 some potential application fields of this technology are pointed out.

3.2 Description of THEW slot variant

The process involves three layers of material. The structure can be considered as a sandwich structure, where the upper part consists of an aluminium plate, the middle part is a titanium or steel sheet metal with a slot on it, and, finally, the lower part is a polymer plate. The aluminium will be stirred and viscoplasticised by the non-consumable rotating tool and it will flow through the titanium (or steel) extrusion die to reach the polymer. The probe penetrates the aluminium and few millimetres in the polymer. Here, the formation of the hook joint is achieved and can be seen in the following figure obtained from the previous works.

Figure 19: Hook joint [2]

Obviously, the probe does not touch the extrusion die and the hook shape is reached through an offset from the centre of the slot in y-direction, while the travelling direction is the x-direction. The main mechanisms which allow the formation of the joint are adhesive bonding and mechanical interlocking.

The function of the extrusion sheet metal is double. Indeed, it behaves as a die to extrude the viscoplasticised aluminum in the polymer plate and it has also the function to protect the polymer from further degradation in case of too high temperatures. For this reason,

since the sheet metal is designed to be a thermal insulator, after different evaluations the best candidate seems to be Ti Gr 1. In the next chapters there will be also an optimisation of the design of the extrusion function of the sheet metal.

To summarise, the different phases of THEW in relation to the previous works are:

1) Machining of the base materials respecting the designed and predetermined dimensions;

2) Positioning of the polymer plate and consequent positioning of the die extrusion plate above it;

3) Identification of the starting position of the welding process and setting of the weld length in the FSW machine;

4) Positioning of the aluminum plate over the extrusion die;

5) Clamping of the system;

6) Z-axis position through a force control system;

7) Setting of the correct process parameters;

8) Implementation of the welding procedure.
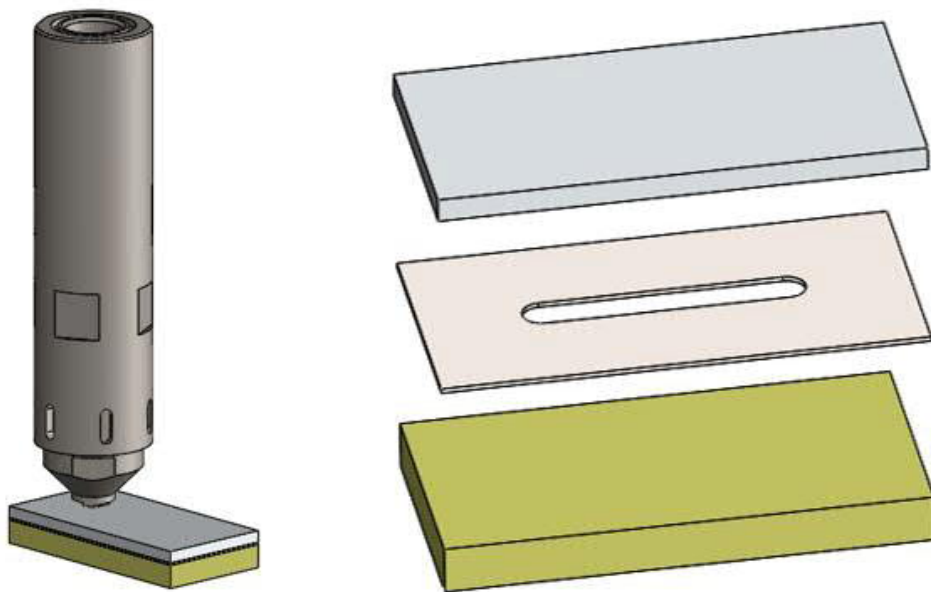
Figure 20: Base materials and process models

3.3 THEW benefits and comparison to other dissimilar materials joining techniques

As already said in the introduction of this work, THEW can be considered as a disruptive technology among the usual ones used to join lightweight and/or dissimilar materials. This is a key issue also from a market point of view since the use of lightweight materials is becoming increasingly required for environmental purposes. The main benefits related to the use of this joining technique can be listed:

1) The THEW joint offers multidirectional mechanical resistance constraints. The other provided solutions to join dissimilar materials provide only a limited mechanical resistance and for thin lightweight components. From the tests a simultaneous resistance to tensile shear and cross tension is highlighted, but torsion resistance is also present. THEW process can be also applied on thicker lightweight components that usually are exploited for structural purposes where a high load-bearing capacity is highly demanded. Some preliminary mechanical tests were made in the previous works on a joint of about 20 mm in length to have a very general overview of the strength offered by these joints. The results are resumed in the following table:

Table 1: Preliminary mechanical tests results [1]

Materials	Maximum Load [kN]	Type of test / Weld direction (in relation to Al-alloy)
AA5754-H111/PEEK	7.24	Tensile Shear/Transversal
	7.33	Tensile Shear/Longitudinal
	2.51	Cross Tension/Transversal
	3.57	Cross Tension/Longitudinal

Figure 21: Tests configurations [1]
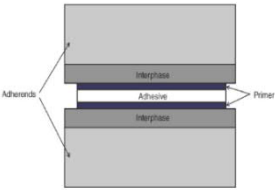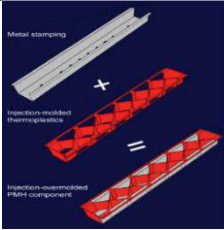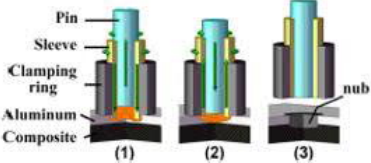
2) THEW can be applied to join dissimilar materials like lightweight metals and thermoplastic polymer-based components;

3) The process allows a very fast setup that leads to potential high productivity;

4) No requirement of pre- or post-processing operations as in mechanical fastening and adhesive bonding, since the welded components are already in a full load-bearing condition;

5) The same THEW tools and equipment can be used to make any kind of continuous joints with free path and characterised by air and liquid tightness;

6) The toughness and ductility of the joint, due to the hook mechanical constraint, ensures to avoid a catastrophic failure of the joint;

7) The process allows to weld lightweight dissimilar materials, that leads to a reduction of the CO_2 emissions, fuel consumption, weight and maintenance costs;

8) The use of THEW process can be fully automatised through a digitalised controlled operation without the need for operators, leading to many savings in different fields;

9) The process is high-energy efficiency and do not emit toxic fumes or radiation. For this reason, it is also environmental friendly process.
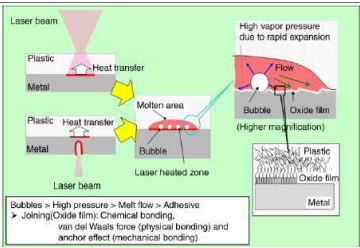
Due to the novelty of this disruptive joining method, some obstacles can be faced since many industries dealt for a long time with other existing methods to join dissimilar materials, such as, adhesive bonding and mechanical joining. So, they based their lightweight structural design on these two methods and the introduction of this technology will change industries habits. However, at the same time this technology represents a new design opportunity in this field.

Finally, after the introduction of the discussed alternative joining methods for dissimilar materials and the benefits and obstacles of THEW technology, it is good to summarise the

advantages and disadvantages of the competitive techniques in order to have a comprehensive view of these joining methods.

Table 2: THEW competitive joining techniques

Alternative joining methods		Advantages	Disadvantages
Name	**Illustration**		
Adhesive bonding		1) Continuous joint 2) High strength-to-weight ratio 3) Design flexibility 4) Used to join large surfaces 5) Does not change the microstructure of the involved materials 6) Prevents galvanic corrosion between dissimilar materials	1) Introduces internal stresses in the bond line 2) Poor temperature resistance and high environment sensitivity 3) Affected by moisture 4) Long curing times 5) Requires pre-processing 6) Difficult to be inspected by NDT
Mechanical joining		1) Does not change the microstructure of the materials, except for hot staking procedures 2) Allows relative motion 3) Threaded joints are reversible	1) Corrosion problems 2) Requires pre-processing 3) Increase in weight, except for integral mechanical attachment methods
Injection overmolding		1) Tight interlocking 2) Low weight and reduced overall costs	1) Higher setup and processing times 2) Expensive equipment
Friction spot joining		1) Short joining cycles 2) Weight saving 3) Environment friendly 4) Reparability	1) Voids occur in the joints 2) Limitations in joint design 3) Low torsion and peeling strength

		(ability to repair the same joint again) 5) Recyclable joints	4) Thickness limitations
Laser welding		1) High flexibility 2) Can be automatized 3) Reduces stress concentrations 4) Short processing times	1) Not applicable to thermoset based composites 2) Very high cost equipment

3.4 THEW applications

THEW process can be exploited for different markets where demanding requirements are of extreme importance and should be fulfilled. Indeed, this process can be applied to all the moving systems which are based on optimised design and materials with dissimilar physical behaviour like lightweight metal alloys and polymer-based components. Nowadays, this is a big engineering challenge and THEW can be an answer for this. This concept can be applied to different industry fields, such as:

1) Automotive: the environmental burden of the current power sources in the automotive sector is still too high. For this reason, electrical power can be an alternative. However, the drawback is the heavy weight of the batteries. To compensate the higher weight, lighter structural solutions can be implemented to increase the car's range;

2) Aeronautic: the continuous request in this field is to have lightweight structures, but still preserving the safe design. Indeed, this industry is seeking for more efficient joining methods;

3) Marine: due to the growing market demand, more efficient transport capacity and environmental friendly solutions are asked, including more lightweight structural solution with a consequent material selection that deals with light engineering materials;

4) Railways: in a world where time is a key issue for competitiveness, a fast and efficient transport of people and goods is of primary importance. For this purpose, lightweight materials solutions should be involved especially in railroad cars design;

5) Defence: the requirement of structures with high strength-to-weight ratio is important to achieve also the objective to move as fast as possible;

6) Wind energy production: the use of lightweight metals and polymer-based components in some of the fundamental moving parts, such as, very large blades, is a novel application where THEW can be exploited;

7) Fuel cell production: the stacking and assembly phase is usually based on mechanical fastening methods, which increase the volume and weight of them, and make harder the assembly phase. THEW can represent a challenge and an opportunity in the stacking phase, leading to a new concept of fuel cells.

4 Materials and Methods

4.1 Introduction

In this chapter there is the analysis of the base materials and the experimental methods and equipment used during the performed tests in the welding laboratory of Aalto University.

In section 4.2 there is the technical description of the welding machine used during the project.

In section 4.3, the testing equipment used during this work is briefly described.

In section 4.4 there is the characterisation of the base materials through the manufacturer datasheets. The chemical composition of them will be analysed and the mechanical properties will be reported.

In section 4.5 the exploited testing methods are presented.

4.2 Welding machine

The machine used for the previous welding experiments of THEW process is ESAB LEGIO FSW 5UT. This machine will be used even in the experiments related to this work, since the objective is to improve the process and to make it in larger dimensions. ESAB LEGIO is designed with a rigid framework for high performance during high-load conditions with a working range (welding head travel) from 1 to 5 meters. The system comprises heavy-duty bearings and the welding head travel is actuated using a ball-screw system.

The welding head is manipulated through a hydraulic actuator which allows the application of high loads minimizing the required space. The contact force is controlled through a PLC (Programmable Logic Controller), which provides a close-loop control system specific for this fundamental parameter.

The spindle is actuated by an AC motor that can provide the torque and the spindle rotation for each specific purpose application. Moreover, a liquid cooling system is used to minimize the wear on the spindle components and the tool.

Since a PLC is used as control system, the machine is characterised by a high operative precision to have high accuracy on the axis positioning and the welding speed. The Z-axis can work either on position control or force control mode. The graphical user interface is designed to regulate the process parameters, the welding path and all the other parameters linked to the machine. In addition, it is even possible to monitor the process in real time to adjust the process parameters in case of necessity and to manage the alarm system.

The machine presents even an anvil with a cooling system and a series of grooves and holes exploited for the clamping system of the piece to be machined [48].

Figure 22: ESAB LEGIO FSW 5 UT available in Aalto University Welding Laboratory

Finally, the specifications of the FSW machine are available online, but the most important of them are included in this work [48]:

Table 3: Specifications of ESAB LEGIO FSW 5 UT [48]

Feature	Specification
Maximum torque $[Nm]$	200
Maximum rotational speed $[rpm]$	3000
Maximum forging force $[kN]$	100
Maximum welding travel speed $[m/min]$	4
Work envelope dimensions (XX, YY, ZZ) $[mm]$	2000*400*300
Welding control (only on Z-axis)	- Force - Position - Speed
Welding angle [°]	0-5
Monitoring parameters	- Spindle speed and torque - Position, speed and force in all the axes

4.3 Testing machines

4.3.1 Mechanical testing equipment

For each structural application and so for welded joints, there is the necessity to conduct mechanical testing to classify the structural reliability and the strength of the joint. For this purpose, MTS Landmark 810 material testing system has been exploited to obtain high performance mechanical tests for the produced joints: tensile shear test and cross tension test. Moreover, also base materials were tested through a simple tensile test. The machine is directly available in the engineering materials laboratory in Aalto University. The properties of this machine are briefly discussed in this section, but they can be found on the producer website.

MTS Landmark 810 can be used for different mechanical tests for both low and high force static and dynamic testing. Indeed, through the wide range of force capacities, servovalve flow ratings, pump capacities, software, and accessories, the machine can be configured to meet the specific material requirements for the testing.

The machine is composed by a floor mounted frame that has very high axial and lateral stiffness to improve the test accuracy and the overall performance of the system. Moreover, on the base of the frame there are isolator pads which behave as dampers from external vibrations. A crosshead, provided with a load cell and characterised by high

stiffness for precise displacement measurement and increased dynamic performance, can slide on the frame columns which allow to maintain load unit alignment over their whole length. This can be obtained through the hydraulic lifts which regulate the crosshead movement. The force transducers present an accurate strain gage design for both static and dynamic test and with a variety of force ratings that can be chosen to meet the specific requirements. A wide system of grips and fixtures can be used to clamp the sample to be tested. A hydraulic actuator is integrally mounted in the base plate to have a better side load capability and more accurate test results. Finally, an actuator manifold is available to mount close coupled accumulators which damp the pressure fluctuations from the hydraulic actuators to furtherly improve the test control and data accuracy [49]. The most important testing machine features can be collected in the table below.

Table 4: MTS Landmark 810 main properties [49]

Force range [*kN*]	25-500
Available performance	Very high
Testable materials	- Plastics - Elastomers - Aluminum - Composites - Steel - Super alloys
Specimen size	- Subsized - Standard - Medium - Large
Test type	- Tension/compression - Fatigue - Creep - Fatigue crack growth - Fracture toughness
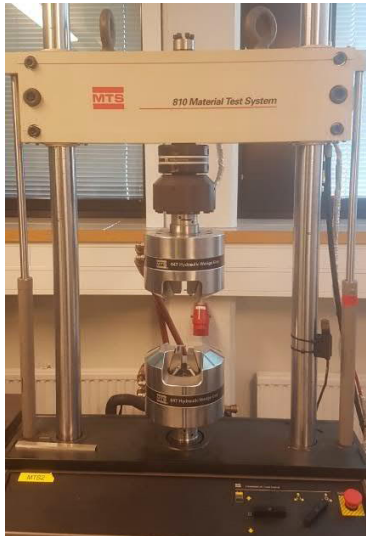
Figure 23: MTS Landmark 810

For the same purpose it was also used a very similar testing machine Zwick Roell Z020 according to the availability in Aalto University Testing Laboratory. The only difference with respect to MTS Landmark 810 is the maximum test load in tensile direction that was 20 kN. The other properties are very similar and for this reason they are not reported in this work, but they are available on [50].

Figure 24: Zwick Roell Z020 testing machine

4.3.2 Optical microscope

For micro-/macrostructural characterisation NIKON Epiphot 200 was used and it is an optical microscope available in material testing laboratory of Aalto University. It is an inverted microscope used for the metallographic analysis. It has an outstanding optical system with CF Optics combined with Infinity Corrected design for greater system flexibility with sharp and clear images. Moreover, since the reticle is inserted at the primary image plane position, the micrometer remains focused without any kind of influence from the state of the analysed sample surface. The design is operator-friendly since there are a lowered stage and controls located within easy reach which facilitates all the operations. In addition, all the imaging modes can be exploited with this microscope: brightfield observation, darkfield observation, Nomarski DIC observation, simple polarization observation and epi-fluorescence observation. The system available in Aalto University presents six objectives with different levels of magnification 2.5x, 5x, 10x, 20x, 50x and 100x. Finally, the images can be recorded through the software NIS-Elements F2.30. Other detailed technical information are available on [51].

Figure 25: Equipment used for microscopic characterisation

4.3.3 Hardness testing machine

The hardness testing machine used in this work was Gnehm Brickers 220. The machine can be used to measure Vickers or Brinell hardness. The system presents a platform where the sample can be positioned in the right position through the help of a light indicator. The platform can be raised to reach the clamping system of the piece. The mark left from the indenter can be analysed through an optical system that allows to collect the dimension of the diagonals.

More detailed technical information are available on [52].

Figure 26: Gnehm Brickers 220 hardness testing machine

4.4 Materials

4.4.1 AA1050

Aluminium alloys are the most widely utilised metal structural materials after iron and steel. They have the potential for application and development in many fields such as aviation, aerospace, automobile, naval, weapons and power electronics. The most important properties of them are low density, high specific strength, easy processing, good corrosion resistance and excellent thermal and electrical conductivity [53].

Aluminium alloys can be divided in two main categories: wrought alloys and casting alloys.

The first category includes all the alloys that usually are subjected to solid state processes (e.g. plastic deformation) in order to produce semiproducts. They can be also differentiated in thermal treated and workhardened (when plastic deformation is used to increase strength) [54].

Casting alloys are used for foundry. Also in this case they can be divided into the ones which can be thermally treated and the ones that can be used as cast which means immediately after solidification [54].
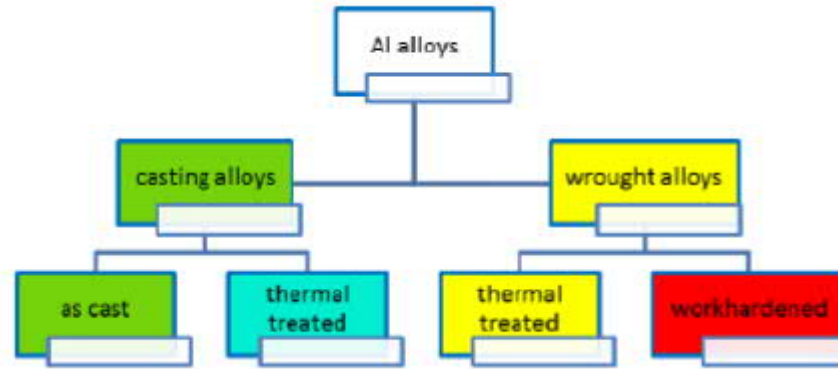
Figure 27: Classification of Al-alloys [54]

AA1050 is a wrought aluminium alloy which belongs to 1000 series. According to the Aluminum Association the first digit represents the main alloying element. 1xxx means that there are not alloying elements and it is called commercially pure aluminium (minimum of 99% of Al in weight). The second digit shows possible alloy modification from the original composition represented by the digit 0. Third and fourth digits do not have any significance, but they are unique to identify a particular alloy. However, for 1000 series the third and fourth digits show the degree of purity (e.g. 1050 implies 99.5% Al).

For our purpose it has been chosen for its excellent both thermal and electrical conductivity and high corrosion resistance. In fact, aluminium is very reactive to the oxygen and so it produces a spontaneous thin layer oxide, called alumina, which passivates the inner part from further corrosion. On the other hand, it has very low mechanical strength, due to low number of solute atoms and precipitated particles which represent barriers against the mobility of the dislocations. However, the strength can be improved by mechanisms of plastic deformation [55]. This kind of alloy is mostly used industrially in chemical process plant equipment and heat sinks, since it has a higher thermal conductivity than other alloys. The material provided by the supplier was in a form of 5 mm thick sheets. The chemical composition of the material is reported in Table 5, while the mechanical, thermal, physical and electrical properties are reported in Table 6:

Table 5: AA1050 chemical composition [56]

Composition	Al	Cu	Fe	Mn	Si	Ti	Mg	Zn
%	99.5-100	0.05	0-0.4	0.01	0.25	0-0.05	0.05	0-0.07

Table 6: AA1050 properties [56][57]

Properties	Values range
Temper	H14/H24
Density $\left[\frac{kg}{m^3}\right]$	$2680 - 2740$
Young's modulus $[GPa]$	$69 - 72$
Proof stress $[MPa]$	$75 - 85$
Tensile strength $[MPa]$	$105 - 145$
Elongation $[\% \, strain]$	8
Compressive strength $[MPa]$	75-85
Hardness-Vickers $[HV]$	33
Melting point $[°C]$	$645 - 658$
Thermal conductivity $\left[\frac{W}{m \cdot °C}\right]$	$224 - 234$
Electrical conductivity $[\%IACS]$	$57.5 - 61.6$
Thermal expansion coefficient $\left[\frac{\mu strain}{°C}\right]$	$22.9 - 24.1$
Specific heat capacity $\left[\frac{J}{kg \, °C}\right]$	893-903

4.4.2 Ti Gr 1

Titanium alloys are characterised by a very high tensile strength to density ratio, high corrosion resistance and ability to withstand moderately high temperatures without creeping. For this reason, they are used in aircraft, spacecraft, naval ships, and missiles. Moreover, since in automotive applications, particularly in motorcycle and automobile racing, a weight reduction is fundamental without losing high strength and rigidity, titanium alloys are designated as the best candidates for these applications. Titanium is also known for its low thermal conductivity which makes it very difficult to be machined with conventional tools. Indeed, during the machining all the energy stays in the working zone and the friction is high, thus there will be overheating. A consequence of this is that the tool wears rapidly, and the material removed is at high temperature that leads to the burning of titanium chips [58][54].

Considering the stability of two phases, elements are split according to their ability to stabilise α (Al equivalent) or β (Mo equivalent) phases:

1. $Mo_{eq} = [Mo]+2.5[Fe]+1.7[Co]+1.7[Mn]+1.25[Cr]+1.25[Ni]+0.66[V]$;
2. $Al_{eq} = [Al]+10[O]+0.32[Sn]+0.16[Zr]$.

Based on the stability of different phases, titanium alloys can be divided in four groups:

1. α alloys: this group of alloys comprises commercially pure (CP) Ti and alloys with only α stabilising. They execute excellent corrosion resistance but with lower strength properties. They can be strengthened by solid solution and cold working. Chemical industry is the field where they are exploited more for their excellent creep and corrosion resistance (e.g. heat exchangers).

2. Near-α alloys: they present low fractions of β stabilisers (up to 2 wt.%) forming less than 10 vol.% of β phase. They are characterised by high creep resistance with good strength. For this reason, this group is used for high temperature applications (≈ 500-550 °C) in the aerospace field (e.g. compressors of turbine engines).

3. α+β alloys: the fraction of β stabilisers is of 4-6 wt.% leading to 5-40 vol.% fraction of β phase at room temperature. It is possible to obtain martensite transformation with high cooling rates from the β phase field to the room temperature. Depending on the different exploited thermal and thermomechanical treatments, several microstructures can be obtained leading to various mechanical properties. Ti6Al4V is the most widespread Ti alloy belonging to this category, because it is the most balanced property profile alloy.

4. Metastable β Ti alloys: they present higher content of β stabilisers (10-15 wt.%) leading to amounts higher than 50 vol.% of α phase in equilibrium. On the other hand, β phase is only in metastable state. They are characterised by high levels of strength with acceptable toughness, fatigue resistance and formability. They can be divided in high strength and heavily stabilised alloys, depending on the percentage of the α stabilisers.

5. Stable β alloys: this group contains significant proportions of β stabilisers (≈ 30 wt.%) and are formed only by β phase. They are characterised by high hardenability and high density, but usually they are not commercialised. [59][60]
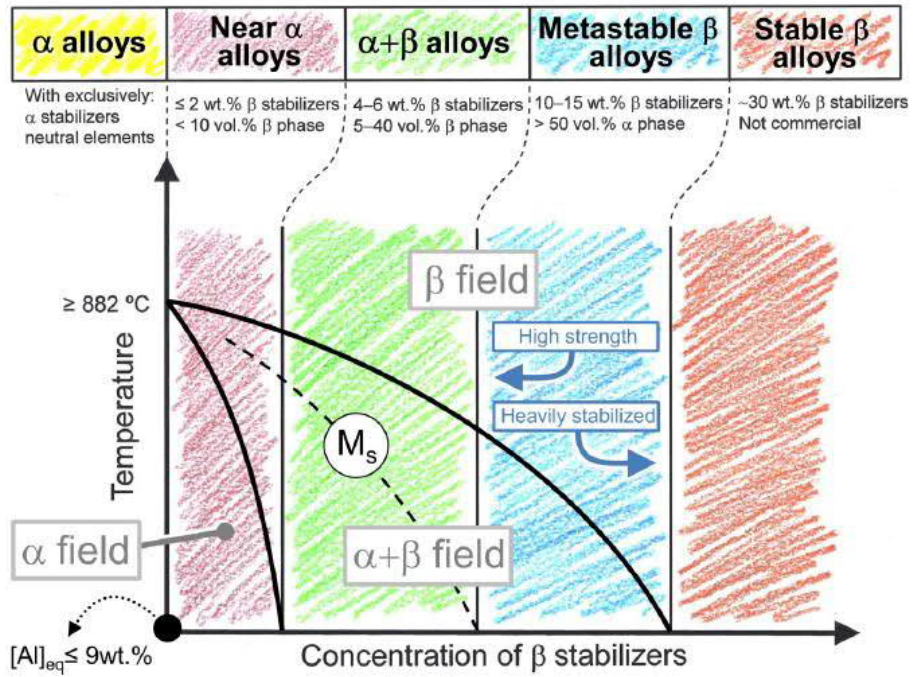
Figure 28: Ti alloys characterisation in β isomorphous phase diagram with martensite start line M$_s$
[59]

Ti Gr 1 belongs to the category of Ti-α alloys. This means that it has percentage of Al$_{eq}$ lower than 9% and it is the highest purity grade commercially available. In general, the mechanical properties of titanium are influenced by oxygen, nitrogen, hydrogen and iron. Indeed, they increase the material hardness, tensile strength and yield strength, but at the same time they reduce the elongation. Moreover, hydrogen activates embrittlement of the material and so its level should be kept very low. Since, as already highlighted Ti Gr 1 presents the lowest percentages of alloy elements, among the Ti alloys it is the one with the lowest strength, but it shows good ductility and toughness leading to high formability. In addition, it exhibits excellent corrosion resistance in highly oxidizing to mildly reducing environments, also including chlorides. Other important properties are its good impact toughness at low temperatures, the good weldability and machinability. Finally, it has also very good creep resistance. This is because the diffusion rate in HCP structures is very low, improving the creep resistance [61][62].

For our purposes, Ti Gr1 has been chosen since it has a low thermal conductivity. Thicknesses of 1 mm and 0.6 mm were used. The specifications of the material are presented in the next tables:

Table 7: Ti Gr 1 chemical composition [57]

Composition	Ti	Fe	O	C	H	N	Other
%	99.1-100	0-0.2	0-0.18	0-0.08	0-0.015	0-0.03	0-0.4

Properties	Values range
Density $\left[\frac{kg}{m^3}\right]$	$4510 - 4520$
Young's modulus $[GPa]$	$100 - 105$
Yield strength $[MPa]$	$172 - 240$
Tensile strength $[MPa]$	$240 - 360$
Elongation $[\% \ strain]$	20-25
Compressive strength $[MPa]$	130-170
Hardness-Vickers $[HV]$	115-125
Melting point $[°C]$	1670
Thermal conductivity $\left[\frac{W}{m·°C}\right]$	$16.3 - 18$
Electrical conductivity $[\%IACS]$	$3 - 3.13$
Thermal expansion coefficient $\left[\frac{\mu strain}{°C}\right]$	$8.5 - 9.3$
Specific heat capacity $\left[\frac{J}{kg \ °C}\right]$	539-541

4.4.3 Polyether ether ketone (PEEK)

Polyether ether ketone, better known as PEEK, is a semicrystalline thermoplastic material with outstanding mechanical and chemical properties retained also at high temperature. It is obtained through the aromatic nucleophilic substitution reaction of the potassium salt of hydroquinone and 4,4'-difluorobenzophenone [63].

Its chemical reaction is depicted in the picture below:

Figure 29: PEEK chemical reaction [64]

PEEK has been chosen for our experiments since it has high melt and glass transition temperature, high chemical resistance and it is melt processable. Indeed, since it is a thermoplastic material, when heated to high temperature, it softens and if we are closed to the melting temperature it melts. So thermoplastic materials, like PEEK, are characterised by reversibility in their transformations. They can be reheated, melted and changed in

terms of shape. This means that they can be reprocessed many times without degrading under the effect of heat. This feature makes them totally different from the thermosets that cannot be reprocessed through the heat. Indeed, in thermoplastic materials the polymeric chains are independent and there is no link between them, while in thermosets during the process of curing are irreversibly hardened through the use of the heat. The curing process will lead to a chemical reaction called crosslinking which allows the formation of strong chemical molecular bonds between molecules from different polymeric chains. Since, crosslinking is an irreversible process, thermosets cannot be remelted. For this reason, thermosets have a melting temperature higher than their degradation temperature [64].

The use of FSW technology will cause the production of heat that can lead to a thermal degradation in case of use of thermosets. Indeed, our choice is to operate with thermoplastics and in particular with PEEK.

Other reasons that lead to use PEEK for our specific purpose is that it presents high tensile strength compared to the other plastics, it is also resistant to attack by organic and aqueous environments and it is an excellent electrical and thermal insulator. The only drawback is that it is very expensive due to its production process. In our experiments plates with a thickness of 5 mm were used. Finally, the specific properties of the PEEK included in our experiments are collected from the manufacturer and they are provided with a thickness of 5 mm.

Table 9: PEEK properties [65]

Properties	Standard methods	Values range
Density [g/cm^3]	DIN EN ISO 1183-1	1.31
Melting temperature [$°C$]	ISO 11357-3	343
Thermal conductivity$\left[\frac{W}{m*K}\right]$	DIN 52612-1	0.25
Thermal capacity $\left[\frac{kJ}{kg*K}\right]$	DIN 52612	1.34
Glass transition temperature [$°C$]	ISO 3146	143
Service temperature [$°C$]	Average	-60-250
Dielectric strength [kV/mm]	IEC 60243	20
Yield stress [MPa]	DIN EN ISO 527	87-110
Elongation [%]	DIN EN ISO 527	20
Tensile modulus of elasticity [MPa]	DIN EN ISO 527	3760-4000

4.4.4 AA5754-H111

This alloy belongs to 5000 series of Al-alloy. To understand the composition and the properties of this Al-alloy, we need to refer to its designation. First, it belongs to wrought alloys that means that semi products are obtained through the exploit of plastic deformation processes. Moreover, 5000 series are Al-Mg alloys. For this reason, they are not heat treatable that leads to the impossibility to use precipitation hardening mechanism to give strength to the alloy. The mechanism of precipitation hardening is obtained through the process of artificial ageing. The process can be explained from the following picture considering a heat treatable Al-alloy e.g. Al-Cu alloy (2000 series).
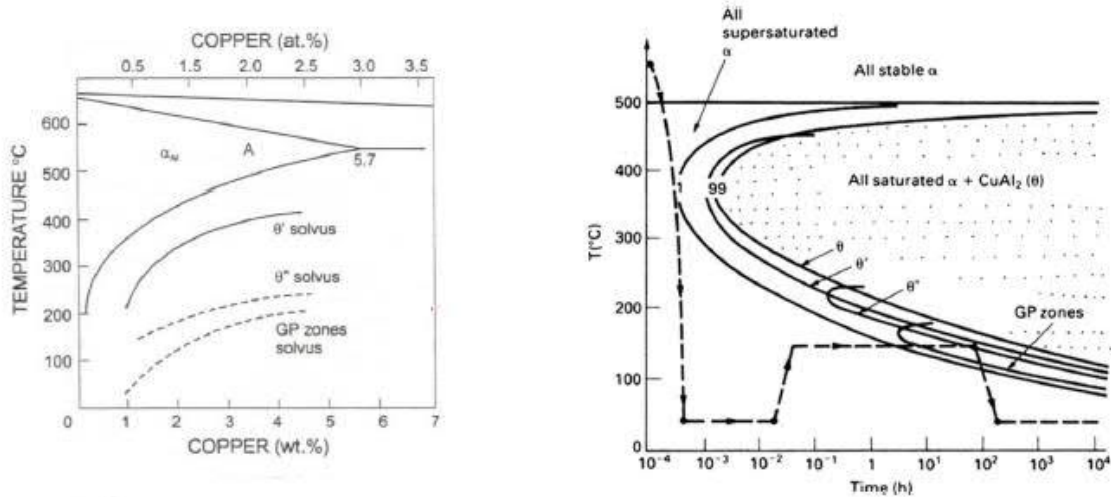
Figure 30: Artificial ageing in Al-Cu alloys [54]

First, there is the solution annealing of the alloy bringing it to the monophasic α region that is a solid solution of Al and Cu. The following quenching will lead to the formation of a supersaturated solid solution where the copper remains entrapped in the crystal lattice of the aluminum. Then, the process of artificial ageing consists to hold the alloy in a range of the temperature between 100 and 300 °C. This allows diffusion of the solute atoms with the formation of tiny uncoherent precipitates dispersed in the alloy matrix. The strengthening derives from the capacity of these precipitates to obstacle the dislocations movement during the plastic deformation and it has different stages leading to the formation of the precipitates. The first of these is the formation of GP zones which leads to the nucleation of densely dispersed small clusters involving few atom layers. However, the GP zones solvus temperature in 5000 series is too low and it is unusual to have this strengthening mechanism. Nevertheless, Mg is the best solid solution strengthener in Al-alloys. For this reason, these alloys are used after quenching in the state of a super saturated solid solution and they can also be strain hardened. Indeed, the temper designation H111 refers to the degree of strain hardening of the alloy. H1 means that they are only strain hardened without any additional thermal treatment to achieve the desired additional strengthening. The second digit can range from 0 to 8 and 8 has been assigned to tempers having a final degree of strain hardening equivalent to a corresponding reduction of area of 75%. So, 1 means that we have a reduction of area equal to an eighth of 75%. Finally, the third digit indicates a possible variation of the two-digit H temper and it is used to indicate that the degree of the hardening is close to the 2 digits of the temper. Thus,

H111 means that the strain hardening is less than the amount of the one indicated by H11 [50] [62] [63].

The main properties of this alloy are the good strength due to the concomitance of two strengthening mechanism (strain hardening and solid solution strengthening), good weldability and corrosion resistance in sea water. The only problem that can occurs can be due to the high Mg content (>3-4%) that leads to tendency for formation of the brittle β-phase (Mg_5Al_8) at grain boundaries. Moreover, β-phase makes the alloy prone to the risk of SCC. Additions of Cr and Mn can improve the situation from this point of view [66]. The properties and the chemical composition of the alloy are listed in the table below and they are obtained from the manufacturer. Plates with a thickness of 5 mm were used.

Table 10: AA5754 chemical composition [68]

Composition	Al	Cu	Fe	Mn	Si	Ti	Mg	Zn
%	94.2-97.4	0-0.1	0-0.4	0-0.5	0-0.4	0-0.15	2.6-3.6	0-0.2

Table 11: AA5754 properties [68]

Properties	Values range
Temper	H111
Density $\left[\frac{kg}{m^3}\right]$	$2650 - 2710$
Young's modulus $[GPa]$	70
Proof stress $[MPa]$	90
Tensile strength $[MPa]$	$190 - 240$
Elongation $[\% \, strain]$	18
Compressive strength $[MPa]$	190-240
Hardness-Brinell $[HB]$	65
Melting point $[°C]$	$595 - 645$
Thermal conductivity $\left[\frac{W}{m \cdot °C}\right]$	132
Electrical conductivity $[\%IACS]$	32.5
Thermal expansion coefficient $\left[\frac{\mu strain}{°C}\right]$	23.7
Specific heat capacity $\left[\frac{J}{kg \, °C}\right]$	879-915

4.5 Testing methods

As already stated in the previous paragraphs the welded joints need to be tested to understand if they can be used for structural purpose. From the literature the most suitable mechanical tests for this application are tensile shear test and cross tension test, that are better explained in the next sections. Moreover, also the base materials were tested to check if the experimental data matched the ones of the manufacturer datasheets. Tensile tests and Vickers hardness tests were made for the base materials selected as the best ones for the development of THEW process.

4.5.1 Tensile test

Tensile test consists in loading with a tensile force a specimen with dog-bone geometry bringing it to the fracture. The dog bone is used to ensure that the fracture will occur in the useful length of the sample since the geometry induces a stress concentration in this part. Indeed, when the fracture of the sample occurs in the midsection it is due to the material reaching the maximum tensile strength. On the other hand, if the fracture occurs very close to the grips or in the grips itself, the failure can be due to improper load or pre-existing defect in the material. Tensile test is done to determinate the typical mechanical properties of a material independently from the specimen dimensions. Indeed, the results available from the machine are load-displacement curve, but they are normalised according to the geometry of the sample to obtain the engineering stress-strain curve where the stress and strain can be defined as:

$$\sigma = \frac{F}{A_0} \quad (1)$$

$$\epsilon = \frac{l - l_0}{l_0} = \frac{\Delta l}{l_0} \quad (2)$$

Where F is the load applied to the sample, A_0 is the initial cross-sectional area of the specimen, l is the instantaneous gauge length and l_0 is the original gauge length.
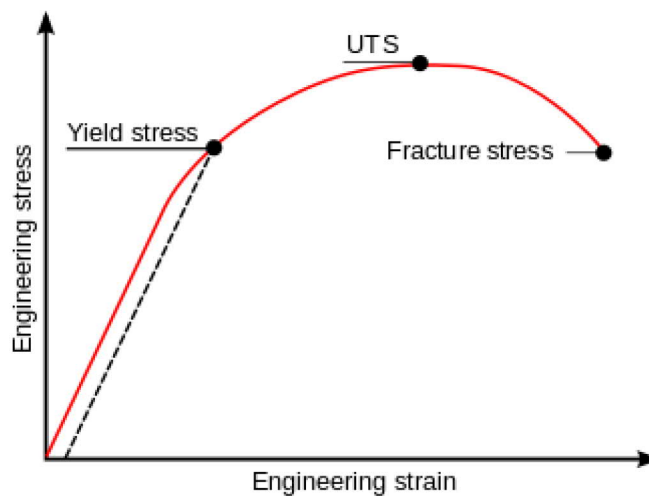

Figure 31: Typical stress-strain curve [69]

From the curve it is possible to see that in first part of the test the material experiences elastic deformation, which means that the stress can be expressed as a linear function of the strain. The slope of this line is known as Young's modulus, E. The elastic deformation is a reversible deformation that means once the load is released, the material recovers its original shape. However, the elastic deformation lasts until the yield strength σ_{ys} is reached. After that stress, the material experiences plastic deformation which is not reversible. There is not a precise way to measure the yield strength, but conventionally it can be determined as the stress obtained through the intersection between the stress-strain curve with a line with slope E, but with an offset of 0.2% on x-axis. This means that the yield strength can be defined as the stress that leaves a plastic deformation of 0.2% in the material. In the plastic region the stress increases not linearly with the strain. The increase in metals is due to the phenomenon of strain hardening. At room temperature deformation, the defects, called dislocations, tend to multiply and to obstruct each other. This phenomenon hinders the deformation, making higher the strength of the material. At a certain point, the maximum value of the stress is reached, and it is called Ultimate Tensile Strength (UTS). From this point the cross-sectional area where the fracture is supposed to happen starts to decrease and this phenomenon is called necking. Since the cross-section reduces, a true stress can be defined considering the actual area and not the original one. If the hypothesis of the conservation of volume in the material are valid, the true stress and strain can be defined as:

$$\sigma_T = \sigma(1 + \epsilon) \quad (3)$$

$$\epsilon_T = \ln(1 + \epsilon) \quad (4)$$

Where σ and ϵ are respectively the engineering stress and strain. However, since we are not interested on them and the engineering ones are reported in manufacturer datasheets, in this work only the engineering stress and strain will be computed.

Finally, the last parameter that can be computed from the tensile stress is percent permanent elongation that is representative of the ductility of the material. It can be computed as:

$$A\% = \frac{l_u - l_0}{l_0} * 100 \quad (5)$$

Where l_0 is the initial gauge length and l_u is the gauge length after fracture.

For all the tests, the traverse speed was 2 mm/min.

4.5.2 Vickers hardness test

The definition of hardness testing is "a test to determine the resistance a material exhibits to permanent deformation by penetration of another harder material". Indeed, the procedure is performed by pressing an indenter on the surface of the material that should be tested. Then, depending on the kind of the test there is a relation between hardness and depth of indenter penetration, or the size of the impression left by the indenter [70].

In this work we exploit Vickers hardness test, where the hardness is determined by measuring the size of the impression left by the indenter. In Vickers hardness test a diamond pyramid indenter is exploited and it is pressed on the surface with a certain load between 1 kgf and 100 kgf [70].
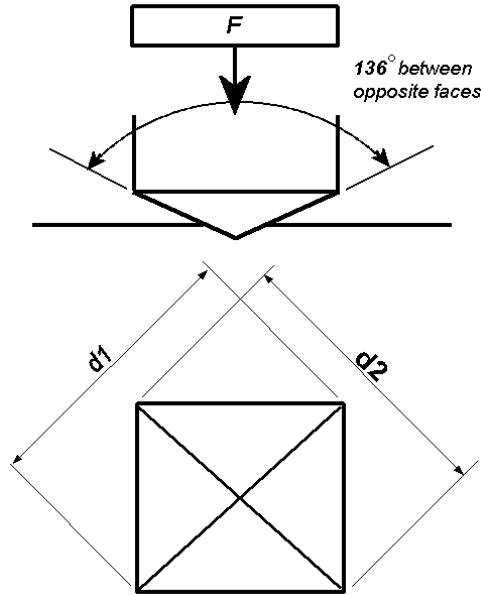
Figure 32: Vickers indenter and impression left on the specimen [71]

The hardness number is computed as:

$$HV \approx 1.854 \frac{F}{d^2} \quad (6)$$

Where F is the load expressed in kgf and d is the arithmetic mean of the two diagonals d_1 and d_2 in mm [71].

4.5.3 Tensile shear test

The first mechanical test that has been carried out for the joints was tensile shear test. As already said, Zwick Roell Z020 was used to perform this kind of test. The temperature was maintained close to room temperature and the traverse speed used for the test was 1 mm/min. After that, the data were collected from the machine and the typical force-displacement plot was obtained with the software Matlab.

Before the test, a very long weld of a length of approximately 350 mm was made in an overlap configuration for an overlap of 60 mm. Since, the welding length is very big, a very precise and advanced clamping was used to weld it as we can see from the welding setup from the next figure.
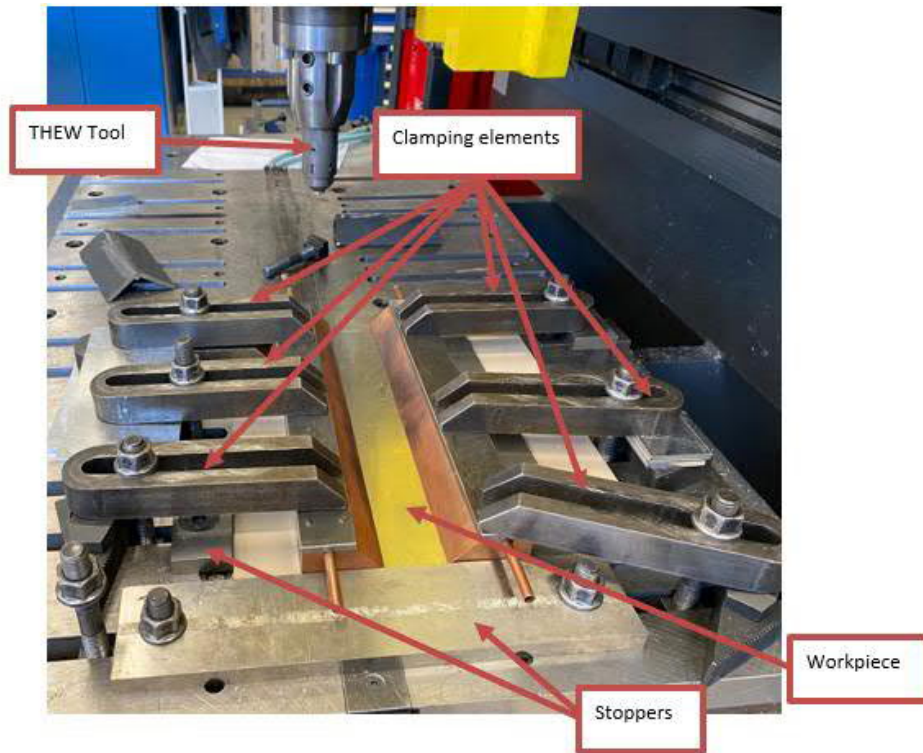
Figure 33: Welding setup for tensile shear test specimens

After that, 5 samples were obtained from the cutting of the piece in a way to have the same dimensions for all of them, following the European Standard used for this test. The designed standard exploited for the testing of our pieces is EN ISO 14273:2016 "Resistance welding-Destructive testing of welds-Specimen dimensions and procedure for tensile shear testing resistance spot and embossed projection welds". As it is also specified in the standard the object of tensile shear testing is to determine the tensile shear force that the test specimen can sustain [72]. Moreover, since the test specimens were obtained through the cutting process of a bigger single piece, the initial and final part of the weld shall be discarded as suggested from the standard.

Key
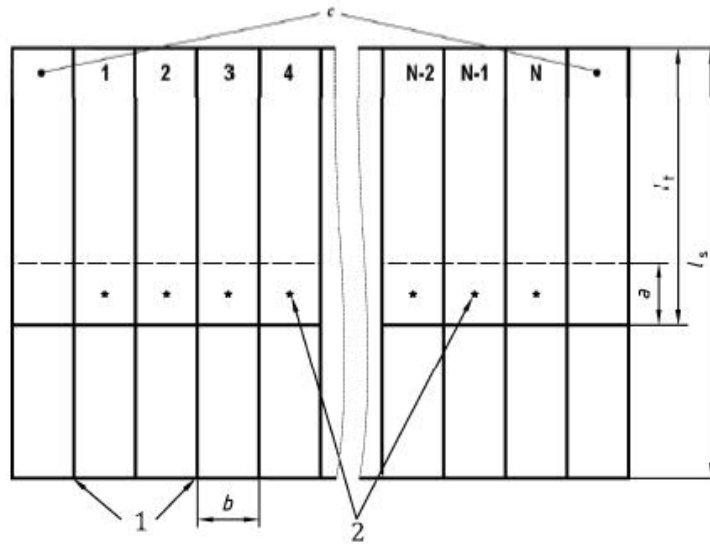
1	cuts	c	discarded
2	welds	N	number of welds tested
a	overlap	l_c	clamping length
b	specimen/clamping width	l_s, l_t, l_f	

Figure 34: Initial weld test piece according to the standard [72]

Figure 35: Initial weld test piece
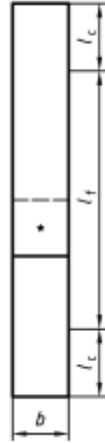
Figure 36: Single weld test specimen [72]
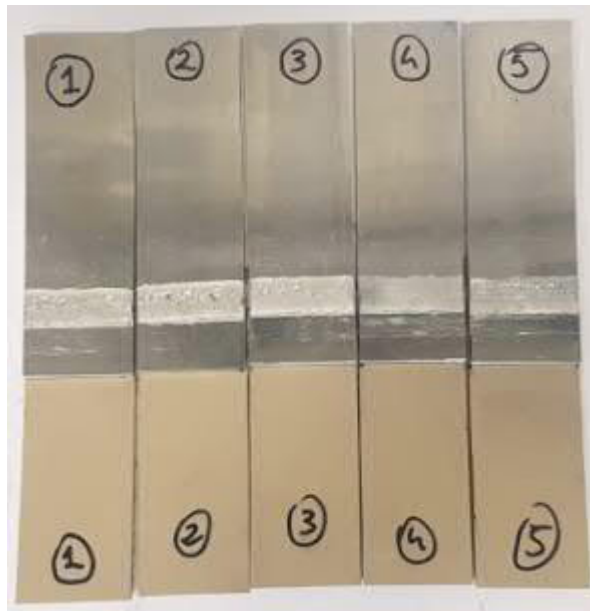
Figure 37: Numbered single weld test specimens

The value of the lengths highlighted in the previous figures are shown in the next table.

Table 12: Tensile shear test specimen dimensions

Symbol		Value [mm]
l_t	Length of individual test pieces	160
l_f	Free length between clamps	120
l_s	Specimen length	260
b	Specimen width	50
a	Overlap	60

Finally, since the thickness of our samples is higher than 3 mm, shim plates of the same thickness of the sheets of the test samples are used to clamp the test pieces in the testing machine. A schematic representation of this configuration is shown in the next figure to clarify the setup before the testing.
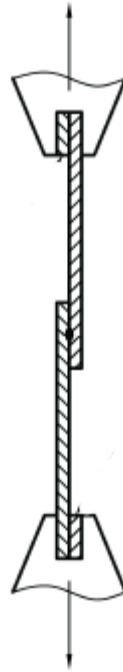
Figure 38: Profile with shim plates [72]
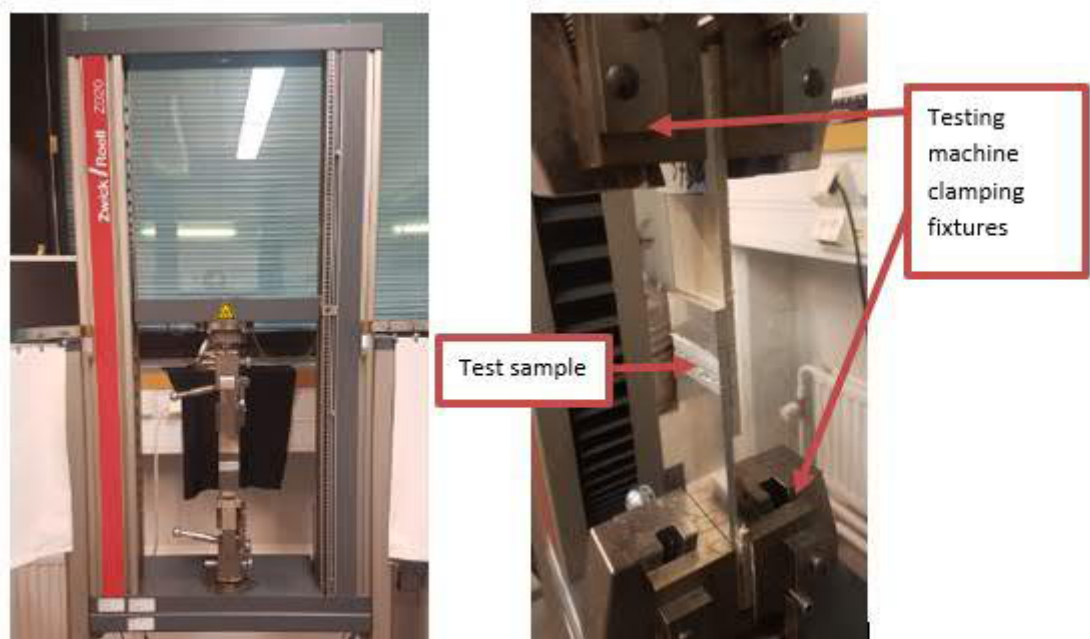
Figure 39: Specimen in testing machine

4.5.4 Cross tension test

The second mechanical test that has been carried out is cross tension test. As already said, MTS Landmark 810 was used to perform this kind of test. The temperature was maintained close to room temperature and the traverse speed used for the test was 1 mm/min. After that, the data were collected from the machine and the typical force-displacement plot was obtained with the software Matlab.

The samples to be welded were prepared according to the standard EN ISO 14272:2016 "Resistance welding-Destructive testing of welds-Specimen dimensions and procedure for cross tension testing of resistance spot and embossed projection welds". The object of the cross-tension test is to obtain the tensile force that the test specimen can withstand.

The test sample consists of two rectangular pieces with two holes used for the clamping in the testing machine through the bolts and specific dimensions must be used, as described from the standard.

Key
1   weld
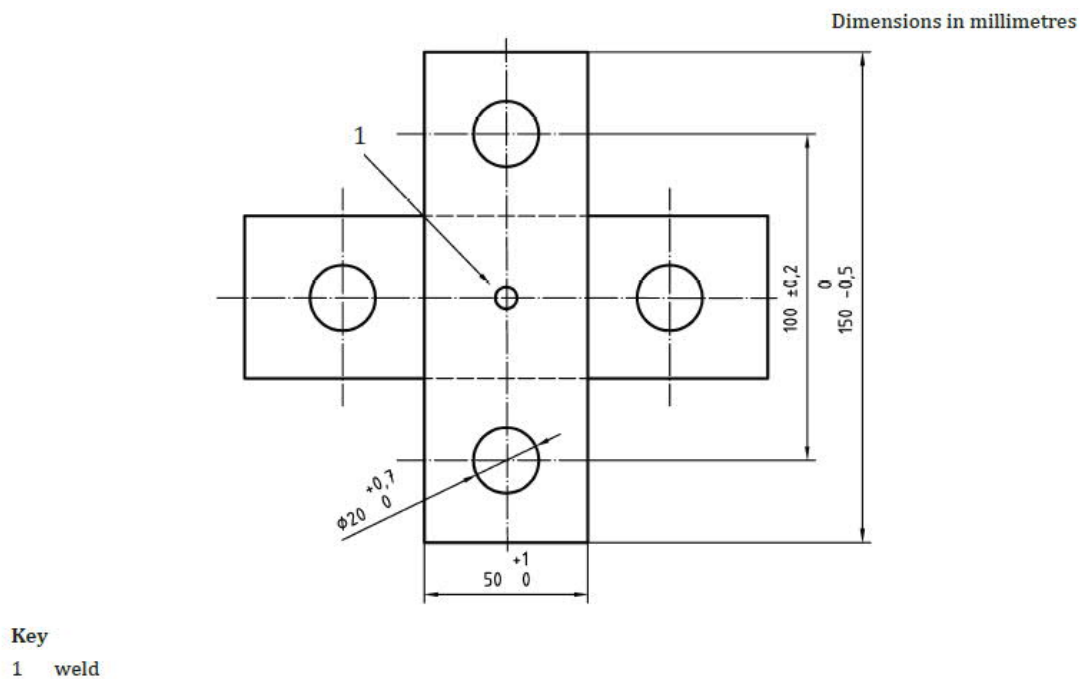
Figure 40: Test sample geometry according to the standard [73]

Also in this test, a specific purpose clamping system was used to make a circular weld with a diameter of 20 mm.
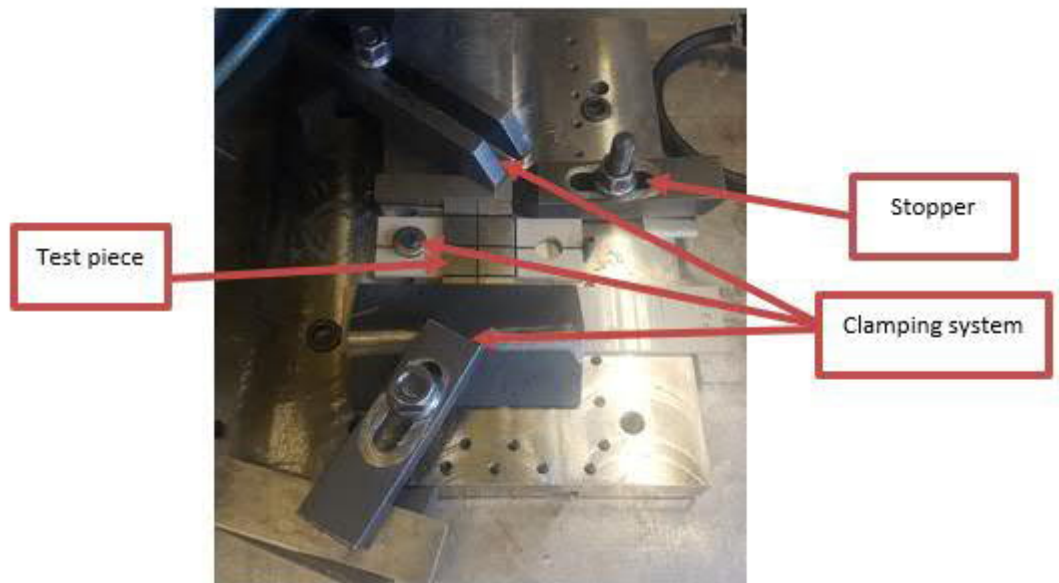
Figure 41: Clamping system for the welding of cross tension samples

For this sample geometry, a circular extrusion die was machined to perform the circular weld and 5 final samples were obtained for the testing.
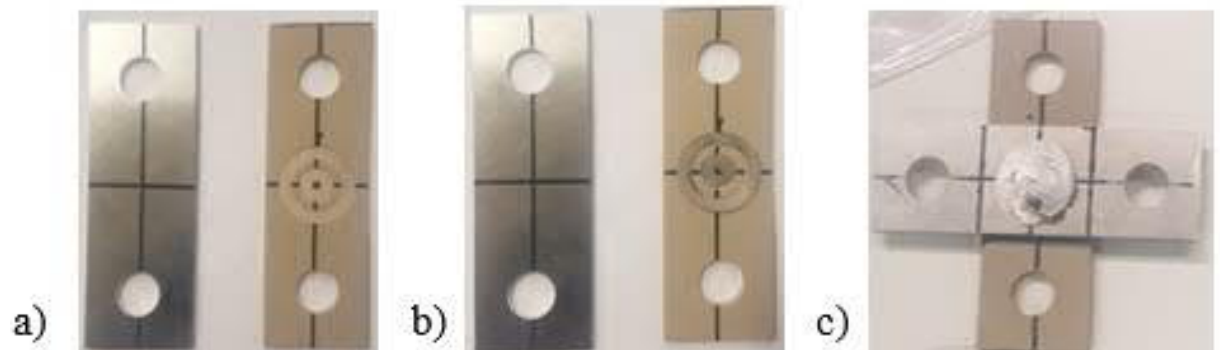
Figure 42: a) Samples to be welded; b) Positioning of the extrusion die; c) Final sample

Figure 43: Sample in the testing machine

4.5.5 Microscopic analysis

After that a proper THEW joint was obtained, the workpiece was cut in different points to analyse the evolution of the joint along the welding path. The samples were mounted through the cold mounting method in acrylic resin (Struers DuroCit Kit). The good surface quality of the samples was ensured through operation of grinding and polishing, using sanding papers with an abrasive grain size from 82 μm to 0.5 μm. For macrostructural analysis no etchant was used in the first phase since it was made only to analyse the geometry of the joint and its evolution along the weld path. On the other hand, in the second phase of the macrostructural analysis, the etchant was used to see the grain orientation and flow. Also in microstructural analysis the samples were etched with a solution of water (60 ml), hydrofluoric acid (15 ml) and phosphoric acid (10 ml) for 35 s. It is worth to specify that the sample was obtained with the best set of preliminary process parameters. The microscope used for these analyses was already described. Another thing to be highlighted is that the overall picture of the joint obtained through the microscope was a composition of many smaller localised pictures, since with the lowest magnification it was not possible to take the overall picture of the joint. Finally, the scratches on the materials were due to the grinding and polishing processes. Indeed, the structure was a sandwich structure with three different materials, which made harder the removal of the scratches. They are acceptable for the macrostructural analysis, but not for the microstructural analysis. For this reason, the microstructural analysis was made after a proper removal of the scratches.

5 Design of tool

5.1 Introduction

In this chapter there is a discussion about the tool design and different steps in its development. Initially, during this work some tools from previous works were used (e.g. friction stir channeling and friction stir welding). The problems related to the use of the old tools was the excessive presence of flash that prevented the closure of the weld joint surface. This is related to the concept of the "third body region". Indeed, in all the friction-based processes a viscoplasticised region is generated and it is processed in a new shape with new properties. Although this region is still in a solid state, it presents a three-dimensional material flow that allows a good mixing between different materials. Usually, in welding processes based on friction mechanism (e.g. FSW), the "third body region" is constrained between the shoulder, the anvil, and the surrounding cold base material and so the region is closed, leading to a flashless process [74]. However, with the use of the old tools there was not an upward force bringing the material up towards the shoulder in order to create a pressure and so a forging action of the shoulder on the material. Moreover, no features were present on the shoulder to bring the material near the probe to obtain a surface closure of the weld. Indeed, a centripetal action of the shoulder is required to close the surface opening detected on the samples made in the previous works experiments.

To summarise, there is the necessity to close the open surface, but simultaneously the aluminum has to penetrate and pressurise the polymer to force it in an upward direction. Moreover, we want to evaluate a new shape of the joint in place of the hook joint. Indeed, a new so called "Crab Claw" joint can be evaluated, which present a symmetric shape. These objectives can be obtained through a specific-purpose design of the shoulder and probe that play a key role to create the two most exploited bonding mechanisms in this process: mechanical interlocking and adhesive bonding.

The chapter is organised in different sections where there is a detailed presentation of the new designed tool.

In section 5.2 there is the classification and characterisation of the material used in the manufacturing process of the tool.

In section 5.3 the design and production of the tool is displayed, while in section 5.4 there is a detailed description of the components of the tool.

In section 5.5 the method to assembly all the components is described and finally in section 5.6 the other tools used for the machining of the samples are displayed.

5.2 Tool material

To understand which material can be the best possible in the process of THEW a small and simple material selection was made considering different constraints related to the application. The use of CES software supported this process of material selection. Indeed, the tool material will influence the weld quality and so it is a key issue in the THEW process. The selection depends on the operational conditions that the tool must face.

A series of constraints will be listed that will be applied in the formulation of Ashby maps for material selection:

1) Resistance to wear due to the friction between the workpiece and the tool;

2) High strength associated to good creep resistance;

3) High resistance to thermal fatigue due to the thermal cycles that the material has to face;

4) Good fracture toughness to prevent crack propagation;

5) Low coefficient of thermal expansion to ensure dimensional stability during the rise of the temperature;

6) Good ductility;

7) Good machinability in order to produce the very small and complex features present on the tool components.

Some of these constraints refer to same material properties and so they can be grouped. For instance, the thermal stresses are proportional to the thermal expansion coefficient, thus thermal fatigue depends on the thermal expansion coefficient.

For the other constraints there are other material parameters that can be exploited in CES software and that will be used to make Ashby maps. First, we can make a map with Yield strength as y-axis and Fracture toughness as x-axis. Among the materials that will pop up, we can select the ones which fulfill also the other requirements.

Moreover, we will consider only metals and alloys, and composites in our selection.
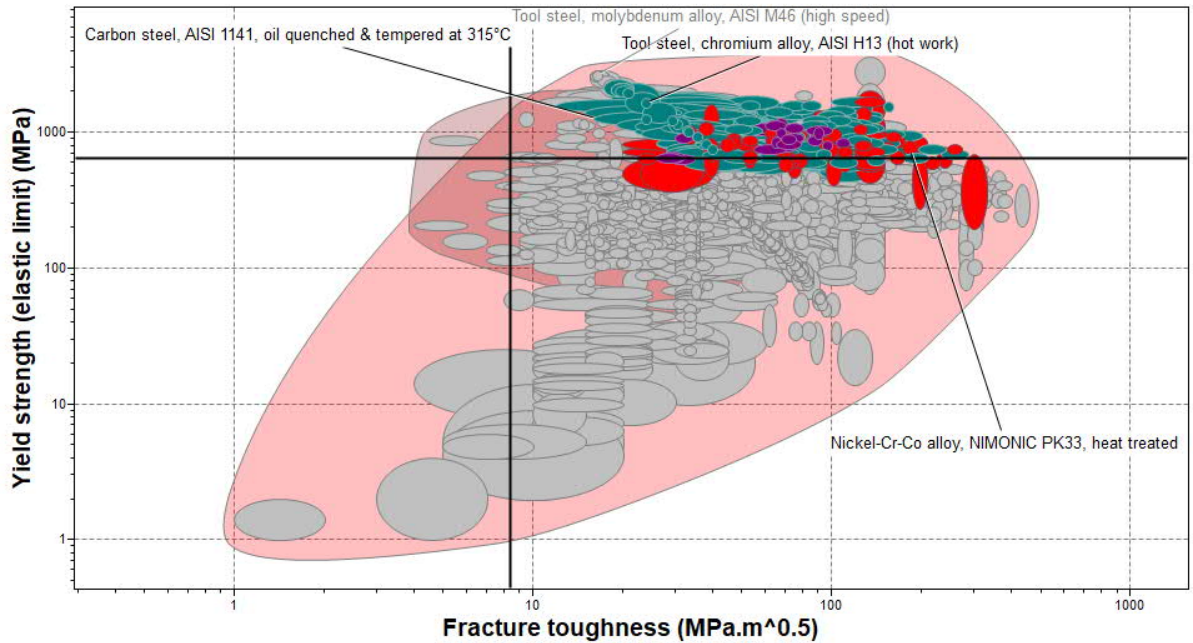
Figure 44: Yield strength-fracture toughness map [57]

As we can see from the map, the best materials for yield strength-fracture toughness are Q&T steels, tool steels and Ni-based superalloys. However, we need also to analyse other properties. For this purpose, another useful map is Elongation-(1/Thermal expansion coefficient). On x-axis we use the inverse of the thermal expansion coefficient to maximise both parameters.
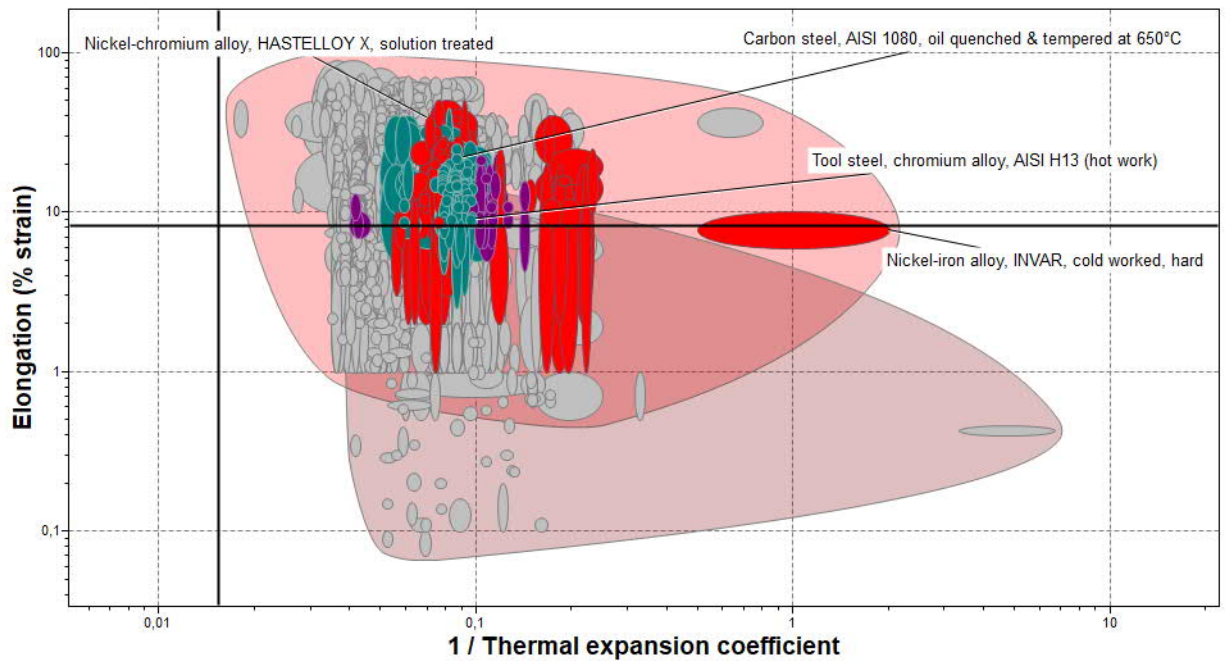
Figure 45: Elongation-(1/Thermal expansion coefficient) [57]

55

Also in this case, the best materials are Ni-based superalloys, Q&T steels and tool steels. Since, in our welding experiments we will use only Al-alloys, which are low melting point alloys, it is useless to consider even an expensive solution like the one represented by Ni-based super alloys. For this reason, they are discarded from this selection. The choice is narrowed between tool steels and Q&T steels. From the literature, the best choice seems tool steels as they have also higher maximum service temperature. Depending also on the market availability, the choice falls on AISI H13.

AISI H13 is a chromium-molybdenum-vanadium hot work tool steel. It is subjected to the heat treatment of quenching and tempering to have the typical microstructure of tempered martensite and retained austenite. Indeed, it has outstanding mechanical properties and it resists to high temperature. Moreover, as it is also indicated on CES datasheet, it has a very good machinability too. The chemical composition and the mechanical properties of the material are reported in the next following tables.

Table 13: AISI H13 chemical composition [57]

Composition	C	Cr	Fe	Mn	Mo	Ni	P	S	Si	V
%	0.32-0.45	4.75-5.5	88.9-92	0.2-0.6	1.1-1.75	0-0.3	0-0.03	0-0.03	0.8-1.25	0.8-1.2

Table 14: AISI H13 mechanical and thermal properties[57]

| Properties	Values range
Heat treatment	Air quenching and tempering at 540 °C
Density $\left[\frac{kg}{m^3}\right]$	7690-7840
Young's modulus $[GPa]$	211-221
Yield strength $[MPa]$	1610-1690
Tensile strength $[MPa]$	1940-2040
Elongation $[\% \ strain]$	8.3-9.7
Compressive strength $[MPa]$	1610-1690
Hardness-Vickers $[HV]$	380-580
Melting point $[°C]$	1460-1500
Thermal conductivity $\left[\frac{W}{m \cdot °C}\right]$	27.5-29.8
Electrical conductivity $[\%IACS]$	3.07-4.23
Thermal expansion coefficient $\left[\frac{\mu strain}{°C}\right]$	10.2-10.7

Finally, since good wear resistance is required due to the friction-based process that is involved, a process of surface hardening is required. For this reason, a process of nitriding was exploited to increase the surface hardness, even at high temperature, the wear resistance, to improve the fatigue life and the corrosion resistance. The process consists to introduce nitrogen into a steel component, through the heating of that in a fused salt bath that contains nitrogen-bearing salts (e.g. NaCN, sodium cyanide) or in a gas stream which includes the presence of cracked ammonia (NH_3). The process allows the formation of

stable nitride precipitates which leads to the surface hardening for a depth of 500 μm. Moreover, the process is conducted at a temperature between 495 and 565 °C which prevents distortion, avoiding a necessary further heat treatment [57].

5.3 Design of the new tool

After the first phase where old tools were used, new probes and shoulders were improved and designed to achieve the objectives of this work. Moreover, also a new holder was produced to have complete set of new tools. The most important modifications compared to the past were made in the probe and shoulder. Indeed, three different probes were designed and developed. In the same way three different variants of the shoulder were produced. On the other hand, no differences were made in the design of the holder. All the different features of the new tools cannot be dispayed since they are sensitive data.

After the first phase of testing, looking at the results, one combination of probe and shoulder was selected to further improve the THEW process and to test the obtained joints.

The phase of design and modeling of the tools was done through the software Solidworks 2018.

5.4 Tool components

5.4.1 Holder

The function of the holder, as suggested by the name, is to hold the shoulder and the probe. Indeed, in the main assembly of the tool (in next sections) it is possible to see that both the shoulder and the probe are tightened to the holder. The other function of the holder is to transfer the torque and all the loads from the welding machine to the tools (shoulder and probe). To obtain the transfer of the torque, the holder should be tightened to the FSW machine through the arranged bolts. In addition, to prevent the coolant leakage the holder should be pressed against the machine walls allowing the perfect housing of the holder. Finally, it has to withstand the mechanical loads deriving from the process.

In the next figure there is a schematic representation of the holder.

Figure 46: Schematic representation of the holder

Figure 47: Manufactured holder

5.4.2 Shoulder

The main purpose of the shoulder in friction based process is to heat the surface of the workpiece through friction and material deformation, to transfer the heat to the weld region, to produce a downward forging action necessary to consolidate the weld joint and to constrain the heated metal beneath the bottom shoulder surface [75] [76]. Nowadays, two main classes of shoulders are commonly used, the conventional one and the scrolled one.

Usually, a conventional shoulder has a concave face with an inclination of a small angle (6-10°) from the flat shoulder. In this way, during the plunging phase the material that is

stirred by the probe is directed towards the shoulder cavity, forming a reservoir of the displaced material. Through, the application of a downward pressure, the material stored in the concave shoulder provides a forging action on the material behind the tool. Through the forward movement of the tool, there will be new material in the cavity that pushes the preexisting material behind the probe [75]. The shoulder used in the previous works was made in this way with a concavity of 5°. In addition, this kind of shoulder should be used with a tilt angle of the tool in the range of 1-3° from the normal of the workpiece to keep the material reservoir and to promote a compressive forging force on the weld by the trailing edge of the shoulder [75].

In scrolled shoulder, the end surface will present some features which help the material friction, shear, and deformation to increase the material stirring and so the weld quality. In this case, the shoulder will have flat surface with spiral channel cut or extruded from the edge of the shoulder to the probe. In this way, there is no necessity to have a tilt angle of the tool. The advantage of the scrolled shoulder is the reduction of the flash by entrapping the viscoplasticised material inside these features. Moreover, the material inside these channels is constantly sheared from the surface increasing deformation and friction for heat production on the surface [75].

In this work three different shoulders were designed. In the next figure there is a representation of the designed shoulders with their respective features that are blacked.
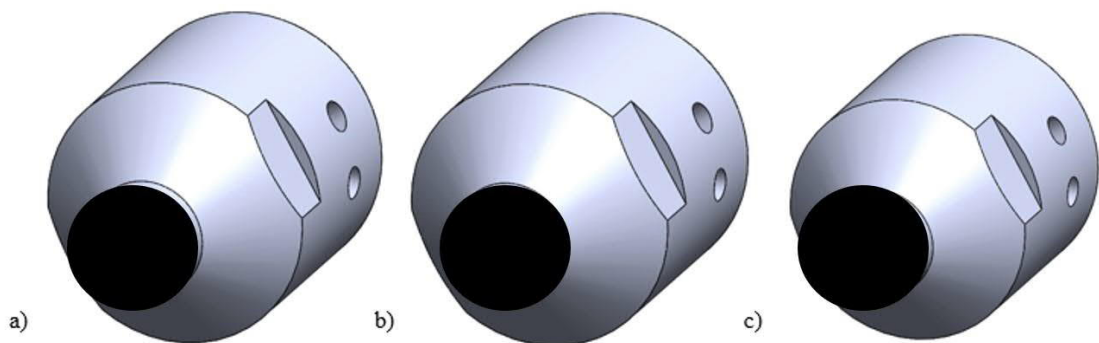
Figure 48: Schematic representation of the shoulders a), b) and c)
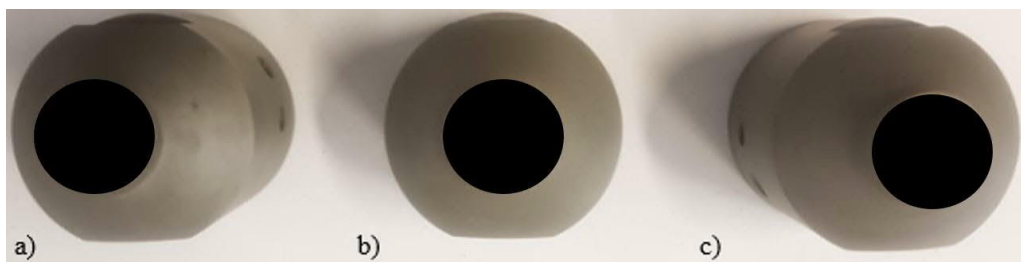
Figure 49: Manufactured shoulders a), b) and c)

The efficiency of these three shoulders was tested and the best one was chosen to achieve the prefixed objectives together with a specific probe.

5.4.3 Probe

The probe has the function to shear and stir the workpiece material in front of the tool, to move the material behind the tool and to move it upwards or downwards depending on the features made on it. Threadless probes are usually used for high strength alloys or highly abrasive alloys, since the threads can be easily worn away. However, threaded probes are the most used to induce upwards/downwards flow of the material depending on the tool rotation. Moreover, the material can circulate more times around the tool through the threads before being deposited behind the tool. Obviously, this phenomenon helps the stirring of the material and the closure of possible voids [75].

In this work, the objective was to close the weld joint surface, but simultaneously to have the penetration of the aluminum inside the polymer. For this purpose, three different probes were designed and manufactured. Also in this case the details are blacked since they are sensitive data.
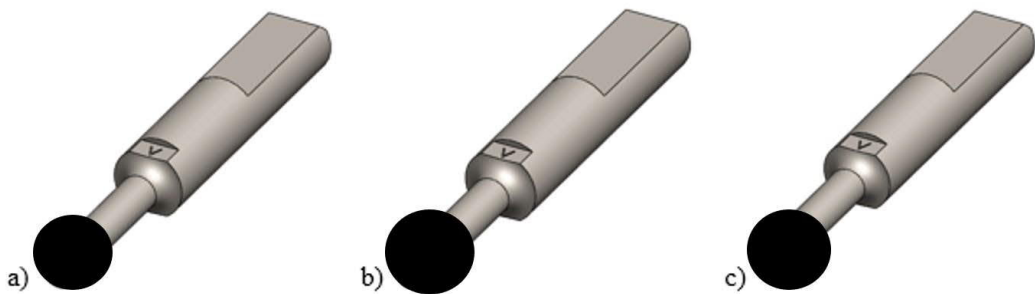
Figure 50: Schematic representation of the probes a), b) and c)

Figure 51: Manufactured probes a), b) and c)

All the probes should leave a channel due to the induced flow of the material. However, this channel should be filled by the upwards flow of the polymer. Indeed, the idea is that the viscoplastic hot aluminum will soften and penetrate the polymer applying on it a pressure which forces it to go up achieving the mechanical interlocking and adhesive bonding between the two dissimilar materials.

As for the shoulder, after different tests the best preliminary probe was chosen, depending on the joint results.

5.5 Assembly of the tool

The designed tool is composed of three parts: holder, shoulder and probe. The probe is tightened inside the holder through dedicated helical threads to screw it inside the holder. To avoid the relative rotation between the holder, that is connected to the welding machine, and the probe, a bolt is used to lock the probe in the determined position. In the same way the shoulder is tightened to the holder through dedicated threads and a couple of bolts is used to lock it to avoid relative rotation with the holder. Finally, the holder is accommodated on the welding machine though the use of two bolts. Teflon taper is exploited on the probe and on the bolt locking the probe in the holder to avoid coolant leakage.

Through the regulation of the screwing of the probe and the shoulder, different probe lengths outside the shoulder can be used. For this reason, this tool is called modular tool as different probe lengths can be obtained.

A schematic view of the final assembly of the tool is represented in the next figure.
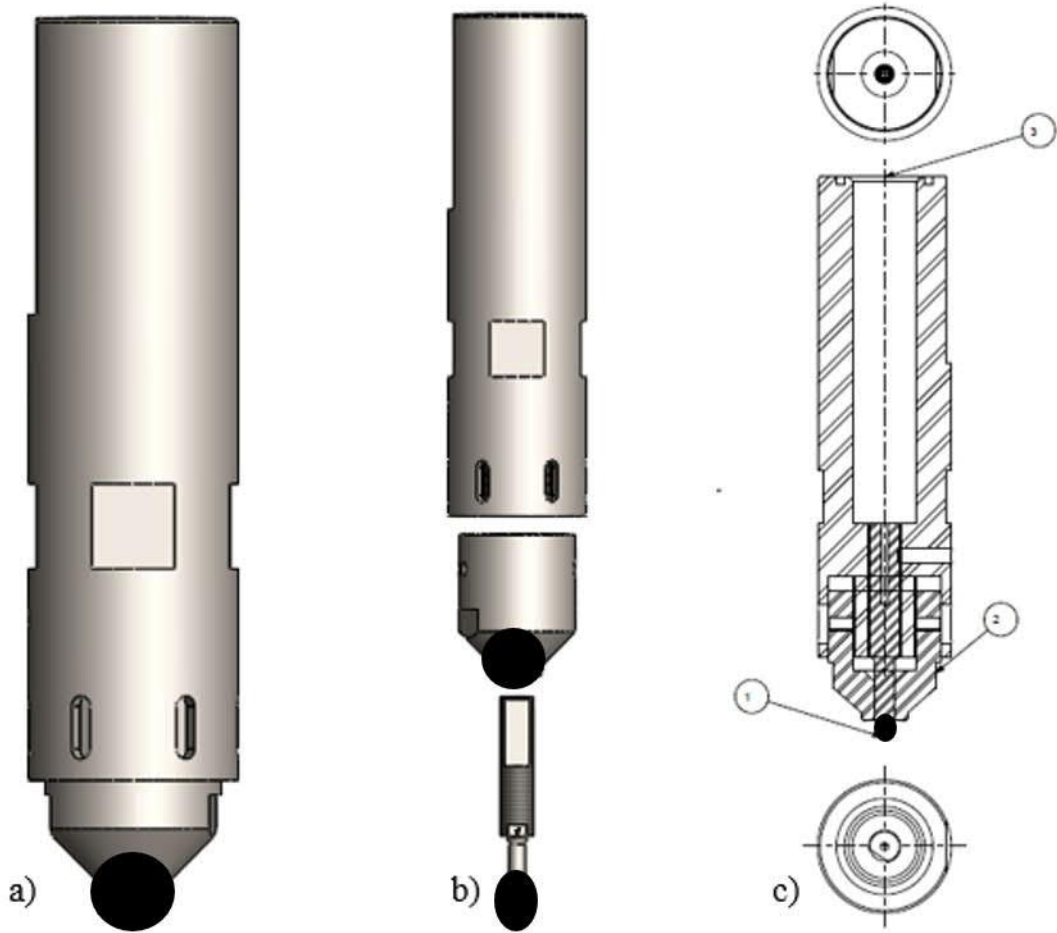
Figure 52: Schematic representation of the modular tool a) tool assembly; b) exploded view; c) tool assembly cross section

Figure 53: Tool assembly

5.6 Machining tools

The tools described in the previous sections are all used for the welding phase. However, before this phase the preparation of the samples to be welded is obtained through a careful machining of them. Since the welding machine is a CNC machine, it can be also used to machine pieces regulating all the process parameters related to the different machining operations. So, drills bit and mills are mounted and used to machine the different samples. In the next figure there is a picture of the used machining tools.

Figure 54: Machining tool, a) collet holder; b) collet; c) mill

6 Development of the process

6.1 Introduction

In this chapter there is the development of the THEW process. All the phases involved in the welding process are discussed.

In section 6.2 there is the establishment of the experimental conditions considering the geometries of the samples, a new clamping system and a new concept of extrusion die.

In section 6.3 performance parameters based on the manual observation of the obtained joints are introduced.

In section 6.4 the most important and explored process parameters for the THEW process are investigated and their influence on the process are explained.

In section of 6.5 the effect of the different modeled tools is investigated with a simultaneous variation of the process parameters. Different results were obtained and through the guidance of the performance parameters the best set of preliminary tools is chosen to improve and further develop the process.

In section 6.6, since for COVID-19 there was a limited access in the laboratory, and it was not possible to do a proper optimisation design for the process parameters, a set of good parameters was selected depending on the results obtained and judged through the criteria explained in section 6.3. It can be possible that these parameters will be the optimal ones, but a proposal to be developed in the future is to have an optimisation plan to have the actual optimal parameters.

In section 6.7 there is the description for linear double side THEW joint, while in section 6.8 the non-linear variant is presented.

6.2 THEW experimental conditions

6.2.1 Test pieces geometry

The materials that were investigated in the process were AA5754 H111, AA1050, Ti Gr 1 and PEEK.

The initial material geometry used during the development of the THEW welding process, was very similar to the previous works. However, one objective of this thesis was to have a longer weld length with a consistency of the joint along this length. For this reason, longer pieces were machined. A minor improvement was to machine the pieces all with the same dimensions. In this way, the clamping process and the positioning of the samples were much easier. The final dimensions of the samples were 200*60*5 for the aluminum and PEEK plates. On the other hand, the titanium sheet metal had the same dimensions, but with 1 mm of thickness.

The test pieces as in the previous works are positioned in a sandwich structure. The PEEK was in the bottom, the titanium in the middle and the aluminum on the top. Since the titanium has the function to extrude the viscoplastic aluminum a slot with the same length

of the weld length (≈150 mm) was machined on it. As already said, the purpose of the titanium was to guide the extrusion of the viscoplastic aluminum towards the PEEK to control the flow of the aluminum in the PEEK. Another important reason to use titanium is to insulate the polymer from the frictional heating produced during the process. Indeed, titanium has a very low thermal conductivity.

In the next figure there is the titanium and polymer geometry according to the previous works approach.

Figure 55: Ti-sheet metal and polymer according to old approach

After some feasibility studies on the welding process the geometry of the pieces was changed. Indeed, 1 mm thick plate distanced the aluminum and the PEEK too much. This leads to a poor deposition of the aluminum in the PEEK. For this reason, the distance between the aluminum and the PEEK was minimised. Initially, the same approach was used but with a thickness of 0.6 mm. After some experiments, the geometry was changed again. Indeed, the titanium was machined in strips that can be embedded in proper machined slots on the PEEK. The thickness of the titanium was reduced to 0.6 mm and the depth of the slots in the PEEK were 0.5 mm leaving only a space of 0.1 mm between the aluminum and the polymer. Moreover, the slots will have a width 1 mm larger than the titanium strips and leave a 4mm wide polymer region that is close to the aluminum (as already said there is a space of 0.1 mm between the aluminum and the PEEK). The drawing and the picture below will clarify the concept. The new approach improves the condition to obtain the joint, but also the machining phase avoiding the slot machining on the titanium.

In addition, also the clamping phase will be easier since there is no risk of movement of the titanium die.
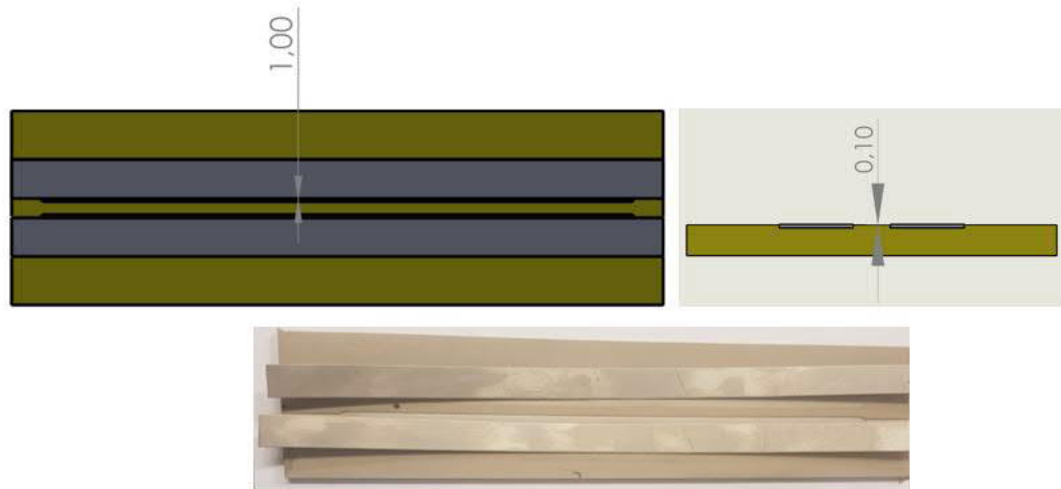
Figure 56: Ti-strips and polymer according to new approach

Once the right process parameters were selected, the attempt to obtain a rectangular and circular weld was developed. In both cases, 200*200 mm aluminum and PEEK plates were used.

6.2.2 Development of a new clamping system

In the previous works the weld length was very short (at maximum 40 mm). This means that a punctual clamping system was enough. One of the objectives of this work was to obtain longer weld length together with the closure of the surface. For this reason, a new clamping system was made. It consists of two stoppers tightened on the anvil of the FSW machine and of two welded sheets with a certain angle.
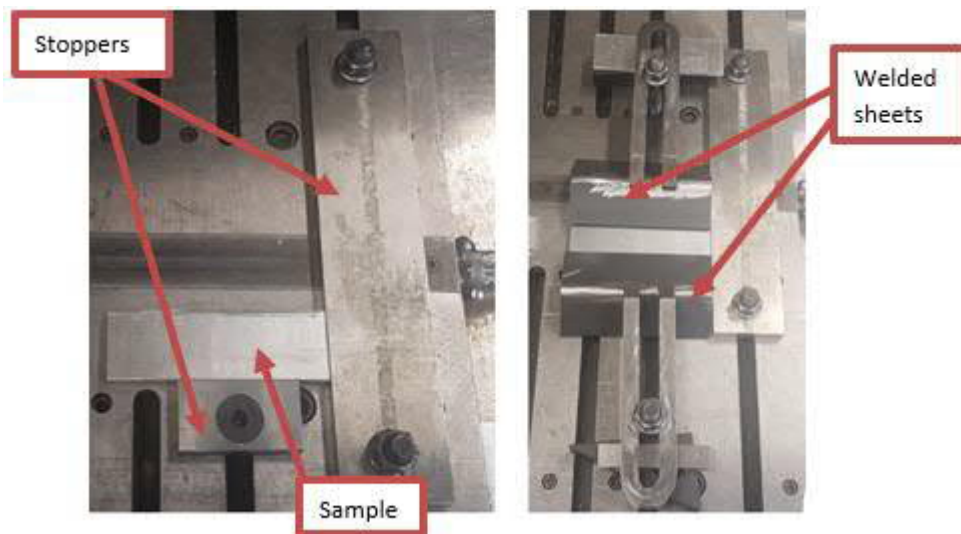
Figure 57: Clamping system

In this way a more uniform pressure will be distributed in the sample avoiding unwanted and unpredictable bending which can compromise the quality of the joint.

6.3 Performance parameters

Due to time problems for COVID-19 pandemic, an optimisation process was not designed for this work. In that case, different joints should be produced varying the process parameters within a designed range and evaluating the respective mechanical properties. Since this process was not feasible, the evaluation of joint was done by manual observation considering a geometrical assessment of the joint and the assessment of the involved joining mechanisms.

The geometrical assessment involves the depth of the deposition of the aluminum inside the polymer, the thickness of the "Crab Claw" joint, the volume of deposition of the aluminum and the closure of the surface.

On the other hand, the joining assessment is based on the different possible joining mechanisms during the process that are adhesive bonding and mechanical interlocking. Indeed, it is evaluated which one of the two mechanisms prevails, but also if there is polymer vaporisation and the degree of flowing up of the polymer into the aluminum.

6.4 Process parameters

To evaluate and achieve a better joint quality, a set of process parameters were investigated depending on their influence on the process. Then, after different experiments a set of right parameters was selected. However, a proposal for future work is to do an optimisation plan to find the optimal parameters.

The analysed parameters are listed below:

1. Rotational speed: the rotational speed is the main parameter which determines the viscoplasticisation of the aluminum. Indeed, it creates friction on its interfaces with the aluminum and it plastically deforms the aluminum. The heat generated by the two effects is responsible of the aluminum viscoplasticisation.

2. Weld position: this parameter is related to the probe length outside the shoulder. Indeed, regulating the ratio between the probe length and the weld position has a main effect on the formation of a proper joint.

3. Dwell time: the parameter dwell time has a direct link on the joint formation. Indeed, too high dwell time leads to melting and consequent vaporisation of the polymer and softening of the aluminum with consequent excessive penetration of the shoulder and flash formation for the overall weld path. Both are due to the steep heat deriving from high dwell time.

4. Travel speed: the regulation of the travel speed is fundamental for the joint formation. Indeed, too high travel speed do not allow a proper material stirring with consequent passage to the visco-plastic domain. At the same time too low travel speed can lead to a concentration of the heat with the usual vaporisation of the polymer and flash presence from the aluminum.

6.5 Best set of preliminary tool selection

In chapter 5 the designed tools were presented. All of them were designed to achieve the formation of a proper joint and closure of the aluminum surface. In this section there is a discussion for the selection of the best set of preliminary tools' combination. In the meanwhile, the process parameters were varied to obtain the right parameters that can be used for a further development of the THEW process. Initially, only AA1050 was involved in the welding process with PEEK. However, in the next subsections there is a discussion about the material that will give the best results in terms of joint.

6.5.1 Probe a)-Shoulder a)

The first tool combination is probe a)-shoulder a). As already said the initial approach was to have an extrusion die of titanium with a thickness of 0.6 mm. The probe was C mm outside the shoulder and a weld depth of B mm was used. In addition, a travel speed of D mm/min, a rotational speed of A rpm and a dwell time of 4 s were applied. The results can be seen in the next figure.

Figure 58: Joint obtained with cylindrical probe and surface features

As we can see from the picture the probe effect is to leave a channel inside the aluminum. Moreover, the aluminum does not penetrate the polymer and the only joining mechanism involved is adhesive bonding between the alloy and the polymer. One action that can be taken in this phase is to increase the length of the probe and so the weld depth. On the other hand, the surface was totally close compared to the experiments from the previous works. This means that the combined effect between the shoulder and the probe is occurring. However, in the plunging region there are too flash. This can be caused by a careless Z-axis zero detection due to the softness of the Al-alloy. Indeed, for Z-axis zero detection we are touching the aluminum surface and if it is soft the probe will penetrate it too much leading to a wrong detection of the zero, which leads to an excessive penetration with consequent high friction and heat release.

The probe length outside the shoulder was increased to C mm and the weld depth to B mm, but the adhesive bonding is still the main joining mechanism.

Figure 59: Joint after the increase of the weld depth

In addition, the surface still presents the flash. Probably, the forging pressure is excessive and for this reason the weld length of the probe outside the shoulder should be increased maintaining the weld depth constant. Another problem of the shoulder is the high quantity of aluminum sticking on it, which avoids a good material stirring and repeatable process. Therefore, another variant of the shoulder is used for the next experiments and since the pull up effect of this probe is too strong, the probe is also changed.

6.5.2 Probe b)-Shoulder b)

The new overall shape of the probe should help the penetration of the aluminum in the polymer. As already said, the probe length outside the shoulder was increased to C mm and the weld depth was maintained constant to B mm. The other parameters were not changed except for the dwell time that was decreased to 2 s to avoid excessive heat generation in the starting point. The old approach of the titanium extrusion die is still used.

Figure 60: Joint obtained with cylindrical + unthreaded conical probe and surface features

As we can see from the picture the "Crab Claw" shape is very clear, but there is still a big channel in the aluminum. Although the new overall shape of the probe helps the aluminum

to flow towards the polymer there is still the presence of the channel. This channel should be filled by the softened and pressurised polymer due to the heat and penetration of the aluminum. For this reason, the second approach was then investigated with the use of the last probe (probe c)) which has different features. In this case a space 1 mm wide and 0.5 mm deep in the polymer can help the flow of the viscoplastic aluminum with consequent pressurisation and softening of the polymer. In addition since there is still the presence of flash and the surface presents occasionally some cracks, the shoulder was also changed.

6.5.3 Probe c)-Shoulder c)

As already said, in these experiments a new extrusion die approach was investigated. Moreover, this probe has features which forces the aluminum penetrate the polymer. The shoulder was also changed in order to obtain a total closure of the surface with a better stirring ability. Indeed, the last shoulder features leads to higher stirring frequency with consequent good effect on the consolidation of the joint. In this way also the sticking of the aluminum is reduced. The parameters were the same of the previous experiment, but the tool rotation was decreased to A rpm and the travel speed to D mm/min. This action will improve the stirring of the aluminum and gives time to the probe to process the aluminum in a more effective way. However, since the travel speed was much lower, also the tool rotation was decreased to avoid a severe heating which leads to a possible degradation of the polymer.

Figure 61: Joint obtained with improved conditions

From the picture we can see that with the help of the improved features of the probe, the aluminum penetrated better the polymer with a consequent light flow of the polymer up. However, even with improved parameters and conditions, and with an improved probe, the joint still shows a small channel due to the fact that the aluminum is not able to soften, penetrate and pressurise the polymer properly. The cause of this can be attributed to the kind of aluminum alloy used in the experiments. Indeed, AA1050 is very soft and ductile as it can be seen from the datasheet and for this reason it is not able to be forced inside the PEEK that is a very strong polymer that is used for structural application. However, this set of tools seems the one which gives best results in terms of performance parameters. Moreover, there is still the presence of flash and the weld depth was sometimes changed of few decimal of millimeters during the process, since there was too much penetration of the shoulder which did not allow to have good surface quality. This means that the process was strongly influenced by the Z-axis zero detection. The high ductility of AA1050 can lead to a wrong detection of the Z-axis zero, that can be a little bit below the surface of the plate, influencing the whole process. After these analysis the conclusion was to try the same

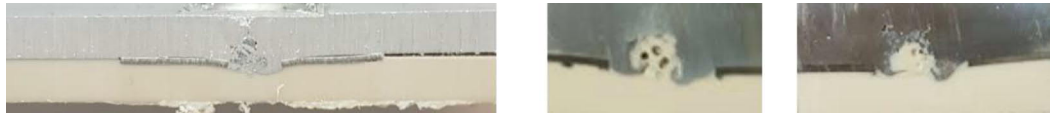process on a stronger Al-alloy (AA5754-H111) with the same tools, process parameters and setup conditions.

Figure 62: AA5754 H111/PEEK joint with improved conditions

From the picture it is possible to see that the joint was improved with this alternative Al-alloy. There is a strong penetration of the aluminum that caused a pressurised outward flow of the polymer creating a proper mechanical interlocking with a crab claw joint. Moreover, due to the effect of the probe features, the aluminum was also pressurised against the shoulder, preventing the flow of the polymer outside of the surface which was the principal cause of the opened surface.

Due to these results, AA5754 H111 was selected as the best candidate for the THEW process and for its further development with an optimisation process to obtain the actual optimal process parameters which is not handled in this work.

6.6 Selection of the best set of preliminary process parameters

As already said in the previous sections, since there was not an optimisation plan due to COVID-19 pandemic, the process parameters were changed step by step and eventually the ones that gave the best results were chosen. In this work only some pictures were shown to demonstrate the different achieved results, but different experiments were made before changing the process parameters until we achieved the right ones. The best process parameters were obtained considering the new extrusion die approach and with AA5754-H111 in place of AA1050. After that we got the best joints in terms of performance parameters, repeated tests were made showing a certain degree of repeatability which led to the selection of the best parameters achievable without an optimisation plan.

They are listed in the following table:

Table 15: Process parameters for THEW process

Process parameters	Value
Rotational speed [rpm]	A
Rotation direction	CW
Weld position [mm]	B
Tool plunge speed [mm/s]	0.2
Reference force [kN]	7
Control	Position
Dwell time [s]	2
Tilt angle [°]	0°
Probe length [mm]	C
Travel speed [mm/min]	D

These parameters were coupled with the best set of preliminary tools which are shoulder c) and probe c) that are shown in the next figure.

Figure 63: Best set of preliminary tools

6.7 Double side THEW joint

After that the THEW joint was developed on one side, it was also attempted to obtain a double side joint to obtain a sandwich structure. To avoid the contact between the two joints since the thickness of the polymer was only 5 mm, an offset of 4 mm for the two welding regions was created.

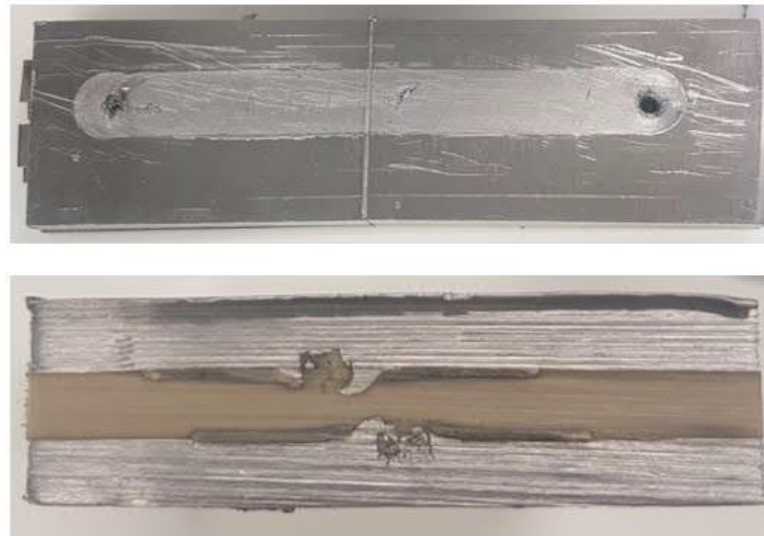The results of the welding process are displayed in the next figure.

Figure 64: Double side THEW joint

From the figure it can be noticed that the surface quality was excellent, no surface openings were detected and there was only the hole at the end of the weld length that is for material conservation (due to the losses of material in the tool plunging phase). In addition, there was a good upward flow of the pressurised polymer. On one side it seems that the "Crab Claw" shape started to form, while on the other side there was the hook joint shape typical of the previous works approach. Indeed, it was due to an improper x-y starting position detection with a consequent offset travel. However, there was also a good mixing of the two materials, no voids and polymer vaporisation were detected. This means that the chosen process parameters were repeatable to obtain a proper joint.

6.8 Rectangular and circular THEW joint

The last step was to develop the THEW joint with different non-linear welding paths. For this reason, it was developed with a circular and rectangular path. Also in this case titanium stripes were used to act as extrusion die. The results are displayed in the next figure.

Figure 65: Rectangular and circular double side THEW joint

However, in some regions of the welding path there was still the presence of flash. This is due to the bending of the aluminum plate because of a punctual clamping system. Indeed, in this case the designed clamping system was unsuitable. However, the results can be considered quite good since we are in a preliminary phase of the THEW process.

7 Mechanical characterisation

7.1 Introduction

In this chapter, there is the mechanical characterisation of the base materials and of the weld joints obtained through the THEW process. The purpose of the tests made for base materials was to compare the obtained values for the mechanical properties to the ones from the datasheets. On the other hand, the characterisation of the THEW joints was necessary to assess which is the maximum load that the joints can withstand.

In section 7.2 the results of the tensile tests for the base materials are presented with the plot of the stress-strain curve obtained experimentally. Moreover, also hardness tests were performed on the metallic base materials (titanium and aluminum). The tests were made only for the selected materials that are the best candidates for a deeper development of THEW technology.

In section 7.3 there are the plots and the maximum loads obtained for the designated mechanical tests for the joints. Indeed, tensile shear test was exploited to find the maximum shear force that the joint can withstand, while cross tension test was made to determine the maximum tensile force. The selected parameters to obtain the joint were the ones which gave the best results in terms of joint consistency and physical appearance (without defects e.g. voids, polymer vaporisation, etc.).

7.2 Mechanical testing of base materials

7.2.1 Hardness tests

HV10 Vickers method was exploited to obtain the hardness values for the base materials. In Vickers method a pyramidal diamond indenter with an angle of 136° is pressed on the surface of the material with a certain force. In HV10 method, 10 kilograms of force are applied on the material, that means 98.1 N in terms of force. After that, the hardness number can be found dividing the applied force to the area of the indentation made on the material.

Three tests were made for each material in different regions and far from the previous footprint to avoid that the hardness value was influenced by the work hardening induced by the plastic deformation of the previous measurements.

The obtained values are reported in the following table.

Table 16: Hardness numbers for the selected base materials

Material	Test 1	Test2	Test 3
AA5754-H111	65.5	65.8	65.8
Titanium Gr 1	123	120	120

These values are very similar to the ones given from the manufacturer datasheet.

7.2.2 Mechanical testing of base materials

The mechanical properties of AA5754-H111, Ti Gr 1 and PEEK were computed through the tensile tests. Only the best candidates among the materials exploited in THEW process were tested. The samples have all the same dimension and an extensometer was mounted before reaching a displacement of 0.5 mm. In the next picture the dimensions of the samples are presented.

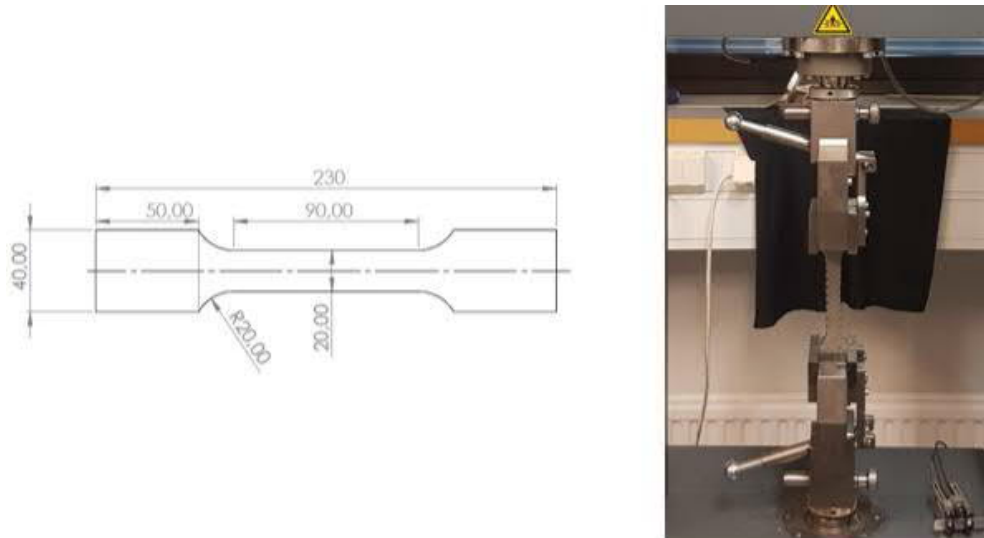*Figure 66: Sample geometry and positioning in testing machine*

In AA5754-H111 and Ti Gr 1 both the rolling direction and transversal direction were tested. Two samples for each direction were tested. The stress-strain curves are reported in the next figure.
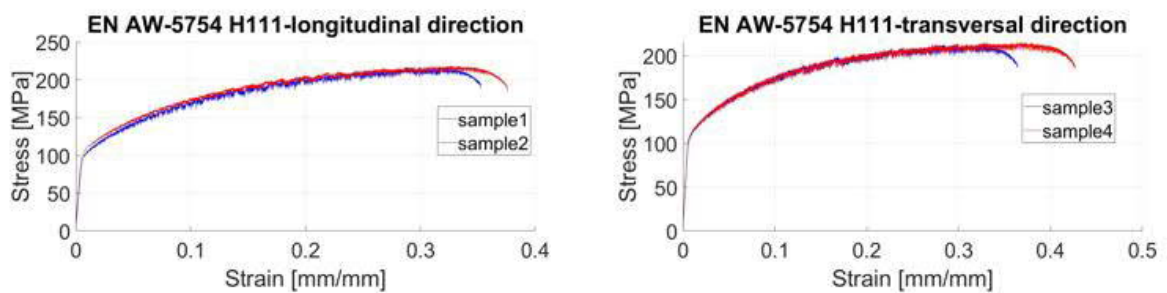

Figure 67: AA5754-H111 stress-strain curves

From the data it was possible also to compute the important mechanical properties for our base materials.

The data are resumed in the next tables.

Table 17: AA5754-H111 mechanical properties in longitudinal direction

Young's modulus [GPa]	Yield strength [MPa]	Ultimate tensile strength [MPa]	Percent permanent elongation (%)
68.29 ± 0.60	106.11± 2.61	217.31±1.41	20±1

Table 18: AA5754-H111 mechanical properties in transversal direction

Young's modulus [GPa]	Yield strength [MPa]	Ultimate tensile strength [MPa]	Percent permanent elongation (%)
67.33 ± 0.18	112.07± 0.03	214.03±1.51	24±2

For AA5754-H111 the experimental data were very closed to the ones given from the manufacturer, except for the yield strength, where the experimental one was much higher than the one from the datasheet. This can be justified considering that the producer puts only the minimum one.

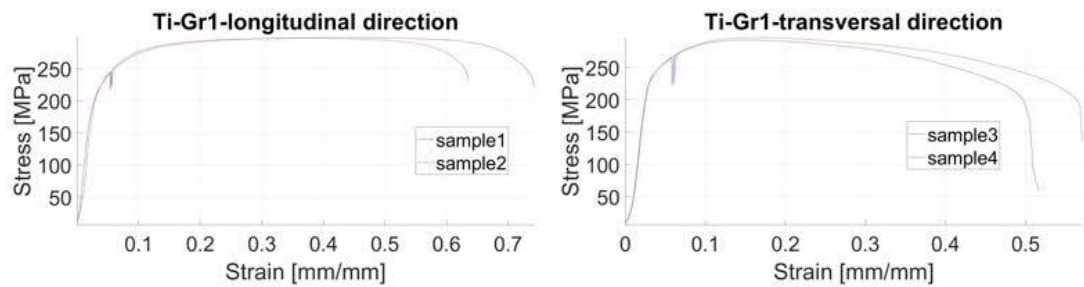The stress-strain curves for Ti Gr 1 are reported in the next figure.

Figure 68: Ti Gr 1 stress-strain curves

Table 19: Ti Gr 1 mechanical properties in longitudinal direction

Young's modulus [GPa]	Yield strength [MPa]	Ultimate tensile strength [MPa]	Percent permanent elongation (%)
100.01±0.05	176.32±1.54	297.74±0.48	55±1

Table 20: Ti Gr 1 mechanical properties in transversal direction

Young's modulus [GPa]	Yield strength [MPa]	Ultimate tensile strength [MPa]	Percent permanent elongation
101.09 ± 2.05	220.78± 0.81	294.19±1.96	46±3

Also in this case the experimental data are according to the datasheets provided by the manufacturer except the percent permanent elongation. Indeed, the experimental one is much higher, but looking in other datasheets it is possible to have Ti Gr 1 with better formability that ensure this range of elongation. For this reason, probably our Ti Gr 1 belongs to this category. The discontinuity which may be found on the curve very close to the yield strength, is only due to the removal of the extensometer, but it is irrelevant for our results.

Finally, PEEK was also tested but in one direction only, since there is no rolling direction that can affect the mechanical properties. The stress-strain curves are reported in the following figure and the inferred mechanical properties were recorded in the next table.
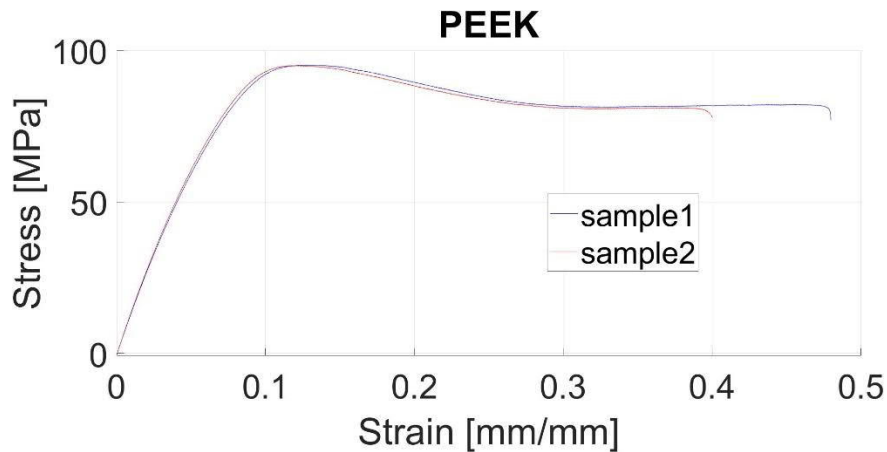

Figure 69: PEEK stress strain curves

Table 21: PEEK mechanical properties

Young's modulus [GPa]	Yield strength [MPa]	Percent permanent elongation
3.84 ± 0.14	95.20± 0.09	33±1

The testing of this last samples demonstrated that also for PEEK the experimental data are according to the manufacturer ones.

7.3 Mechanical testing of the joints

This section contains the mechanical tests for the weld joints obtained through the THEW technology considering the best option among the selected material and tools.

7.3.1 Tensile shear test

In next figure there is the force-displacement curves obtained from the tensile shear test of the samples produced through the THEW process. All the samples were cut from one long weld where the set of right process parameters was exploited.
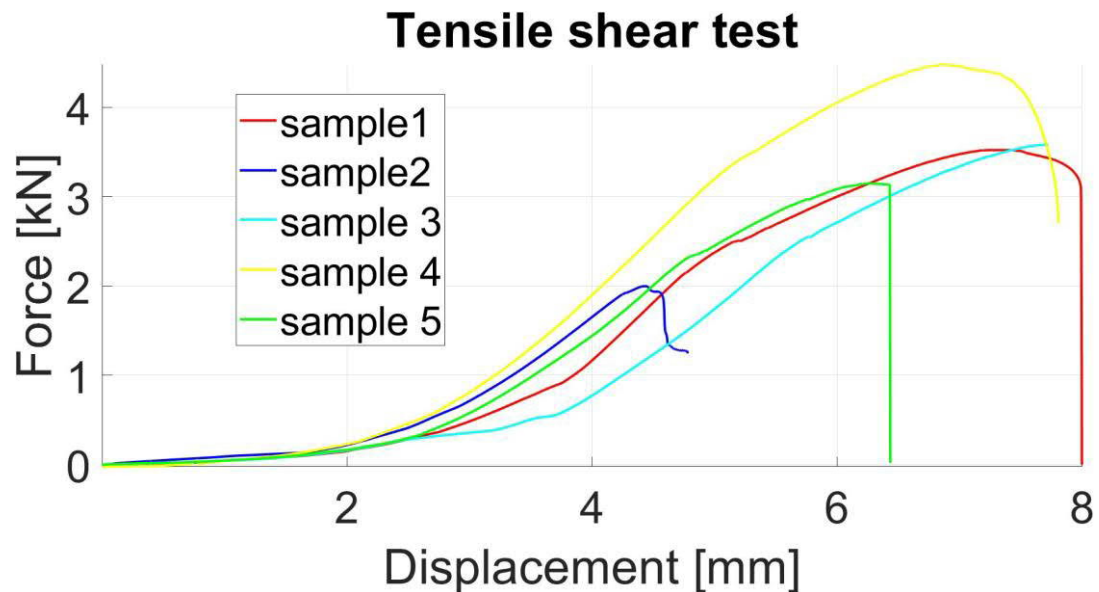

Figure 70: Force-displacement curves for the tensile shear test samples

For all the samples the joint has an initial phase of elastic deformation to which corresponds an increase of the load that is roughly linear after a phase of big displacements with small load. Then, it reaches a peak to collapse suddenly. Since there is a very small linear region and then the linearity approximation is not valid anymore, this means that the sample starts to yield before reaching the peak and fracture. The behaviour of the curves is almost the same, but the sample 2 presents a lower peak load. The description of the fracture modes in the next lines will clarify the reason for that. The maximum recorded failure load for these samples was for sample 4 with a peak load of 4.48 kN.

The failure mode was similar for the samples 1, 3 and 5. Indeed, they have also a similar peak load, respectively 3.52 kN, 3.58 kN and 3.15 kN. As we can see from the picture representing the fracture area, the failure starts in the PEEK very close to the joint and then it propagates in a straight line until the fracture was reached. Moreover, there are traces of liquified PEEK close to the titanium strips. This effect creates an adhesive bonding but at the same time it can be the initiation point for the fracture propagation, since the liquified PEEK is less strong. Moreover, the fracture does not occur in the joint, but very close to that. This means that the force recorded by the machine during the test was based on the strength of the weaker material that is the PEEK. This means that the joint strength can be even higher since it does not fracture. However, looking at the samples after the test some bending of the aluminum plates was noticeable, that means that during the test it is not

measured precisely the effective shear resistance of the joint since there is a not negligible bending effect, which can influences the results. To have a confirmation of these assumptions, the tests should be repeated in another configuration to avoid the bending effect. The solution can be to have the same overlap configuration, but on both sides of the PEEK. Even if there are the bending problems the results are promising since the fracture does not occur in the joint.
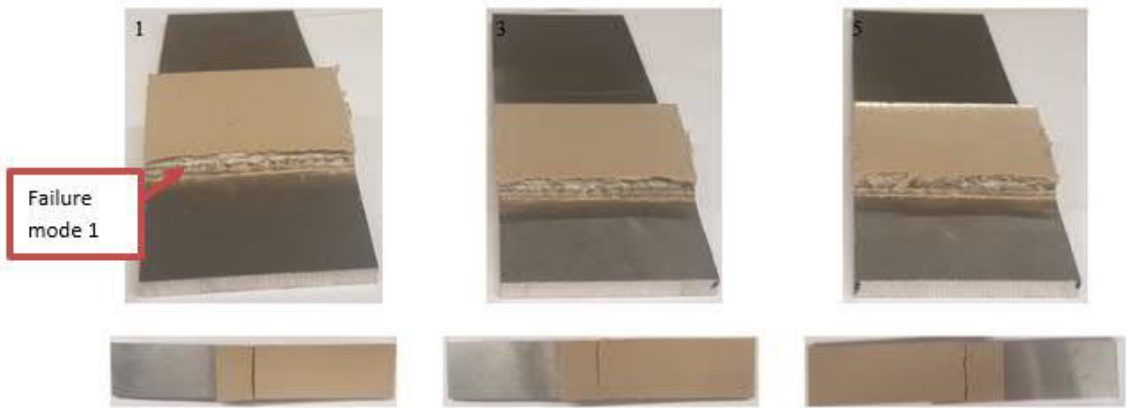

Figure 71: Samples 1,3 and 5 after fracture

Sample 2 presents the lowest peak load that is 2.00 kN. This result has its roots in the presence of a crack on the surface as it is noticeable from the next picture. This is a confirmation that the closure of the surface was a crucial result since it influences the strength of the overall system. Indeed, in this case the fracture occurs in the aluminum, but still out of the joint. Luckily, the surface on the other samples was closed.

Figure 72: Sample 2 after fracture

Finally, sample 4 has the highest peak load. In this case, the failure mode was different. The integrity of the shape of the crab claw joint and the non-fractured PEEK highlighted

that there was a tearing of the polymer surface with a consequent failure when the aluminum was totally detached from the polymer. This can be due to the introduction from the sharp edges of the joint geometry shape of a stress concentration in PEEK area close to the weld region. This can be confirmed by the presence of entrapped polymer in the "Crab Claw" joint shape of the aluminum. Also in this case, there is a noticeable presence of the bending effect of the aluminum plate that can influences our results in terms of shear resistance. The suggestion is to retry the tests with the suggested configuration in the lines above.

Figure 73: Sample 4 after fracture

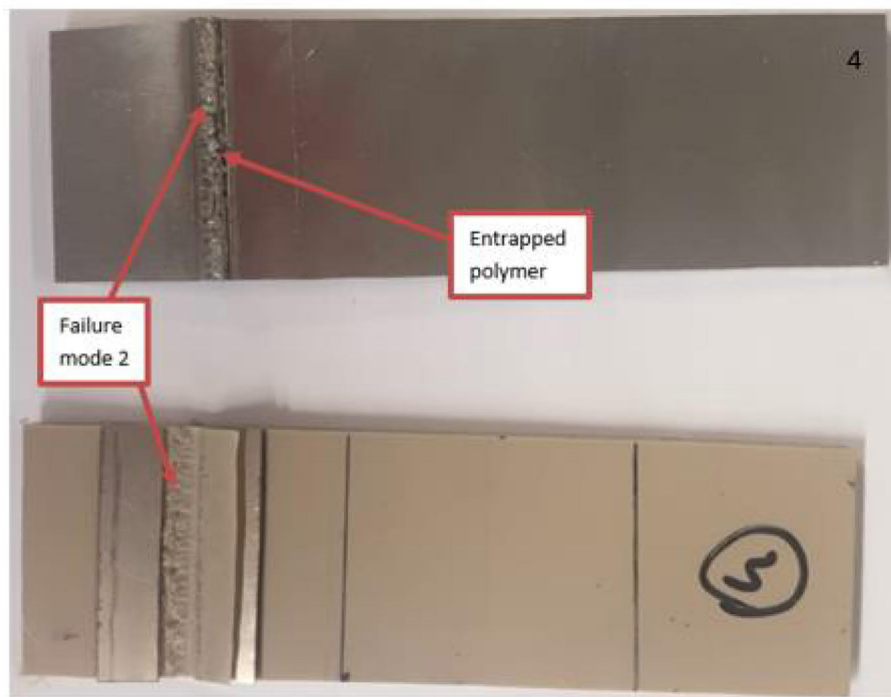To summarise the failure mode 1 was due to the weakness of the liquified polymer, while failure mode 2 was due to the stress intensification in the polymer close to the sharp edges of the joint which exert a tearing action on the polymer. The fracture in the aluminum due to the presence of the crack was not considered as a failure mode since it was due to inaccuracies during the welding process.

7.3.2 Cross tension test

In next figure there is the force-displacement curves obtained from the cross-tension test of the samples produced through the THEW process. All the samples were made exploiting the set of right process parameters evaluated previously.
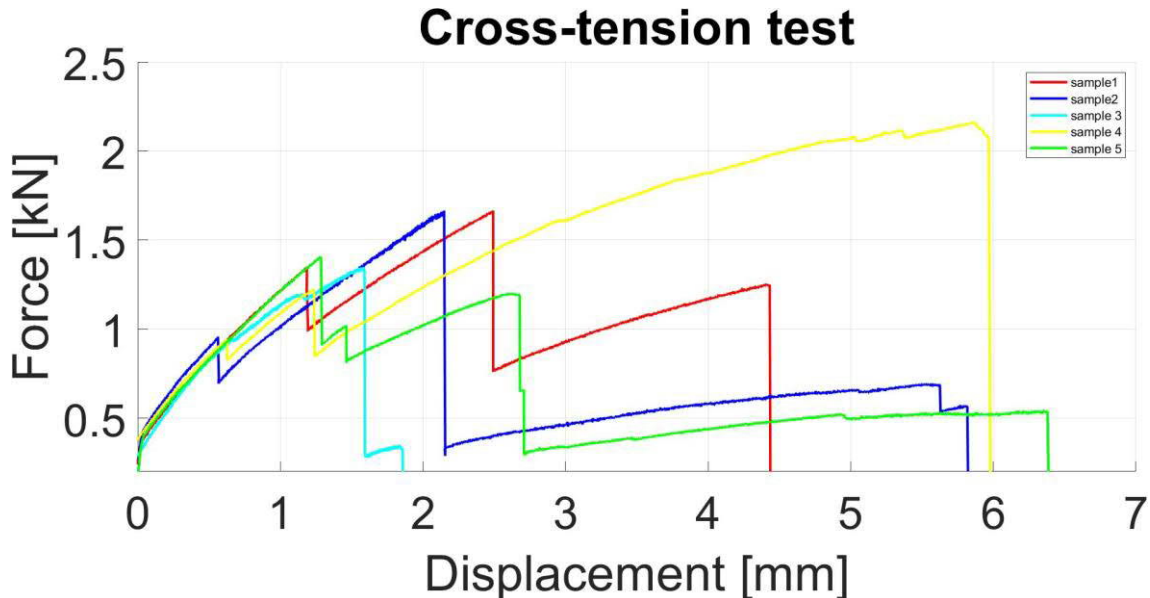

Figure 74: Force-displacement curves for the cross-tension test samples

From the picture we can notice that for all the samples the joint have an initial phase of elastic deformation, that can be approximated to a linear relationship between the load and the displacement, and then there is a deviation from linearity until it reaches a local peak with consequent load drop. After that, it starts to increase again linearly until it reaches another local peak. The process was iterated until the last local peak and after the joint fractures. The explanation of this behaviour can be justified considering that it is not a punctual joint, but there was a circular joint with many points of anchoring. The maximum load was recorded for sample 4 and it was 2.16 kN.

The failure mode was very similar for each sample, except for sample 3 that has also the lowest peak load equal to 1.34 kN. The reason of that looking at the fracture surface was that no penetration of aluminum in the polymer occurred. For this reason, the joint was based only on the adhesive bonding due to the visible local liquification of the polymer. For the other samples, the fracture still occurred in the polymer close to the weld area. This means that the weld joint was very strong, and it can be confirmed by the strong penetration of the aluminum in the polymer, with consequent anchoring effect. There were still traces of molten polymer that contributes to the adhesive bonding effect. Also in this case, the strength of the joint relied on the two competitive effects of joining which are adhesive bonding and mechanical interlocking. As in tensile shear tests, the reason for the fracture in the PEEK very close to the joint was based on the weakness of the molten polymer in this area, where the crack initiation took place. For the sake of completeness, the maximum loads for samples 1, 2 and 5 were respectively 1.67 kN, 1.66 kN and 1.41 kN.

The fracture surfaces are displayed in the next picture.

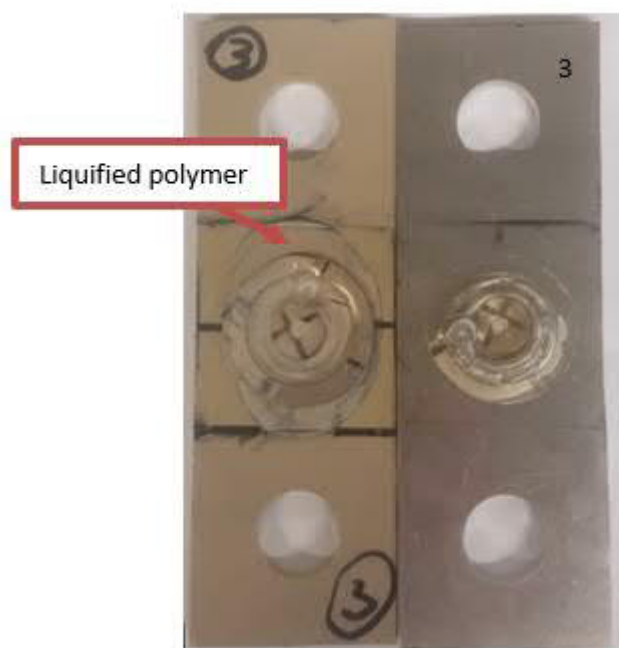

Figure 75: Samples 1, 2, 4 and 5 after fracture

Figure 76: Sample 3 after fracture

To summarise, also in cross-tension test failure mode 1 was predominant. The failure due to the lack of penetration of aluminum in the polymer cannot be considered a proper failure mode since it was due to inaccuracies of the process and it was related to an improper joint.

8 Microscopic analysis

8.1 Introduction

As already specified the obtained joint was analysed through optical microscope to examine the overall joint geometry, the involved joining mechanism, the possible presence of polymer vaporisation and finally to inspect the differences between the processed zone and the base material.

In section 8.2 macrostructural analysis of the THEW joint was performed while in section 8.3 the microstructural analysis was carried out.

In section 8.4 the joint was characterised from a geometric point of view.

The analyses were made in different section of the sample. The weld path had a length of 100 mm and the cross section was analysed for 3 samples. For this reason, the specimen was cut in three points as it is clarified from the following drawing.
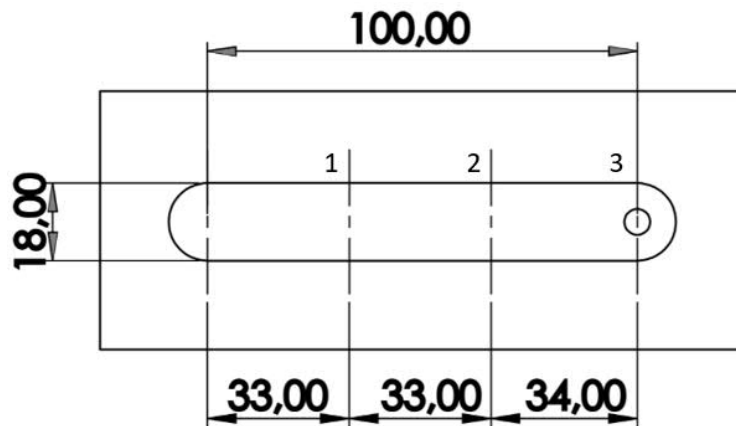

Figure 77: Cutting points and sample geometry

8.2 Macrostructural characterisation of THEW joint

From the previous drawing it is easy to understand that three different cross sections along the welding path were analysed. Moreover, as already said the overall picture of the joint was obtained from the combination of pictures extracted in different points of the analysed sample. The pictures were extracted considering different optical views. The first set of the pictures was focused on the aluminum, the second set on the polymer and, finally, the third set was made only on the aluminum since the etchant was specific for the aluminum. Differently from the approach of the previous works, a larger consistency of the joint along the welding path was retraceable. This is due to a better development of the surrounding conditions and thanks to a different approach (different process parameters and tools). Indeed, there is an upward flow of the pressurised polymer, but it is restricted in a precise region and it does not prevent the downward flow of the viscoplasticised of the aluminum inside the polymer.

All the samples were analysed with a magnification of 2.5X.

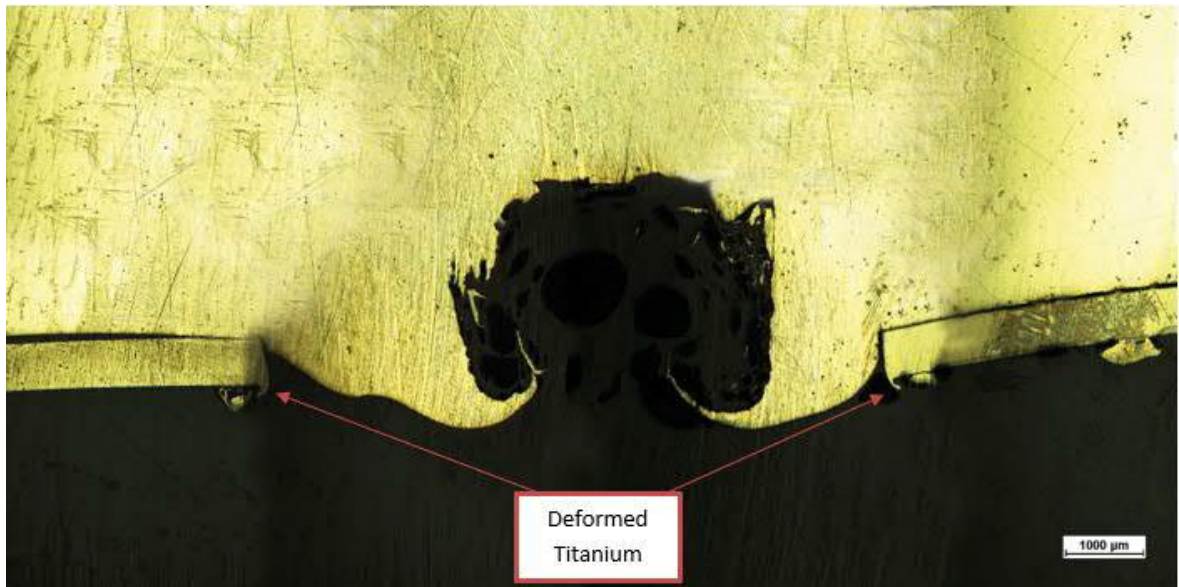## 8.2.1 Macrostructural analysis before etching

Aluminum focused

Figure 78: Sample 1 (Al focused)

In sample 1 the "Crab Claw" joint is very evident. Indeed, two claws extend from the aluminum matrix which ensures a strong mechanical interlocking with the polymer. The presence of the aluminum particles in the polymer is retraceable in some points. This can be due to the flow of the pressurised polymer inside the "Crab Claw" joint. Moreover, there is also a strong deformation of the extrusion die in correspondence of the internal points. This can be due also to a possible contact between the tool and the extrusion die if the tool is not perfectly centered or the titanium moves inside the grooves on the polymer. The bending of the extrusion die is due to two simultaneous effects, which are the softening of the polymer and the forging action of the shoulder. In addition, this Ti-alloy is very easy to be deformed since it is the softest among the Ti-alloys and it has great formability as shown from the tensile tests done on the base materials. The two claws ensure a mechanical interlocking between the aluminum and the polymer. In addition, also adhesive effect can be present due to the melting of the polymer and consequent solidification.
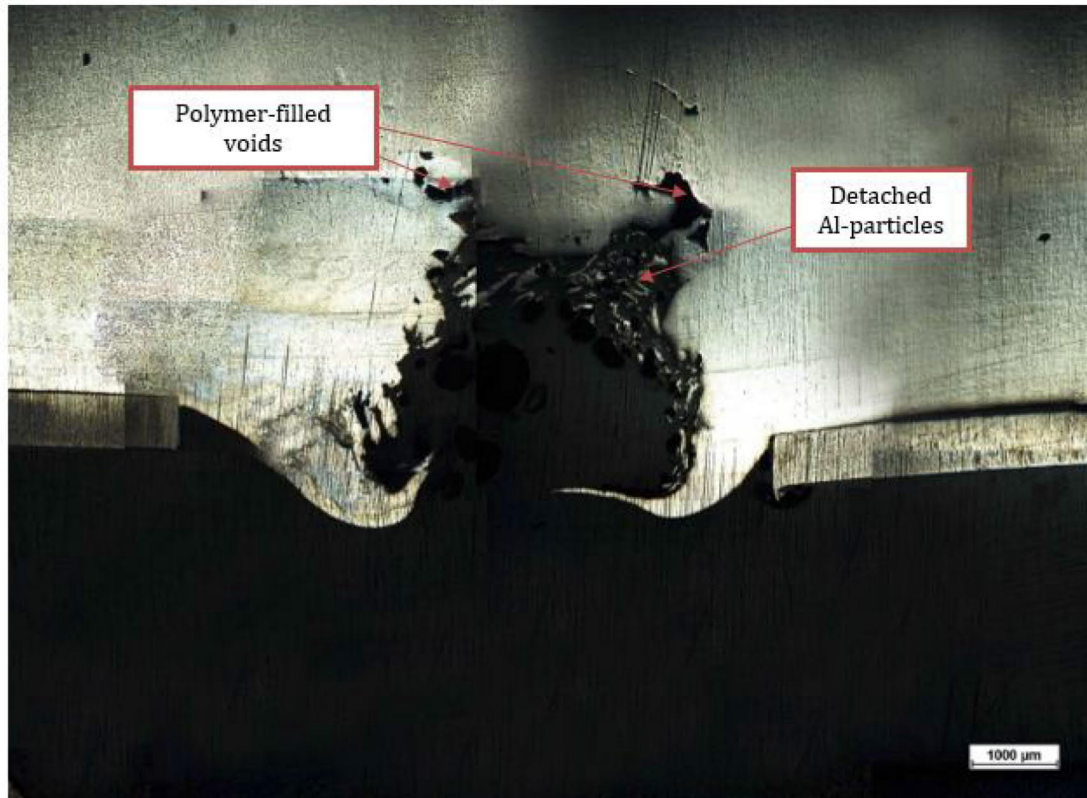
Figure 79: Sample 2 (Al focused)

Sample 2 shows that the "Crab Claw" geometry is still present. However, there is still also the presence of detached aluminum particles inside a polymer matrix and voids filled with polymer in the upper part of the processed aluminum. All these phenomena are always associated to the strong upward flow of the polymer and the non-uniform consolidation of the aluminum material layers. In addition, there is a small space between the aluminum and the titanium extrusion die due to the bending of the sheet metal and the flow of the liquified polymer inside. Finally, the weld surface is closed, and this was one of the objectives of this work compared to the previous ones.
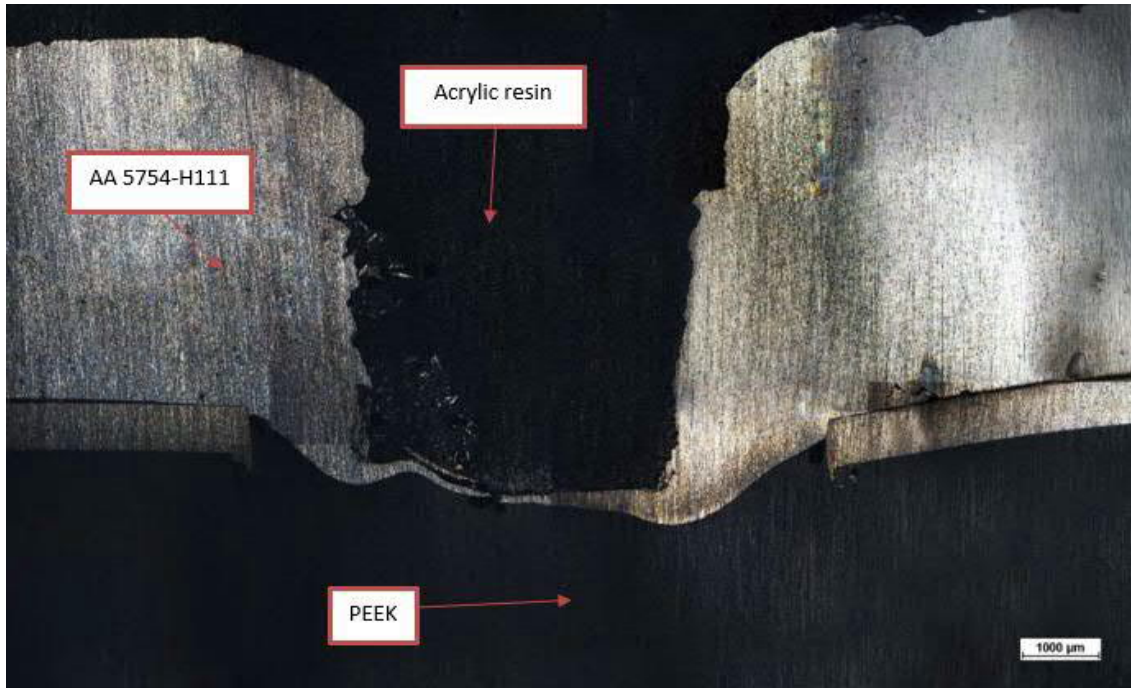
Figure 80: Sample 3 (Al focused)

In sample 3 there is no joint since it is located in the point where the tool plunged out at the end of the welding path. Indeed, the upper part is the acrylic resin used for the cold mounting of the sample, while in the lower part there is the PEEK. However, this last sample is very important to understand the conditions in the precise time instant when the probe is inside the material during the travelling.

As we have seen from the previous samples, a larger consistency of the joint shape was guaranteed through this process compared to the previous works where the joint hook shape was guaranteed for the 35% of the path with a length of the path equal to 41 mm [1].

Polymer focused

This set of micrographs was done with a focus on the polymer to see its condition after the welding process.
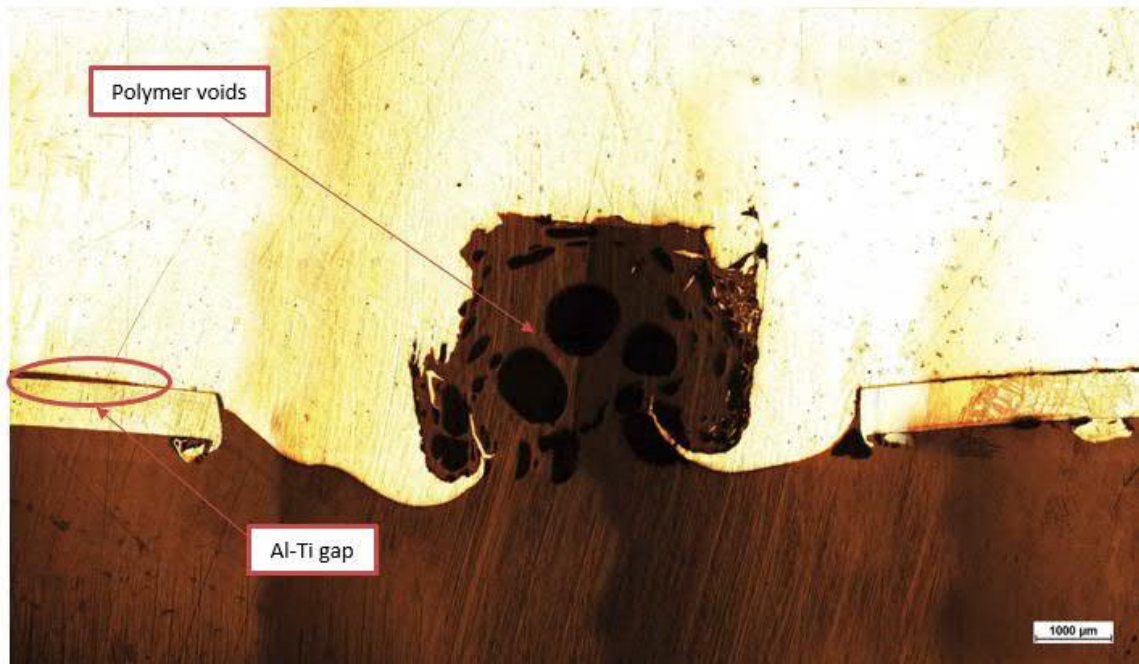
Figure 81: Sample 1 (Polymer focused)

Sample 1 reveals the presence of voids in the processed polymer which is entrapped in the "Crab Claw" shape of the aluminum. The voids lead to this typical sponge structure. They are more concentrated on the aluminum-polymer interface since here the high temperature due to the processing of the aluminum led to a partial vaporisation of the polymer. In addition, it is possible to notice the gap between the aluminum and the titanium sheet metal which is filled by the liquified polymer. This can create a further adhesive bonding between the three materials forming the sandwich structure.

Figure 82: Sample 2 (Polymer focused)

In sample 2 the same features already described in sample 1 can be found. Again, the voids are very concentrated in aluminum-polymer interface and so in the processed zone. However, in this case a void in titanium-polymer is also retraceable. This means that probably in that point the titanium reached a temperature to liquify and vaporise the polymer. In addition, in the top right corner there is a mixture of detached aluminum particles in the polymer matrix.
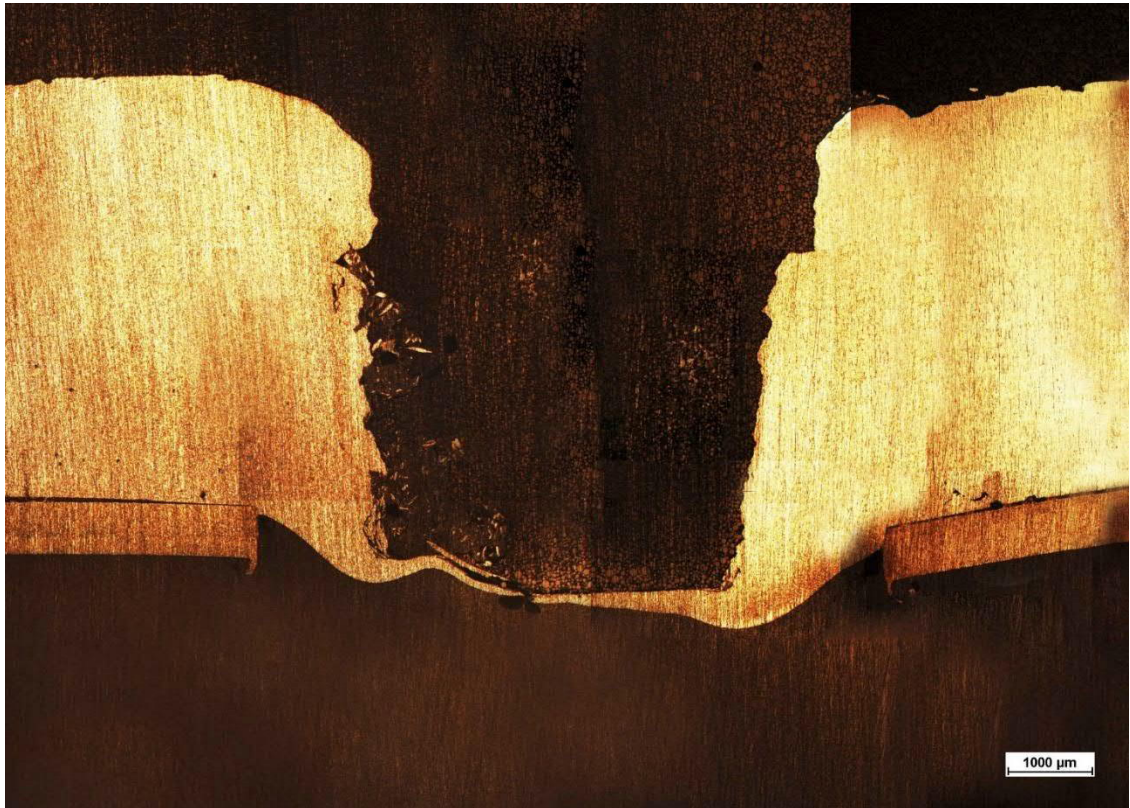
Figure 83: Sample 3 (Polymer focused)

Finally, as already stated, in sample 3 there is no joint since it is the point where the tool plunged out. However, now it is easily possible to distinguish the polymer from the acrylic resin that is in the upper part. In addition, this picture is useful to understand the actual conditions when the probe is inside the material during the travelling.

8.2.2 Macrostructural analysis after etching

In this section a macrostructural analysis of the aluminum region of the joint is made to reveal the flow of the material and the grain structure thanks to the use of a proper etchant. In addition, the objective is also to check the presence of the precipitates due to the deformation process induced by the rotation of the tool, but these can be better seen by higher magnification as explained in next subsection. One cross section was analysed to highlight the described features.
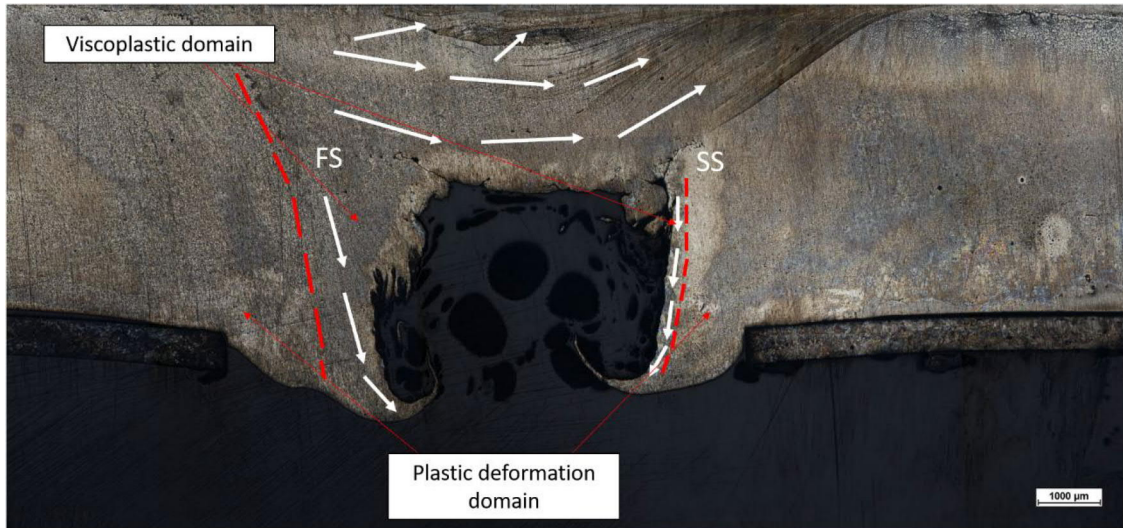

Figure 84: Cross section after etching

As we can see it is quite distinguishable the flow of the material with also the interface between the two flows direction. Indeed, on the interface, where there is the material separation a crack starts to advance from the aluminum interface. However, thanks to the pressure induced by the shoulder the crack does not propagate. Here, we can understand the importance of the shoulder which has the role to consolidate the joint through the forging action.

Finally, it is also possible to notice the interface between the viscoplastic domain where a flow of the material is noticeable and the plastically deformed region, where only a small plastic deformation is noticeable. Indeed, the boundary between the stirred zone and the base material is evident. On the shear side the flow of the material involves only a small layer of material, while on the flow side the layer is much thicker. Moreover, also the pull up of the material in the upper part is distinguishable.

8.3 Microstructural characterisation of THEW joint

One section of the THEW joint was extracted to analyse the microstructure of the joint. In the next picture the numbers indicate the analysed points. The micrographs were taken through the use of optical microscope with four different magnifications (2.5X, 20X, 50X and 100X).

Figure 85: Observed regions

First, it is noticeable a grain refinement due to the dynamic recrystallisation induced by the process and the grains in region close to the claws are elongated and they have a unidirectional flow.
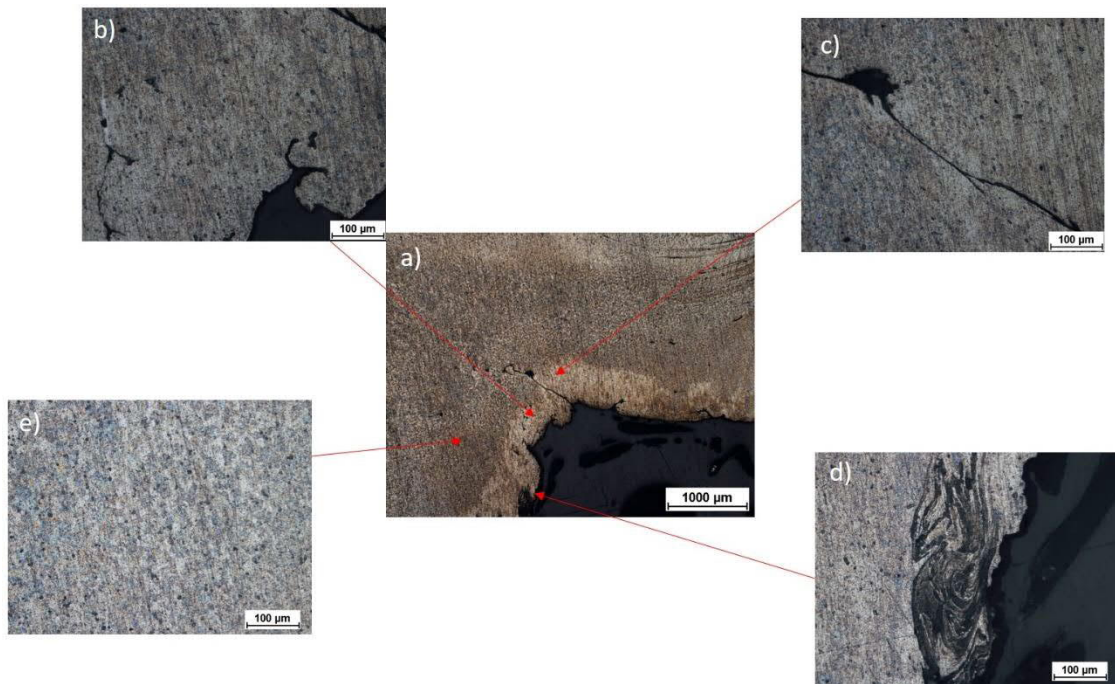
Figure 86: Micrograph at point 1; a) 2.5X; b), c), d) and e) 20X

The picture shows the presence of a crack which propagates from the aluminum interface to the top part. The origin of this crack can be due to the non-consolidated mix of materials from different regions. In addition, the pressurised polymer helps the opening of the crack since it tries to find the easiest path to flow up. However, the pressure induced from the shoulder prevents the propagation of the crack. Moreover, it is very distinguishable the grain structure with the presence of black dots which can be Fe- or Mg-based precipitates

due to the deformation induced by the process, but an EDS analysis can help to determine the composition. In figure 86 d) the mixing between the polymer and the aluminum at the interface is shown.
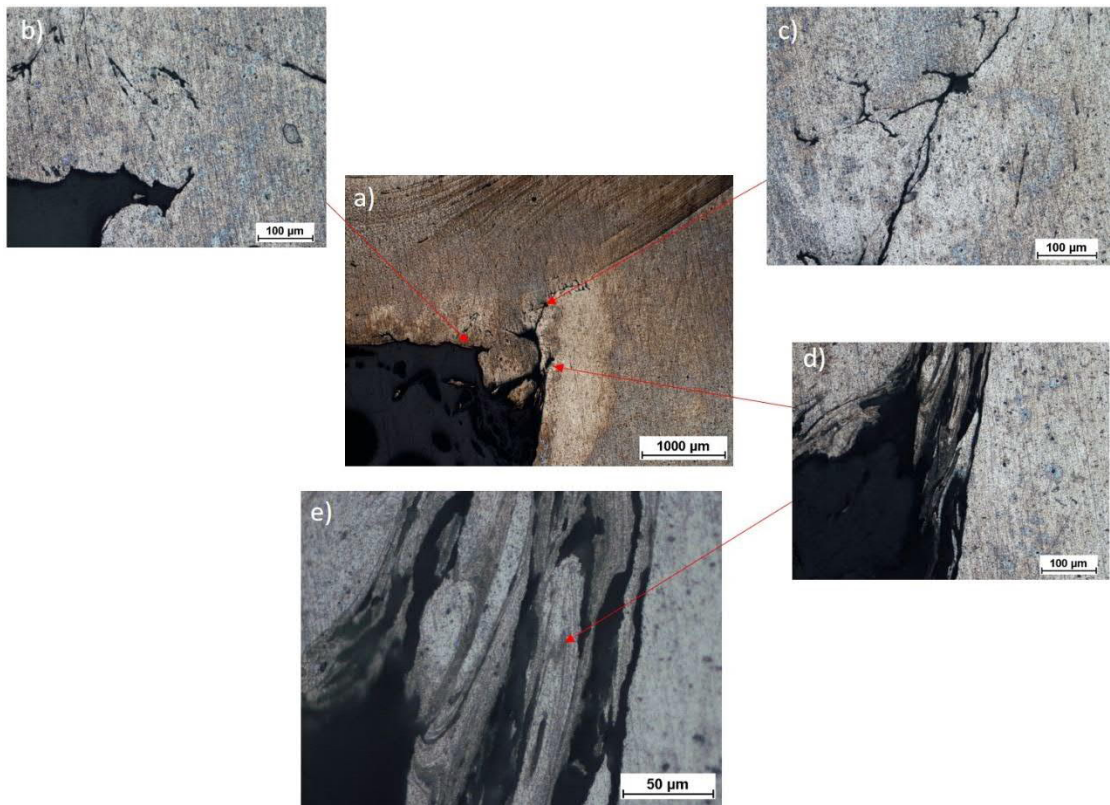
Figure 87: Micrograph at point 2; a) 2.5X; b), c) and d) 20X; e) 50X

Figure 87 shows the presence of surface irregularities due to the contact with the probe during the joining process. A crack still advances from the aluminum interface as in the previous case and a flake structure protrudes from the interface towards the polymer. In figure 87 e) with higher magnification it is possible to notice the mixing between the polymer and the aluminum with the strongly elongated structure of the aluminum grains due to the unidirectional flow of the material.
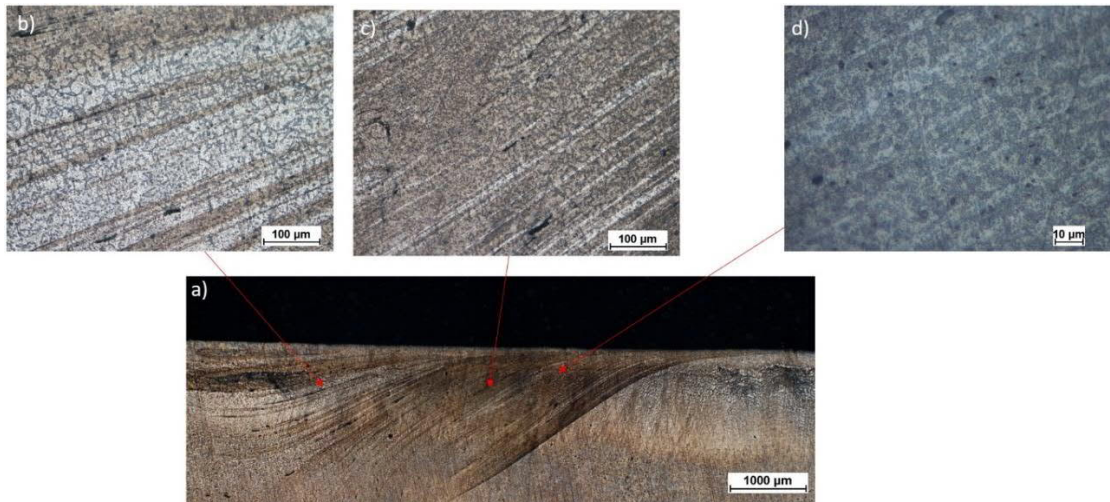
Figure 88: Micrograph at points 3-4; a) 2.5X; b) and c) 20X; d) 100 X

Figure 88 shows an alternation of light and dark lines in the microstructure of the aluminum due to the stirring of the material which leads to the formation of different levels of mixed material that pile up. In addition, the grain boundaries are much more distinguishable in this picture. Some voids are present due to the non-uniform mixing of the material.

Figure 89: Micrograph at points 5; a) 2.5X; b), c), d) and e) 20X; f) 50 X

In figure 89 the characteristic "Crab Claw" shape is distinguishable with the mechanical interlocking deriving from it. The grains are elongated in the region of the claw following the direction of the material flow. Moreover, a gap between the aluminum and the titanium

is noticeable and, in this region, the liquified polymer can flow leading to an additional adhesive effect. The surface irregularities are still present, and they are due to the contact with the rotative probe.
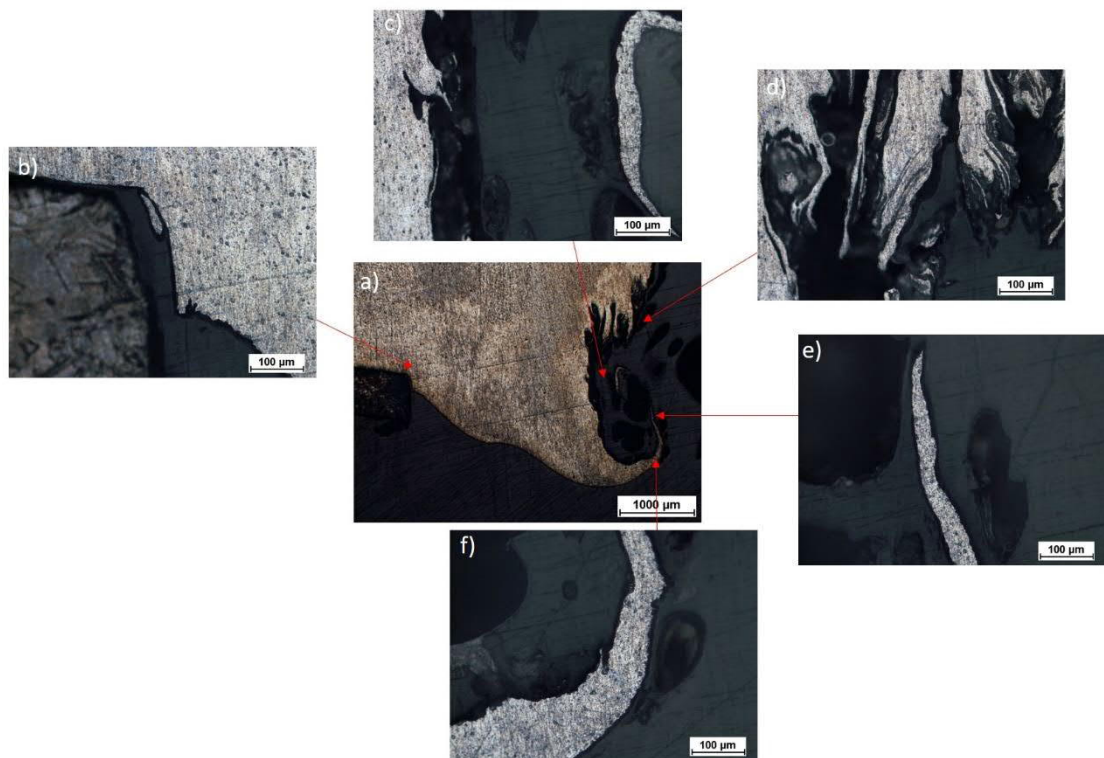
Figure 90: Micrograph at points 6; a) 2.5X; b), c), d), e) and f) 20X

Figure 90 is the specular of figure 89. Indeed, the same features for the claw can be noticed. In addition, on the top part there is a flake structure protruding from the aluminum plate where the mix between the polymer and the aluminum is evident. Due to the stirring of the material, there is also one particle of aluminum completely detached from the plate and surrounded by the polymer matrix.

8.4 Geometric characterisation of THEW joint

The THEW joint was also characterised from a geometric point of view. From the following picture the main dimensions are specified, and the numerical values are reported in the next table.
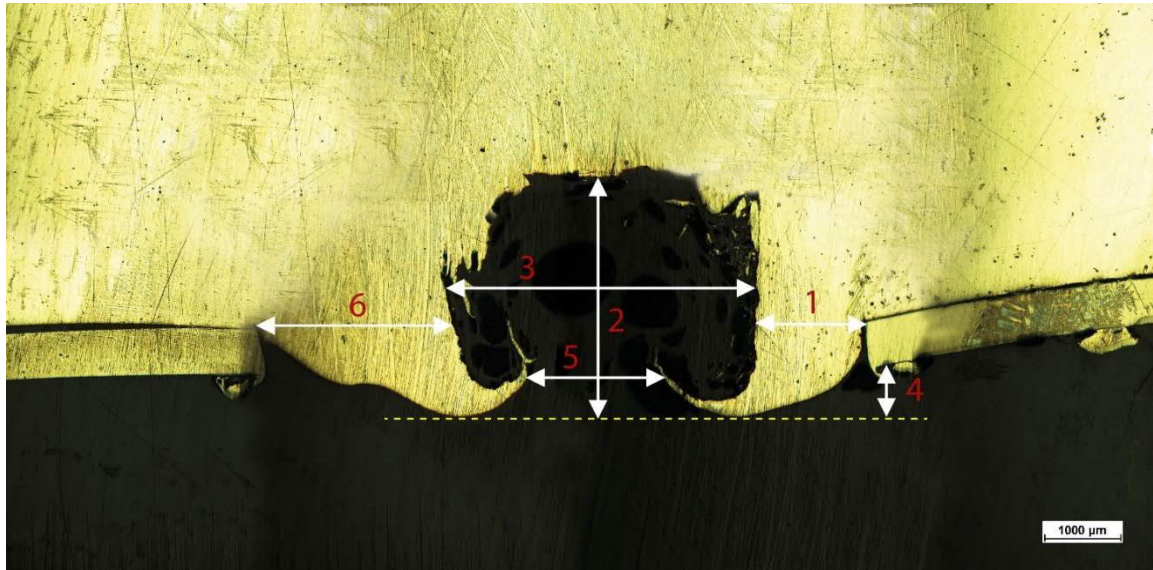
Figure 91: Measurements for THEW joint

Table 22: Overall dimensions for THEW joint

Dimension in the picture	Length [mm]
1	1.382
2	3.176
3	4.118
4	0.735
5	1.882
6	2.647

9 Conclusion and future work

9.1 Conclusion

This work was described as an extension of the previous works made in Aalto University under the supervision of the Professor Pedro Vilaça involving a joining between an Al-alloy with a polymer.

Since they are dissimilar materials the joining process was challenging and after the previous works attempts a new approach was proposed in this last work. The objective was to bring the THEW joining into feasibility through this new approach and in this section a summary of the work and the results obtained were proposed.

Initially, the previous conditions and results were analysed to establish a new experimental plan. Ti Gr 1 was proposed as alternative material for the extrusion die and AA1050 as the new candidate for the Al-alloy. On the other hand, the selected thermoplastic polymer was PEEK.

After the analysis of the previous work conditions, some problems popped up. The necessity to have a closed surface with a longer welding path led to establish some requirements for a new set of tools and a new clamping system.

The new set of tools was carefully designed with also a material selection. The purpose was to obtain a completely closed surface on the joint with a new symmetric geometry for the joint shape. For this reason, three different shoulders and probes were designed and tested to select the best one.

A new clamping system was designed to have a better positioning and force distribution since the welding path length was increased from the previous works. The new system consists of two stoppers and a couple welded sheets which allowed a better pressure distribution to avoid unacceptable bending of the involved sheets that can compromise the welding quality.

In the meanwhile, new process parameters were proposed to carry out the testing phase and they were varied to get the best set of preliminary process parameters. Indeed, due to COVID-19 pandemic it was not possible to design an optimisation plan to have the specific optimal parameters and tools, since this operation requires a large amount of samples and time. Hence, our analysis was done through a manual observation of established performance parameters of the tested samples till we achieved a good joint.

After some experiments and looking at previous works, the results suggested us to reduce the distance between the Al-alloy and the polymer. For this purpose, the extrusion die with a thickness of 1 mm was first replaced by a die with a thickness of 0.6 mm. After that, since the distance was still too big the extrusion die was replaced by a couple of titanium strips with the same thickness of 0.6 mm embedded in pre-machined grooves with a depth of 0.5 mm. The details of this new approach are described in chapter 6.

The preliminary experiments revealed also that the selected Al-alloy, when viscoplasticised through the stirring induced by the probe, was not able to deposit in the polymer, leading to the presence of a channel without any upward flow of the polymer.

Indeed, this Al-alloy was not able to provoke the softening of the polymer with a consequent deposition in it. For this reason, the pressure induced by the viscoplasticised aluminum was not enough to pressurise the polymer to cause its upward flow. Due to these results this base material was replaced by AA5754-H111 with consequent instantaneous improvements in the results in terms of joint and closure of the surface.

After this testing phase, the best set of preliminary process parameters, tools and surrounding conditions was established to obtain the first successful THEW joint with a totally new approach.

The process was also exploited to build the first double side THEW joint and non-linear THEW joint with good results confirming the good track for this preliminary evaluation of the THEW joining process.

The new joints were tested involving two mechanical tests: tensile shear test and cross-tension test. The maximum loads that the joint can withstand for both the tests were recorded. They are also resumed in the following table.

Table 23: Maximum peak loads

Mechanical test	Maximum peak load [kN]
Tensile shear test	4.48
Cross-tension test	2.16

Two failure modes were found during these tests. Failure mode 1 occurred very close to the joint and the failure propagated in the PEEK following a straight path. In this case, traces of liquified PEEK close to the titanium strips were found. The liquified PEEK was weaker and so it behaved as initiation point for the fracture. On the other hand, failure mode 2 consisted of the tearing of the polymer surface with a consequent failure when the aluminum was totally detached from the polymer. This can be due to the introduction from the sharp edges of the crab claw geometry of a stress concentration in PEEK area close to the weld region. Indeed, for this last case entrapped polymer was found in the "Crab Claw" shape. Failure mode 1 was prevalent for both tensile shear test and cross-tension test.

Finally, macrostructural and microstructural analyses were made to evaluate the possible presence of polymer vaporisation, different involved joining mechanisms, the overall joint geometry and differences between the processed zone and the base material. From a macroscopic point of view the "Crab Claw" joint shape was obtained and its consistency along the welding path was demonstrated. Some voids in the polymer were detected very close to the aluminum interface and in some cases also on titanium interface. This can be due a partial vaporisation of the polymer in contact with the hot viscoplasticised aluminum. Moreover, a good mixture of aluminum and polymer was also highlighted. On the other hand, from a microscopic point of view a unidirectional flow of material was evidenced with elongated grains in this direction. In general, grain refinement was present due to the dynamic recrystallisation induced by the plastic deformation intrinsic in the process. Fine Fe- or Mg-based precipitates were found in the microstructure due the mixing of

material induced by the process. However, deeper microscope analyses are required to establish the composition of them. Finally, the characteristic "Crab Claw" shape was analysed focusing on the mechanical interlocking caused by this shape which ensures the high resistance of the joint.

9.2 Future work

As already said this work was the implementation of a new approach of the THEW joint. Since it was a preliminary approach different improvements and ideas for the future are suggested in this section.

Optimisation of process parameters:

- Due to COVID-19 pandemic no optimisation plan was designed to find the actual optimal process parameters for the selected combination of base materials. For this reason an optimisation plan can be designed following different algorithms (Taguchi or Box-Behnken methods).

- Improvement of the process parameters to minimise the polymer vaporisation.

Testing and modeling of the THEW joint:

- Improvement of the setup for tensile shear test and testing of different welding paths for cross-tension test.

- Modeling of the THEW joint to compare experimental results with numerical ones.

- Helium leak test to verify the presence of small leaks in the joint.

Improvement of the THEW tools:

- Different new geometries for probe and shoulder can be designed and tested to maximise the deposition of the visco-plasticised aluminum.

Improvement of the surrounding conditions:

- New clamping system can be designed with integrated cooling system especially for non-linear welding path.

Testing of welding path variants:

- Multiple non-linear welding paths on the same sample.

Testing of other engineering materials:

- Possibility to evaluate the process for other set of thermoplastic polymers and lightweight metals.

References

[1]   P. Khadka, P. Santos Vilaca da Silva, and X. Xu, "Joining Polymer to Aluminium by Through Hole Extrusion Welding," in *Seminar on Advanced Polymer-Metal Hybrid Structures*.

[2]   G. S. Meikandaan, "Evaluation of new spot variant approach for joining of dissimilar materials," Aalto University, 2019.

[3]   S. T. Amancio-Filho and L. A. Blaga, *Joining of Polymer-Metal Hybrid Structures*. Wiley Publications, 2018.

[4]   S. T. Amancio Filho, "Friction Riveting development and analysis of a new joining technique for polymer-metal multi-material structures," *Riv. Ital. della Saldatura*, vol. 63, no. 2, pp. 197–208, 2011.

[5]   J. L. Hecht, "Macrocomposites Made By Injection Molding," no. 3, 1986.

[6]   K. Martinsen, S. J. Hu, and B. E. Carlson, "Joining of dissimilar materials," *CIRP Ann. - Manuf. Technol.*, vol. 64, no. 2, pp. 679–699, 2015, doi: 10.1016/j.cirp.2015.05.006.

[7]   G. Meschut, V. Janzen, and T. Olfermann, "Innovative and highly productive joining technologies for multi-material lightweight car body structures," *J. Mater. Eng. Perform.*, vol. 23, no. 5, pp. 1515–1523, 2014, doi: 10.1007/s11665-014-0962-3.

[8]   F. C. Campbell, *Joining: understanding the basics*. ASM International, 2011.

[9]   R. W. Messler, "Joining composite materials and structures: Some thought-provoking possibilities," *J. Thermoplast. Compos. Mater.*, vol. 17, no. 1, pp. 51–75, 2004, doi: 10.1177/0892705704033336.

[10]   R. W. Messler, "Introduction to Joining," *Join. Adv. Mater.*, pp. 3–24, 1993, doi: 10.1016/b978-0-7506-9008-9.50004-x.

[11]   P. Kah, R. Suoranta, J. Martikainen, and C. Magnus, "Techniques for joining dissimilar materials: Metals and polymers," *Rev. Adv. Mater. Sci.*, vol. 36, no. 2, pp. 152–164, 2014.

[12]   R. W. Messler, "Mechanical Fasteners, Integral Attachments, and Other Mechanical Joining Methods," *Join. Mater. Struct.*, pp. 105–176, 2004, doi: 10.1016/b978-075067757-8/50003-8.

[13]   J. A. Speck, *Mechanical Fastening, Joining, and Assembly*, 2nd ed. CRC Press, 2017.

[14]   M. Screws, "Mechanical Fastening," *Handb. Plast. Join.*, pp. 175–201, 2009, doi: 10.1016/b978-0-8155-1581-4.50020-2.

[15]   A. B. Abibe, "Friction-based Injection Clinching Joining (F-ICJ): a new joining method for hybrid lightweight structures," pp. 1–138, 2015.

[16]   S. T. Amancio-Filho, J. F. Dos Santos, and M. Beyer, "S.T. AMANCIO-FILHO, J.F. DOS SANTOS, M. BEYER; .pdf," S.T. AMANCIO-FILHO, J.F. DOS SANTOS, M. BEYER, 2010.

[17]   M. Sônego, A. B. Abibe, J. F. dos Santos, L. B. Canto, and S. T. Amancio-Filho, "Friction-

based Injection Clinching (F-ICJ) of glass-fiber reinforced PA66 and Aluminium Hybrid Structures," *Investig. Mech. Prop. Magnes. Met. matrix Compos. with a fine Dispers. CeO2 Part.*, no. 1, pp. 2665–2672, 2014, doi: 10.2466/pr0.1981.48.1.335.

[18]   E. Bruckner, S. Friederich, and M. Gehde, "Material and process influences during the riveting of technical plastics," vol. 2, Fugen von Kunststoffen, 2013, pp. 98–103.

[19]   E. Bruckner, S. Friederich, and M. Gehde, "Ultrasonic Upsetting: A new method of Ultrasonic Staking to join hybrid material combinations.," 2015.

[20]   M. Gude, W. Hufenbach, R. Kupfer, A. Freund, and C. Vogel, "Development of novel form-locked joints for textile reinforced thermoplastices and metallic components," *J. Mater. Process. Technol.*, vol. 216, pp. 140–145, 2015, doi: 10.1016/j.jmatprotec.2014.09.007.

[21]   M. Mohammadi, J. R. Dryden, and L. Jiang, "Stress concentration around a hole in a radially inhomogeneous plate," *Int. J. Solids Struct.*, vol. 48, no. 3–4, pp. 483–491, 2011, doi: 10.1016/j.ijsolstr.2010.10.013.

[22]   D. Taylor, "Predicting Fatigue Limit and Fatigue Life," *Theory Crit. Distances*, pp. 163–197, 2007.

[23]   R. D. Adams, J. Comyn, and W. C. Wake, *Structural adhesive joints in engineering*, 2nd ed. United Kingdom: Chapman and Hall, 1997.

[24]   R. Pearson, "Thermoset Adhesives," *Encycl. Mater. Sci. Technol.*, pp. 9204–9208, 2001, doi: 10.1016/b0-08-043152-6/01658-2.

[25]   A. Baldan, "Adhesively-bonded joints in metallic alloys , polymers and composite materials : Mechanical," *Rev. Lit. Arts Am.*, vol. 9, pp. 4729–4797, 2004.

[26]   A. Higgins, "Adhesive bonding of aircraft structures," *Int. J. Adhes. Adhes.*, vol. 20, no. 5, pp. 367–376, 2000, doi: 10.1016/S0143-7496(00)00006-3.

[27]   V. C. Cagle, H. Lee, and K. Neville, *Handbook of adhesive bonding*. McGraw Hill, 1973.

[28]   H. Y. Nezhad and D. Stratakis, "PROCESS-INDUCED DEFECTS PERFORMANCE OF AEROSPACE COMPOSITES IN THE PRESENCE OF PROCESS-INDUCED DEFECTS SCHOOL OF AEROSPACE , TRANSPORT AND MANUFACTURING AEROSPACE MATERIALS MASTER OF SCIENCE Academic Year : 2016 - 2017 Supervisor : Dr Hamed Yazdani Nezhad," no. September, 2017, doi: 10.13140/RG.2.2.20580.83848.

[29]   G. Wypych, "Mechanisms of Adhesion," *Handb. Adhes. Promot.*, pp. 5–44, 2018, doi: 10.1016/b978-1-927885-29-1.50004-3.

[30]   R. W. Messler, "Adhesive Bonding and Cementing," in *Joining of Materials and Structures*, 2004, pp. 177 – 226.

[31]   D. N. Markatos, "Experimental investigation of the effect of defects, non-detectable by means of conventional non destructive techniques, on the mode I fracture toughness of adhesively bonded composite joints," University of Patras, 2015.

[32]   S. Lathabai, "Joining of aluminium and its alloys," in *Fundamentals of Aluminium*

Metallurgy, Woodhead Publishing Limited, 2011, pp. 607–654.

[33]   E. M. Petrie, "Adhesives for the assembly of aircraft structures and components. Decades of performance improvement, with the new applications of the horizon," *Met. Finish.*, vol. 106, no. 2, pp. 26–31, 2008, doi: 10.1016/S0026-0576(08)80035-9.

[34]   M. Sercer and P. Raos, "Joining of Plastics and Composites," *Weld. Eng. Technol.*, pp. 1–31, 2010.

[35]   Z. Tadmor and C. G. Gogos, *Principles of Polymer Processing*. New York: Wiley, 2006.

[36]   T. Gendo, K. Nishiguchi, M. Asakawa, and S. Tanioka, ", April 16 – 19 (2007).," in *Proceedings of SAE World Congress and Exhibition*, 2007.

[37]   S. Amancio-Filho and J. Dos Santos, "Joining of polymers and polymer–metal hybrid structures: recent developments and trends," *Polym. Eng. Sci.*, vol. 49, no. 8, pp. 1461–1476, 2009, doi: 10.1002/pen.

[38]   Y. Kawahito, A. Tange, S. Kubota, and S. Katayama, "Development of direct laser joining for metal and plastic," *ICALEO 2006 - 25th Int. Congr. Appl. Laser Electro-Optics, Congr. Proc.*, vol. 604, no. 2006, 2006, doi: 10.2351/1.5060840.

[39]   A. Gisario, M. Mehrpouya, and E. Pizzi, "Dissimilar joining of transparent Poly(ethylene terephthalate) to aluminum 7075 sheets using a diode laser," *J. Laser Appl.*, vol. 29, no. 2, p. 022418, 2017, doi: 10.2351/1.4983268.

[40]   S. M. Goushegir, N. Scharnagl, J. F. dos Santos, and S. T. Amancio-Filho, "XPS analysis of the interface between AA2024-T3/CF-PPS friction spot joints," *Surf. Interface Anal.*, vol. 48, no. 8, pp. 706–711, 2016, doi: 10.1002/sia.5816.

[41]   S. M. Goushegir, J. F. dos Santos, and S. T. Amancio-Filho, "Friction Spot Joining of aluminum AA2024/carbon-fiber reinforced poly(phenylene sulfide) composite single lap joints: Microstructure and mechanical performance," *Mater. Des.*, vol. 54, pp. 196–206, 2014, doi: 10.1016/j.matdes.2013.08.034.

[42]   S. T. Amancio-Filho, C. Bueno, J. F. dos Santos, N. Huber, and E. Hage, "On the feasibility of friction spot joining in magnesium/fiber-reinforced polymer composite hybrid structures," *Mater. Sci. Eng. A*, vol. 528, no. 10–11, pp. 3841–3848, 2011, doi: 10.1016/j.msea.2011.01.085.

[43]   K. Nagatsuka, S. Yoshida, A. Tsuchiya, and K. Nakata, "Direct joining of carbon-fiber-reinforced plastic to an aluminum alloy using friction lap joining," *Compos. Part B Eng.*, vol. 73, pp. 82–88, 2015, doi: 10.1016/j.compositesb.2014.12.029.

[44]   K. Nagatsuka, T. Onoda, T. Okada, and K. Nakata, "Direct dissimilar joining of aluminium alloys and polyamide 6 by friction lap joining*," *Weld. Int.*, vol. 31, no. 1, pp. 9–16, 2017, doi: 10.1080/09507116.2016.1223185.

[45]   F. C. Liu, J. Liao, and K. Nakata, "Joining of metal to plastic using friction lap welding," *Mater. Des.*, vol. 54, pp. 236–244, 2014, doi: 10.1016/j.matdes.2013.08.056.

[46]   O. J. Zoellner and J. A. Evans, "Plastic-Metal Hybrid. A New Development in the Injection

Molding Technology," in *Annual Technical Conference of the Society of Plastics Engineers*, 2002, pp. 1 – 4.

[47] M. Grujicic, "Injection overmolding of polymer-metal hybrid structures," *Join. Polym. Hybrid Struct. Princ. Appl.*, vol. 1, no. 4, pp. 275–305, 2018, doi: 10.1002/9781119429807.ch10.

[48] Esab, "Available: https://www.esabna.com/us/en/products/welding-automation-robotics/friction-stir-welding-fsw/carriers-manipulators/gantries/legio-friction-stir-welding-system.cfm." .

[49] MTS, "Available: https://www.upc.edu/sct/ca/documents_equipament/d_77_id-412.pdf." .

[50] Zwick Roell, "Available: https://www.zwickroell.com/-/media/files/sharepoint/vertriebsdoku_pi/02_284_allroundline_z005_up_to_z020_materials_testing_machine_pi_en.pdf." .

[51] Texhokom, "Available: http://www.tehno.com/specification/epiphot-300-200.pdf." .

[52] G. Harteprufer, "Available: http://www.gnehm-haertepruefer.ch/english.html." .

[53] J. Zhang, B. Song, Q. Wei, D. Bourell, and Y. Shi, "A review of selective laser melting of aluminum alloys: Processing, microstructure, property and developing trends," *J. Mater. Sci. Technol.*, vol. 35, no. 2, pp. 270–284, 2019, doi: 10.1016/j.jmst.2018.09.004.

[54] M. Vedani, "Al-alloys. Applied metallurgy course slides." Politecnico di Milano, 2018.

[55] M. Mhedhbi, M. Khlif, and C. Bradai, "Investigations of microstructural and mechanical properties evolution of AA1050 alloy sheets deformed by cold-rolling process and heat treatment annealing," *J. Mater. Environ. Sci.*, vol. 8, no. 8, pp. 2967–2974, 2017.

[56] Alumeco, "EN AW-1050A," 2020. [Online]. Available: https://www.alumeco.com/aluminium/plates/raw/en-aw-1050a/5-x-1000-x-2000-mm/p/390/3747.

[57] Granta Design, "CES Edupack." 2019.

[58] Continental, "Titanium applications," 2020. [Online]. Available: https://continentalsteel.com/titanium/applications/.

[59] P. Barriobero-Vila, "Phase transformation kinetics during continuous heating of α+β and metastable β titanium alloys," TU Wien, 2015.

[60] B. A. Kazi and M. M. Abdul, "Parametric optimization of machining Ti-alloys in respect to surface roughness - A review," *Appl. Mech. Mater.*, vol. 152–154, pp. 468–473, 2012, doi: 10.4028/www.scientific.net/AMM.152-154.468.

[61] M. Vedani, "Ti-alloys. Applied metallurgy course slides." Politecnico di Milano, 2018.

[62] Matthey Lamineries, "Available: https://www.matthey.ch/fileadmin/user_upload/downloads/fichetechnique/EN/Ti_Grade

_1_C.pdf." .

[63]   G.H. Melton et al., *"Engineering Thermoplastics", Applied Plastics Engineering Handbook*. 2011.

[64]   Matmatch, "Available: https://matmatch.com/learn/material/polyether-ether-ketone-peek." .

[65]   Vink Finland, "Available: https://www.vink.fi/media/import/fi_Vink_SUSTA_PEEK_natural_Datasheet.pdf." .

[66]   R. Ilola, "Engineering metals and alloys course slides." Aalto University, 2020.

[67]   eFunda, "Available: https://www.efunda.com/materials/alloys/aluminum/temper.cfm." .

[68]   Alumeco, "Available: https://www.alumeco.com/aluminium/plates/raw/en-aw-5754/8-x-1020-x-2020-mm/p/391/3792." .

[69]   Wikipedia, "Available: https://commons.wikimedia.org/wiki/File:Stress-strain_curve.svg." .

[70]   Struers, "Available: https://www.struers.com/en/Knowledge/Hardness-testing#hardness-testing-how-to." .

[71]   Gordonengland, "Available:https://www.gordonengland.co.uk/hardness/vickers.htm." .

[72]   BS EN ISO, "Resistance welding — Destructive testing of welds — Specimen dimensions and procedure for tensile shear testing resistance spot and embossed projection welds." 2016.

[73]   BS EN ISO, "Resistance welding — Destructive testing of welds — Specimen dimensions and procedure for cross tension testing of resistance spot and embossed projection welds," no. February. 2017.

[74]   P. Vilaça, J. Gandra, and C. Vidal, "Linear Friction Based Processing Technologies for Aluminum Alloys: Surfacing, Stir Welding and Stir Channeling," in *Aluminium Alloys, New Trends in Fabrication and Applications*, 2012.

[75]   Y. N. Zhang, X. Cao, S. Larose, and P. Wanjara, "Review of tools for friction stir welding and processing," *Can. Metall. Q.*, vol. 51, no. 3, pp. 250–261, 2012, doi: 10.1179/1879139512Y.0000000015.

[76]   D. Yan, "Study of shoulder flow zone formation in thick section FSW of 6061 Al alloy using scroll shoulder tool," 2008.